UNIVERSITY *of the*
WESTERN CAPE

In vitro investigation of putative interactions between the RING finger domain of Retinoblastoma Binding Protein 6 (RBBP6) and various substrates

UNIVERSITY of the
WESTERN CAPE

by

Christopher Jerome Witbooi

Supervisor: David J. R. Pugh DPhil (Oxon)

A thesis submitted in partial fulfilment of the requirements for the degree of Master of Science in Biotechnology

University of the Western Cape
2015

Abstract

Retinoblastoma Binding Protein 6 (RBBP6) is a RING finger-containing protein which plays a critical role in the 3'-end processing of mRNA transcripts. It is a constituent of the human pre-mRNA processing complex but also interacts directly with core splicing-associated proteins. RBBP6 also interacts with both major tumour suppressor proteins p53 and pRb and is known to play a critical role in suppression of p53 during development, in cooperation with MDM2. Through its RING finger it interacts with the C-terminus of the oncogenic protein Y-Box Binding Protein 1 (YB-1) both *in vitro* and *in vivo*, catalysing its ubiquitination and degradation in the proteasome. YB-1 is closely associated with tumour progression, poor patient prognosis and chemotherapeutic resistance, making it a promising target for therapeutic intervention. Unpublished data from our laboratory suggests that RBBP6 is able to poly-ubiquitinate YB-1 *in vitro*, using UbcH1 as the ubiquitin-conjugating enzyme (E2).

This study aims to identify RBBP6 RING protein-protein interactions involved in the down regulation of YB-1 by RBBP6. These interactions include the C-terminal fragment of YB-1 (substrate), MDM2 (E3) and UbcH1 (E2). The C-terminal fragment of YB-1, denoted YB-$1_{220\text{-}324}$, was successfully cloned and expressed in bacteria and demonstrated to interact directly with the RBBP6 RING finger domain in *in vitro* affinity pull down assays. This is in good agreement with our unpublished data that RBBP6 is able to ubiquitinate full length YB-1 as well as the YB-$1_{220\text{-}324}$ fragment.

UbcH1 was successfully expressed and shown to interact directly with RBBP6 RING in *in vitro* affinity pull down assays. This is also in agreement with our data showing that RBBP6 is able to ubiquitinate YB-1 using UbcH1 as E2. ^{15}N-labelled samples of RBBP6 RING was successfully expressed in bacteria and used to investigate the putative interaction with UbcH1 in NMR-based chemical shift perturbation assays. However no interaction was observed, possibly because the sample of UbcH1 was subsequently found using mass spectrometery to be partially degraded.

GST-tagged RBBP6 RING was able to precipitate MDM2 from HeLa lysate. This extends previous reports that full length RBBP6 and MDM2 interact directly and play a role in the suppression of p53 during development. The result was validated by showing that GST-MDM2 was able to precipitate RBBP6 RING in *in vitro*.

This study includes a side project which involved the cloning and expression of DWNN-GG. GST-HA-DWNN-GG was successfully cloned and expressed in bacteria. An HA tag was included immediately upstream of DWNN-GG for immunodetection using anti-HA antibodies; the construct was designed

UNIVERSITY of the WESTERN CAPE

in such as way that it could be re-used to generate HA-tagged versions of existing constructs cloned into pGEX-6P-2.

The above findings lay the foundation for future structural and functional studies of the involvement of RBBP6 in regulation of the cancer-related proteins p53 and YB-1, which may have far-reaching consequences in the fight against cancer.

Declaration

UNIVERSITY *of the*
WESTERN CAPE

UNIVERSITY of the
WESTERN CAPE

By submitting this thesis, I declare that the entirety of the work contained therein is my own original work, that I am the sole author thereof (save to the extent explicitly otherwise stated), that reproduction and publication thereof by the University of the Western Cape will not infringe any third party rights and that I have not previously in its entirety or in part submitted it for obtaining any qualification.

December 2015

Acknowledgements

I would like to thank Prof. David Pugh for his guidance and support throughout my undertaking of this degree. Thank you to Dr. Andrew Faro for every piece of advice and guidance through every experiment and with the help in improving my problem solving skills. Then I would like to thank my entire lab for their assistance and advice. To my family and friends for the support over the years and for being with me every step of the way, it is much appreciated. I would like to make special reference to my girlfriend Jasmine Fembers for bearing with my sulking over results for the last couple of years.

Finally I would like to thank the National Research Foundation for the funding of this research project.

UNIVERSITY of the
WESTERN CAPE

List of Abbreviations

Abbreviation	*Full Name*
Amp	Ampicillin
APS	Ammonium persulphate
bp	Base pairs
BSA	Bovine serum albumin
CV	Column volumes
DNA	Deoxyribonucleic acid
dNTPs	2'-deoxynucleoside 5'-triphosphate
DWNN	Domain with no name
E1	Ubiquitin activating enzyme
E2	Ubiquitin conjugating enzyme
E3	Ubiquitin ligase
GST	glutathione S-transferase
HA	Hemagglutinin
Hip2	Huntington interacting protein 2
His	Histidine
Ip	Immune-precipitation
IPTG	Isopropyl-1-thio -D-galactoside
kDa	Kilo Dalton
LB	Luria Bertani
MDM2	Mouse double minute
MDR1	Multidrug resistance gene 1
Mpe1	Mutant PCFII extrogenic suppressor 1
MWCO	Molecular weight cut-off
N-terminus	Amino terminus
P2P-R	Proliferation potential protein-related
p53	Protein 53
PACT	p53-associated cellular protein-testes derived
PAGE	Polyacrylamide gel electrophoresis
PBS	Phosphate buffer saline
PCR	Polymerase chain reaction
PVDF	Polyvinyldifluoride

UNIVERSITY of the
WESTERN CAPE

RBBP6	Retinoblastoma binding protein 6
RBQ-1	Retinoblastoma-binding Q-protein 1
RING	Really interesting new gene
SDS	Sodium dodecyl sulphate
TBE	Tris Borate EDTA
TEMED	*N,N,N',N'*-tetramethylethylenediamine
UPS	Ubiquitin proteasome system
YB-1	Y-box binding protein 1

UNIVERSITY of the
WESTERN CAPE

List of Figures

Figure title	*Page number*
Figure 1: The domain structure of the RBBP6 family	*3*
Figure 2: The Zn ion coordination of the RING finger domain	5
Figure 3: The domain organization of YB-1	9
Figure 4: Schematic of the protein binding sites on YB-1	10
Figure 5: The proposed mechanism for YB-1 nuclear translocation	13
Figure 6: The p53/Mdm2 negative feedback loop	15
Figure 7: The Ubiquitin Proteasome System	16
Figure 8: The domain organisation of UbcH1	18
Figure 3.1: Construct map of pGEX-6p-2-HA-DWNN-GG	29
Figure 3.2: DNA sequence and amino acid translation of HA-DWNN-GG	30
Figure 3.3: Successful cloning of HA-DWNN-GG into pGEX-p6-2	31
Figure 3.4.: Purification of HA-DWNN-GG	33
Figure 3.5: Endogenous RBBP6 is able to co-precipitate endogenous YB-1	34
Figure 3.6.: Purification of the RBBP6 RING finger domain	36
Figure 3.7: Purification of ^{15}N-labelled RBBP6 RING finger domain	37
Figure 3.8: Construct map of pGEX-6p-2-HA-YB-$1_{220-324}$ -6xHis	38
Figure 3.9: DNA sequence and mRNA translation of YB-$1_{220-324}$	39
Figure 3.10: Cloning of wild type YB-$1_{220-324}$ into pGEX-HA-DWNN-GG	40
Figure 3.11: Sub-cloning of YB-$1_{220-324}$-RRRR mutant into pGEX-HA-DWNN-GG	41
Figure 3.12: Sub-cloning of YB-$1_{220-324}$-KRRR mutant into pGEX-HA-DWNN-GG	42

UNIVERSITY of the

Figure 3.13: Purification of HA-YB-$1_{220-324}$-6xHis fusion protein	43
Figure 3.14: Expression and purification of GST-YB-$1_{220-324}$ mutants -RRRR and -KRRR	44
Figure 3.15: Immunodetection of HA-YB-$1_{220-324}$-6xHis WT (KKKK) precipitated by GST-RBBP6 RING	45
Figure 3.16: Immunodetection of RBBP6 RING precipitated by GST-HA-YB-$1_{220-324}$-6xHis	46
Figure 3.17: Immunodetection of RBBP6 RING precipitated by GST-HA-YB-$1_{220-324}$-6xHis-KKKK and -RRRR	48
Figure 3.18: Expression and purification of UbcH1	50
Figure 3.19: Immunodetection of recombinant RBBP6 RING precipitated by GST-UbcH1	51
Figure 3.20: ^{15}N-HSQC spectra of the RBBP6 RING finger with and without unlabelled UbcH1	53
Figure 3.21: Immunodetection of endogenous MDM2 precipitated by GST-R3	56
Figure 3.22: Immunodetection of RBBP6-RING precipitated by GST-MDM2	56
Figure 3.23: Alignment of the experimental sequence read of HA-DWNN-GG (Sbjct) with the expected sequence (Query)	68
Figure 3.24: Sequence alignment of wild type YB-$1_{220-324}$	68
Figure 3.25: Sequence alignment of wild type YB-$1_{220-324}$ (top) against RRRR (bottom).	69
Figure 3.26: Sequence alignment of wild type YB-$1_{220-324}$ (top) against KRRR (bottom).	69

UNIVERSITY of the WESTERN CAPE

List of tables

Table title	*Page numbers*
Table B1: List of chemicals, kits and suppliers	70
Table B2: List of general stock solutions and buffers	71
Table 3.1: Oligonucleotides used to amplify the HA-DWNN-GG fragment.	30
Table 3.2: Oligonucleotides used to amplify the YB-$1_{220\text{-}324}$ fragment	39

Table of content

Abstract ... ii
Declaration ... iv
Acknowledgements ... v
List of Abbreviations ... vi
List of Figures ... viii
List of tables ... x
Table of content ... xi
Chapter 1 ... 1
Literature review ... 1
1.1. Introduction ... 1
1.2. Retinoblastoma Binding Protein 6 (RBBP6) ... 2
1.2.1. Structure of RBBP6 ... 2
1.2.2. Role of RBBP6 in mRNA processing ... 4
1.2.3. Role of RBBP6 as an ubiquitin-ligase (E3) ... 5
1.2.4. Role of RBBP6 in tumourigenesis ... 7
1.2.5. Unpublished data relating to the ubiquitination activity of RBBP6 ... 7
1.3. Y-Box Binding Protein 1 (YB-1) ... 8
1.3.1. Structure of YB-1 ... 8
1.3.2. Functions and regulation of YB-1 ... 10
1.4. Murine Double Minute 2 (MDM2) ... 14
1.5. The ubiqutin-conjugating enzyme UbcH1 ... 15
1.5.1. Ubiquitin Proteasome System (UPS) ... 15
1.5.2. Structure and function of UbcH1 ... 17
1.6. Aims and Objectives ... 18
Chapter 2 ... 20
Methods and Materials ... 20
2.1. Antibodies used ... 20
2.2. Bacterial cultures ... 20
2.2.1. Bacterial strains used ... 20
2.2.2. Antibiotic selection ... 21
2.2.3. Bacterial transformation ... 21
2.3. DNA cloning ... 21

UNIVERSITY of the
WESTERN CAPE

2.3.1. Isolation of plasmid DNA 21
2.3.2. PCR amplification of gene fragments 21
2.3.3. Restriction enzyme digestion of DNA 22
2.3.4. Ligation of DNA 22
2.3.5. Agarose gel electrophoresis of DNA 22
2.4. Recombinant protein expression 23
2.4.1. Protein expression in rich media 23
2.4.2. Protein expression in labelled media 23
2.5. Protein purification 23
2.5.1. Protein extraction 23
2.5.2. Affinity purification 23
2.5.3. Cleavage of recombinant protein 24
2.5.4. Size exclusion chromatography 24
2.5.5. HisTRAP affinity chromatography 24
2.6. SDS-PAGE gel electrophoresis 24
2.7. Immuno-detection of proteins 25
2.8. Affinity pull-down assays 25
2.9. Co-immunoprecipitation 26
Chapter 3 27
Investigation of interactions involved in the regulation of YB-1 by RBBP6 27
3.1. Introduction 27
3.2. Generation of a GST-HA-DWNN-GG expression construct 29
3.2.1. Cloning of HA-DWNN-GG into pGEX-6P-2 29
3.2.2. Expression and purification of HA-DWNN-GG 32
3.3. RBBP6 interacts with YB-1 in mammalian cell lysates 33
3.3.1. Co-immunoprecipitation of YB-1 by RBBP6 33
3.4. The RING finger of RBBP6 interacts with the CTD of YB-1 in vitro 35
3.4.1. Expression and purification of the RING finger domain from RBBP6 35
3.4.2. Cloning of wild type YB-1$_{220-324}$ for expression in bacteria 38
3.4.3. Cloning of YB-1$_{220-324}$-RRRR and -RKKK mutants 41
3.4.4. Expression and purification of wild type YB-1$_{220-324}$ and the RRRR and RKKK mutants 43
3.4.5. The RING finger of RBBP6 and the YB-1$_{220-324}$ fragment co-precipitate each other in GST pull-down assays 45
3.5. UbcH1 interacts with the RING finger of RBBP6 in vitro 49

UNIVERSITY of the
WESTERN CAPE

3.5.1. Expression and purification of UbcH1 49
3.5.2. UbcH1 binds to the RING finger domain of RBBP6 in vitro 51
3.5.3. Chemical shift perturbation of ^{15}N-labelled RBBP6-RING finger by un-labelled UbcH1 52
3.6. MDM2 interacts directly with the RING finger domain of RBBP6 in vitro 55
3.6.1. Co-precipitation of endogenous MDM2 by the R3 fragment of RBBP6 55
3.6.2. Co-precipitation of recombinant RBBP6-RING by recombinant MDM2 in vitro 56
Chapter 4 58
Discussion and conclusions 58
References 61
Appendix 68
B1. List of chemicals, kits and suppliers 70
B2 List of general stock solutions and buffers 71

UNIVERSITY of the
WESTERN CAPE

Chapter 1

Literature review

1.1. Introduction

Retinoblastoma Binding Protein 6 (RBBP6), also known as p53 Associated Cellular Protein Testis-derived (PACT) or Retinoblastoma Binding Q protein 1 (RBQ-1), is a RING finger-containing protein that forms part of the 3'-end polyadenylation complex in humans and plays a role in regulation of 3'-end processing in yeast and humans (Lee and Moore. 2014; Di Giammartino *et al*., 2014). It also acts as a negative regulator of p53 by activating the poly-ubiquitination activity of Murine Double Minute 2 (MDM2) (Li *et al*., 2007).

In 2008 Chibi and co-workers showed using a yeast 2-hybrid screen that the RING finger domain of RBBP6 interacts directly with the C-terminal domain of transcription factor Y-Box Binding Protein 1 (YB-1) and with the transcriptional repressor zBTB38 (Chibi *et al.,* 2008). RBBP6 has subsequently been shown to catalyse the ubiquitination and degradation of both YB-1 and zBTB38 *in vitro* and *in vivo*. Knockdown of RBBP6 leads to accumulation of zBTB38, leading to sensitivity to DNA damage (Miotto *et al*., 2014). The functional consequences of suppression of YB-1 by RBBP6 are still being established.

YB-1 is a multifunctional, pro-cancerous transcription factor whose transcriptional activity is strongly correlated with aggressive tumourigenesis, metastasis and chemotherapeutic resistance as well as poor prognosis in a number of cancers, in particular breast cancer (Basaki *et al*., 2010). Over-expression of YB-1 is associated with drug resistant tumours by promoting transcriptional activation of ATP-binding cassette transporter P-glycoprotein, which is encoded by the drug resistant gene Multi Drug Resistant gene 1 (MDR1)(Chattopadhyay *et al*., 2008).

The yeast 2-hybrid screen utilised by Chibi and co-workers localised the interaction between RBBP6 and YB-1 to the extreme C-terminus of YB-1, residues 262-324. Previous attempts to express the above region of YB-1 in bacteria failed, presumably because it was too small to form a structured protein. The first aim of this work was therefore to identify and express a larger region of the C-

UNIVERSITY of the WESTERN CAPE

terminus of YB-1 suitable for *in vitro* interaction studies with the RING finger of RBBP6, with the eventual aim of carrying out NMR-based interaction studies.

Fully *in vitro* ubiquitination studies carried out in our laboratory suggest that RBBP6 is able to catalyse poly-ubiquitination of YB-1 in conjunction with the ubiquitin-conjugating enzyme UbcH1 (A Faro and D.J.R. Pugh, manuscript in preparation). If this is true we would expect to find an interaction between RBBP6 and UbcH1 *in vitro*. A second aim of this work was therefore to over-express both UbcH1 and the RING finger from RBBP6 in bacteria and test their interaction using immunoprecipitation and NMR-based interaction studies.

The work of Li and co-workers cited above suggests that RBBP6 cooperates with MDM2 in poly-ubiquitinating p53, leading them to propose that RBBP6 acts as a molecular scaffold, bringing MDM2 and p53 together on the p53-binding domain identified in the C-terminus of RBBP6 (Simons *et al.*, 1997, Li *et al.,* 2007). An alternative explanation, suggested by our own unpublished data, is that RBBP6 and MDM2 interact through their respective RING finger domains, in a manner similar to that by which MDM2 and MDMX interact (Wang *at el*., 2011). In order to test this hypothesis, a third aim of the thesis was to express the RING finger domains of both proteins in bacteria and investigate their interaction *in vitro* using immunoprecipitation and NMR.

UNIVERSITY of the
WESTERN CAPE

The investigations described in the following chapters are aimed at furthering our understanding of the role played by RBBP6 in regulating proteins involved in cancer, including p53, MDM2, YB-1 and UbcH1, primarily by understanding the interactions between them. The hope is that by understanding more about these interactions we may be able to design ways of modulating them that may, eventually, lead to the development of novel anti-cancer therapies. At the very least it would enable us to design non-interacting mutants of the proteins that can serve as negative controls in functional assays.

1.2. Retinoblastoma Binding Protein 6 (RBBP6)

1.2.1. Structure of RBBP6

Orthologues of human RBBP6 are found in all eukaryotic, but not in prokaryotic, genomes, in many cases at single copy number. Analysis of the amino acid sequences reveals the presence of domains previously identified in other proteins, as shown in Figure 1. All eukaryotes express an isoform containing the DWNN domain, a zinc knuckle and a RING finger domain, reading from the N-terminus. Zinc knuckles are found in many other proteins, in many of which they play a role in nucleic acid binding (Krishna *et al*., 2003). RING fingers are found in many E3 ubiquitin ligases, where

their function is to bind to the ubiquitin-conjugated E2, promoting transfer of ubiquitin to the substrate. The DWNN domain is found only in members of the RBBP6 protein family, always at the N-terminus, and has a structure similar to that of ubiquitin (Pugh *et al*., 2006). Lower eukaryotes such as fungi and plants contain only these three domains whereas higher eukaryotes contain additional domains, including regions resembling an SR domain, a proline-rich domain and regions reported to promote interaction with p53, pRb and nuclear localisation (Pugh *et al*., 2006; Simons *et al*., 1997; Witte and Scott 1997).

The single human RBBP6 gene gives rise to a number of different transcripts (and thereby protein isoforms) through a combination of alternative splicing and alternative promoters (Pugh *et al*., 2006; Pretorius *et al*., 2013). Isoform 1 consists of the full length protein of 1792 amino acid residues; Isoforms 2 and 4 represent alternatively-spliced fragments of 1752 and 952 residues respectively (Pugh *et al.,* 2006). Isoform 3 is a 13 kDa protein that is expressed from an alternative promoter; of its 118 residues the first 100 are the same as isoform 1 and contain primarily the DWNN domain. The last 18 residues of isoform 3 are unique to this isoform. The function of isoform 3 remains unclear but in 2011 Mbita and co-workers reported it is regulated independently of isoform 1 and is deregulated in various cancers, possibly playing a role in cell cycle regulation (Mbita *et al.,* 2011). Di Giammartino and co-workers have since reported that isoform 3 regulates mRNA splicing by competing with the DWNN domain on full length RBBP6 (Di Giammartino *et al.,* 2014).

UNIVERSITY of the
WESTERN CAPE

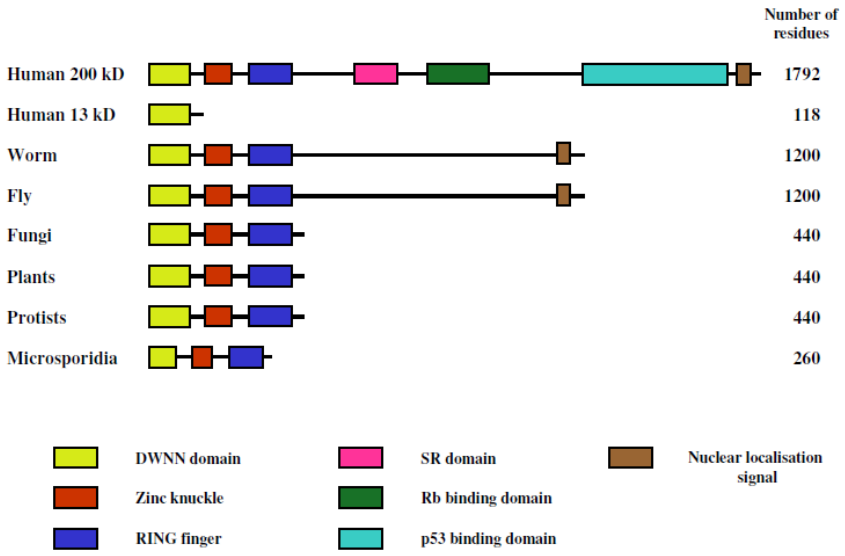

Figure 1: The domain structure of the RBBP6 family. All eukaryotic genomes contain a minimal isoform containing the DWNN, zinc knuckle and the RING finger domains. In this thesis the fragment of human RBBP6 consisting of these three domains is referred to as R3. Higher eukaryotes include C-terminal extensions as well as an independently-expressed fragment consisting almost exclusively of the DWNN domain. RBBP6 has not been found in prokaryotes, which may be attributed to the role of RBBP6 in RNA processing. Figure adapted from Pugh *et al,*. (2006).

1.2.2. Role of RBBP6 in mRNA processing

The *Saccharomyces cerevisiae* orthologue of human RBBP6, which is known as Mutant PCFII Extrogenic suppressor 1 (Mpe1), is a 440 residue protein containing the DWNN domain, the zinc knuckle and the RING finger domain (Vo *et al*., 2001). Vo and colleagues identified Mpe1 to be an integral component of the Cleavage and Polyadenylation Factor (CPF). They demonstrated that Mpe1 is essential for mRNA processing by inactivating it with an antibody specific to the protein which resulted in defective 3'-end mRNA processing in yeast. They concluded that Mpe1 is essential for specific cleavage and polyadenylation of pre-mRNA, by promoting the complexing of Cleavage Factor One (CF1) complex with the CPF. Later Shi and co-workers showed that RBBP6 is a member of the human 3'-end processing complex by isolating and purifying a functional human pre-mRNA processing complex which they then subjected to mass spectrometry to identify the component proteins (Shi *et al.,* 2009). More recently Lee and Moore have directly confirmed Mpe1 role in complexing CF1 with CPF, and shown that the DWNN domain is essential for this function (Lee and Moore 2014). These findings are in good agreement with the demonstration by Di Giammartino and co-workers using nuclear extracts of human cells that knockdown of RBBP6 abolished 3'-end cleavage but not poly-adenylation (Di Giammartina *et al*., 2014). 3'-end cleavage was restored following addition of a recombinant fragment of RBBP6 comprising the DWNN - zinc knuckle - RING finger, which in this thesis is referred to as R3. They concluded that RBBP6 is a regulator of 3'-end processing.

UNIVERSITY of the
WESTERN CAPE

Consistent with a role in mRNA processing, human RBBP6 contains a serine/arginine (SR) rich region similar to those found in many pre-mRNA splicing factors (Witte *et al*., 1997). Furthermore RBBP6 has been reported to localize to nuclear speckles, to which elements of the splicing machinery are known to localize (Mbita *et al*., 2012). Witte and Scott showed that a truncated form of RBBP6, which they named Proliferation Potential-Related protein (P2P-R), associates closely with heterogeneous nuclear ribonucleoproteins (hnRNPs), which are involved in RNA processing, and can be purified using a protocol specific for hnRNPs (Witte and Scott, 1997). They also showed that P2P-R co-precipitates with SmB, one of the core splicing proteins. Another of the core splicing proteins, SmG, was shown by Chibi and co-workers to interact with the N-terminal DWNN domain of human RBBP6 in a yeast 2-hybrid screen (Chibi *et al.,* 2008).

1.2.3. Role of RBBP6 as an ubiquitin-ligase (E3)

In addition to its role in mRNA processing, RBBP6 is known to play a role in ubiquitination through its RING finger domain. As described above, RING fingers are found in many E3 ubiquitin-ligase enzymes where their function is to recruit the ubiquitin-conjugated E2 so that the ubiquitin can be transferred to the substrate, which is recruit by the substrate-binding domain also forming part of the E3 (Kim *et al*., 2007).

The structure of the RING finger domain from human RBBP6 was solved by Nuclear Magnetic Resonance Spectroscopy (NMR) in 2011 and found to coordinate 2 zinc ions by 8 cysteine residues in a C4C4 configuration (Kappo *et al*., 2011). The topology is identical to that of the C3HC4 RING illustrated schematically in Figure 2, although in RBBP6 the histidine is replaced by a cysteine. Similar to many other RING finger domains, the RBBP6 RING was found to form a homodimer in solution and the dimerization interface was found to be identical to that found in the MDM2 homodimer and the BARD/BRCA1 and MDM2/MDMX heterodimers (Brzovic *et al.,* 2002 and Linke *et al.,* 2008). In many cases dimerization has been shown to be essential for E3 ligase activity (Plechanovova *et al*., 2012).

UNIVERSITY of the
WESTERN CAPE

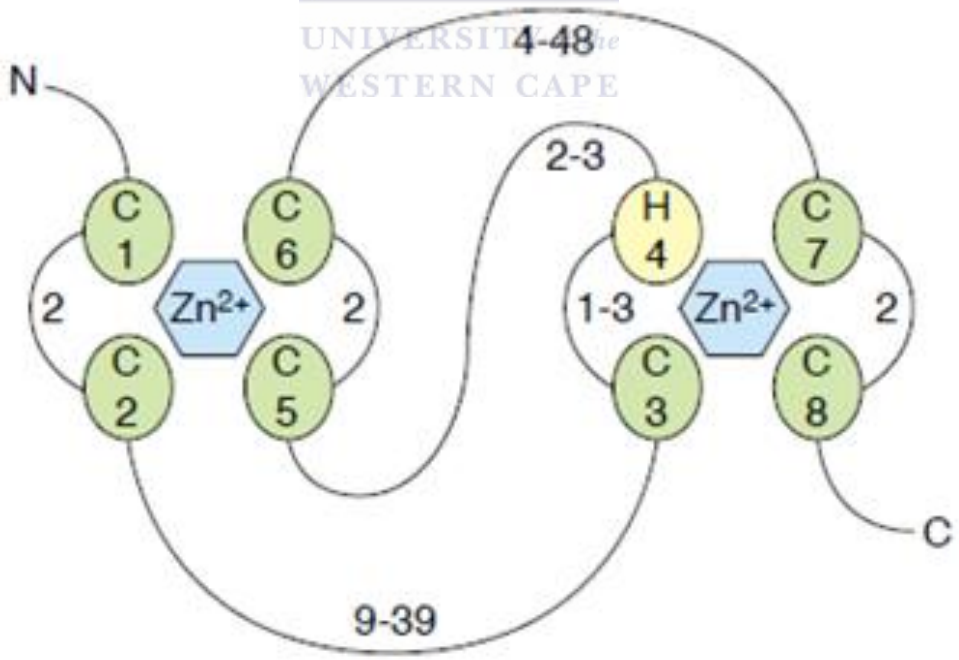

Figure 2: The Zn ion coordination of the RING finger domain. The metal-ligand pairs 1 and 3 coordinate one zinc ion, while pairs 2 and 4 coordinate the second one in a 'cross-brace' arrangement. This schematic illustrates a C3HC4 RING; in RBBP6 the histidine ligand is replaced by cysteine, making it a C4C4 RING. Figure taken from Kosarev *et al* 2002.

Using RBBP6-knockout mice, Li and co-workers showed that RBBP6 acts as a suppressor of the tumour suppressor p53 during development. The tumour suppressors p53 and pRb play essential roles in regulating cell cycle progression and apoptosis, in response to different stresses like DNA damage and abnormal proliferative signals (Weinberg 2006). These proteins must be tightly controlled for normal cell growth and the prevention of tumour development (Weinberg 2006). This is the function of MDM2, which mediates the ubiquitination of p53 and its degradation in the 26S proteasome (Yang *et al*., 2004). Li and co-workers showed that knockout of RBBP6 leads to over-expression of p53 and widespread ectopic apoptosis, resulting in lethality by embryonic day 7.5. In a p53 negative background the embryos survived longer (until day 11.5), indicating the presence of an interaction between p53 and RBBP6 at the genetic level. They went on to demonstrate that at the protein level RBBP6 interacts directly with MDM2. They concluded from this that RBBP6 is required for poly-ubiquitination of p53 by MDM2, making it an essential part of the MDM2/p53 regulatory system. Their results suggest that suppression of p53 by RBBP6 is definitely important during development, when p53 levels need to be kept low to avoid inappropriate apoptosis and when the role of p53 in tumour suppression is likely to be less important than in the mature organism. These finding are consistent with those of Mather and colleagues who earlier concluded that RBBP6 is essential for embryonic development in *Drosophila melanogaster* (Mather *et al*., 2005).

The work of Li and co-workers suggests that RBBP6 facilitates ubiquitination of p53, but does not itself take part in ubiquitination. They proposed that RBBP6 may play the role of a scaffolding protein, involving the binding of p53 to a previously-identified site on the C-terminus of RBBP6, thereby bringing MDM2 into close proximity with p53 (Simons *et al.,* 1997). However it is also possible that RBBP6 plays a role similar to that played by MDMX, which activates the poly-ubiquitination activity of MDM2 by forming a heterodimer with MDM2 through their respective RING finger domains (Wang *et al*., 2011).

In addition to p53, other proteins have been identified as possible substrates for ubiquitination by RBBP6. These include Y-Box Binding Protein 1 (YB-1), which is described in detail below, and the transcriptional repressor zBTB38. An interaction between RBBP6 and zBTB38 was first identified by Chibi and co-workers (Chibi *et al*., 2008) using a yeast 2-hybrid screen and subsequently Miotto and co-workers reported that RBBP6 catalyses ubiquitination and degradation of zBTB38, leading to up-regulation of the replication factor MCM10 (Miotto *et al*., 2014). They concluded that RBBP6 is a causal factor in cancer by stabilizing the replication factor MCM10 which promotes genomic stability.

1.2.4. Role of RBBP6 in tumourigenesis

Due to the extensive involvement of YB-1 in a host of different cancers, regulation of YB-1 by RBBP6 implicates RBBP6 in regulation many of these cancers. Consistent with this, there is direct evidence for the involvement of RBBP6 in a number of cancers.

Oesophageal cancer

Yoshitake and co-workers reported that RBBP6 is over-expressed in oesophageal cancer cells but not in normal oesophageal epithelial cells (Yoshitake *et al*., 2004). They went on to generate antibodies against RBBP6 with which they were able to decrease the size of tumours. They concluded that RBBP6 may be an ideal target for immunotherapy for patients with oesophageal cancer.

Lung cancer

Knockdown of RBBP6 with siRNA in lung cancer cells resulted in an increase in Bax/Bcl2 mRNA which suggests that RBBP6 has an anti-apoptotic effect in lung cancer cells (Motadi *et al.,* 2010). This may be due to RBBP6 having a negative effect on p53 which results in enhanced cell proliferation and inhibition of apoptosis.

UNIVERSITY of the
WESTERN CAPE

Colon cancer

Chen and co-workers reported in 2013 that over-expression of RBBP6 is predictive of poor prognosis in colon cancer. They also reported that when RBBP6 over-expression is combined with mutant p53 patient prognosis worsens dramatically over a short period (Chen *et al*., 2013).

Gastric cancer

Morisaki and co-workers showed using mass spectrometry and RT-PCR that RBBP6 is up-regulated in gastric cancer cells but not in normal cells. They identified RBBP6 as a promising biomarker and therapeutic target for gastric cancer (Marisaki *et al*., 2014).

1.2.5. Unpublished data relating to the ubiquitination activity of RBBP6

Using fully *in vitro* ubiquitination assays, members of our laboratory have shown that the R3 fragment of human RBBP6 (residues 1-335) is able to poly-ubiquitinate p53 with the assistance of MDM2, leading to degradation of p53 in the proteasome (LS Jooste, A. Faro and D.J.R. Pugh, manuscript in preparation). Acting independently R3 and MDM2 were able to mono- or multiply

mono-ubiquitinate p53, but degradation in the proteasome only happened in the presence of both R3 and MDM2. This is consistent with the findings of Wang and colleagues (Wang *et al.,* 2011) that MDM2 is unable to poly-ubiquitinate on its own, but must be activated by MDMX. It is also consistent with the findings of Li and co-workers (Li *et al.*, 2007) that RBBP6 is unable to catalyse degradation of p53 *in vivo*. However our finding that R3 is able to mono-ubiquitinate p53 is novel. Furthermore, the fact that R3 is able to activate the poly-ubiquitination activity of p53 *in vitro* calls into question the scaffold model of RBBP6 activity, because R3 is a far smaller protein than RBBP6 and does not contain the reported p53-binding domain located near the C-terminus of RBBP6.

Results from our laboratory have also shown that the R3 fragment of RBBP6 is able catalyse poly-ubiquitination of Y-Box Binding Protein-1 (YB-1), with the assistance of the ubiquitin-conjugating enzyme UbcH1 (A. Faro and D.J.R. Pugh, manuscript in preparation). The importance of YB-1 is discussed in more depth in the following section.

1.3. Y-Box Binding Protein 1 (YB-1)

YB-1 is a DNA and RNA binding protein that is involved in a number of processes including mRNA packaging, regulation of mRNA stability, pre-mRNA transcription and splicing, translation and DNA repair (Dmitry *et al*., 2013). It belongs to the Y-Box Binding family of proteins and was first discovered for its ability to bind the inverted Y-box motif (CCAAT) in the promoter of major histocompatibility complex class II genes (Didier *et al*., 1988). Y-Box Binding proteins are divided into 3 subfamilies: the first subfamily, YB-1, is specific to somatic cells, and includes human YB-1, Chicken CHK-YB-1, rabbit p50, mouse MSY-1, bovine EFI-A and FRGY from *Xenopus leavis*. The second subfamily, YB-2, is specific to germ cells and includes mouse MYS-2 and the human proteins dbpC and contrin. The third subfamily, YB-3, contains proteins that are synthesized only during embryonic development. Two isoforms of YB-3 mRNA, a short and a long one, are produced by alternative spicing of pre-mRNA. Proteins in this subfamily include dbpA protein, mouse MSY-3, and YB-3 from *X. leavis* (Eliseeva *et al.,* 2011).

UNIVERSITY of the
WESTERN CAPE

1.3.1. Structure of YB-1

Despite migrating on SDS-PAGE at an apparent molecular weight of 50 kDa, which accounts for the alternative name p50, YB-1 has a molecular weight of only 36 kDa. It is made up of three domains: an N-terminal alanine/proline rich domain (A/P domain), which has no regular secondary structure and appears to be intrinsically disordered (Dmitry *et al*., 2013); a cold shock domain (CSD), which has a five stranded β-barrel structure similar to that of bacterial CSD and consensus sequences RNP-1

(K/N-G-F/Y-G-F-I/V) and RNP-2 (V-F-V-H-F) that mediate interaction with nucleic acids (Kloks *et al*., 2002); and a C-terminal domain (CTD) which contains alternating clusters of positively and negatively charged amino acids (Fig 3 A) (Dmitry *et al*., 2013). This domain also appears to be intrinsically disordered with an irregular secondary structure. The state of folding of these three domains is clearly illustrated by the PONDR VL_XT server (www.pondr.com), which predicts the A/P domain and the CTD to be unfolded (Fig 3 B) (Eliseeva *et al*., 2011).

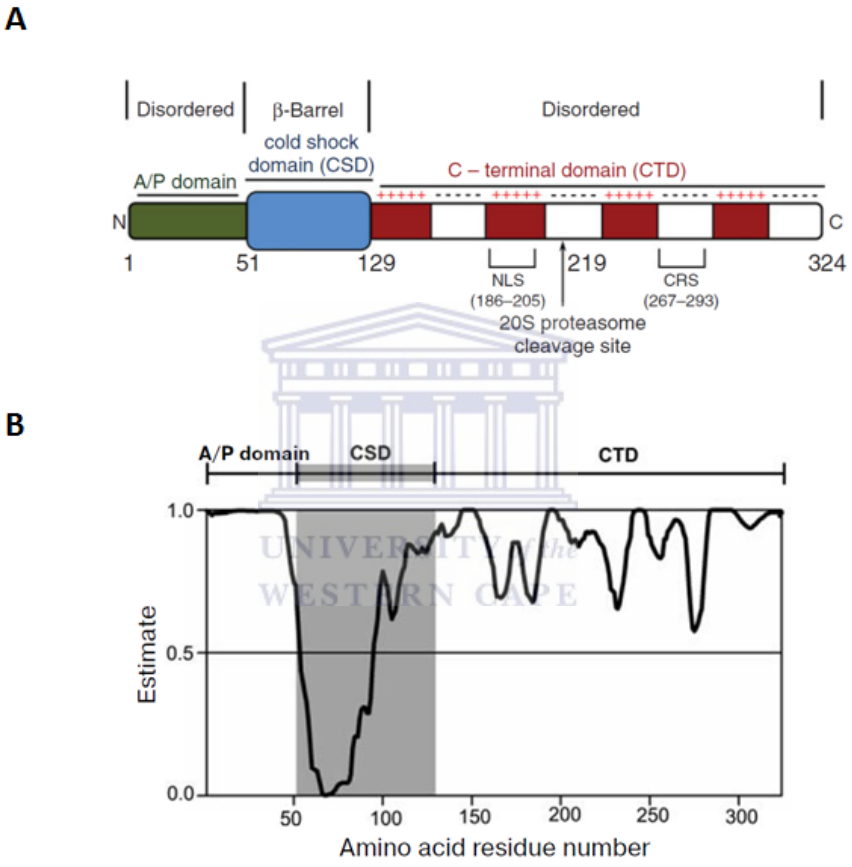

Figure 3: The domain organization of YB-1. (A) YB-1 is a 324 amino acid residue protein composed of three domains: the disordered A/P domain (residues 1-50), the β-barrel shaped CSD (residues 51-128) and the disordered CTD with clusters of positively and negatively charged amino acids (residues 129-324). Figure taken from Dmitry *et al.*(2013). (B) The A/P domain and CTD of YB-1 appear to be disordered based on the PONDR VL_XT (www.pondr.com) algorithm. Values ≥0.5 correspond to disorder. On the other hand the CSD appears well folded. Figure taken from Eliseeva *et al.*(2011).

It is also well known that many disordered proteins only adopt a fixed tertiary structure upon binding to a specific ligand, as is the case with p53 (Uversky and Dunker. 2010). Thus the structure of YB-1 may vary depending on the type of ligand (DNA, RNA or its numerous protein binding partners) and region of interaction. YB-1 has the ability to form homo-multimeric complexes up to 800 or 1000 kDa (Evdokimova *et al.,* 1995); this may be due to the formation of salt-bridges between positively charged arginines and negatively charges aspartic and glutamic acids, which are abundant in the

CTD. Another contributor to the oligemeric properties of YB-1 is the formation of hydrogen bonds between the guanidine groups of arginine and aromatic groups of phenylalanine and tyrosine which are also abundant in YB-1.

All three domains of YB-1 are involved in protein-protein interactions as well as nucleic acid binding (Fig 4). The A/P domain contains binding sites for p53, cyclin D1 and the splicing factor SRp30c. The CSD contains binding sites for Akt kinase and FBX33 (Sutherland *et al*., 2005; Luts *et al*., 2006). The CTD contains the majority of the protein binding sites, including sites for hnRNP K, hnRNP D, RBBP6, p53, TATA-binding protein among others, as shown in Figure 4 (Eliseeva *et al*., 2011). Of particular interest in Figure 4 is the number of tumour suppressor proteins that interact with YB-1, which again highlights its importance in tumourigenesis.

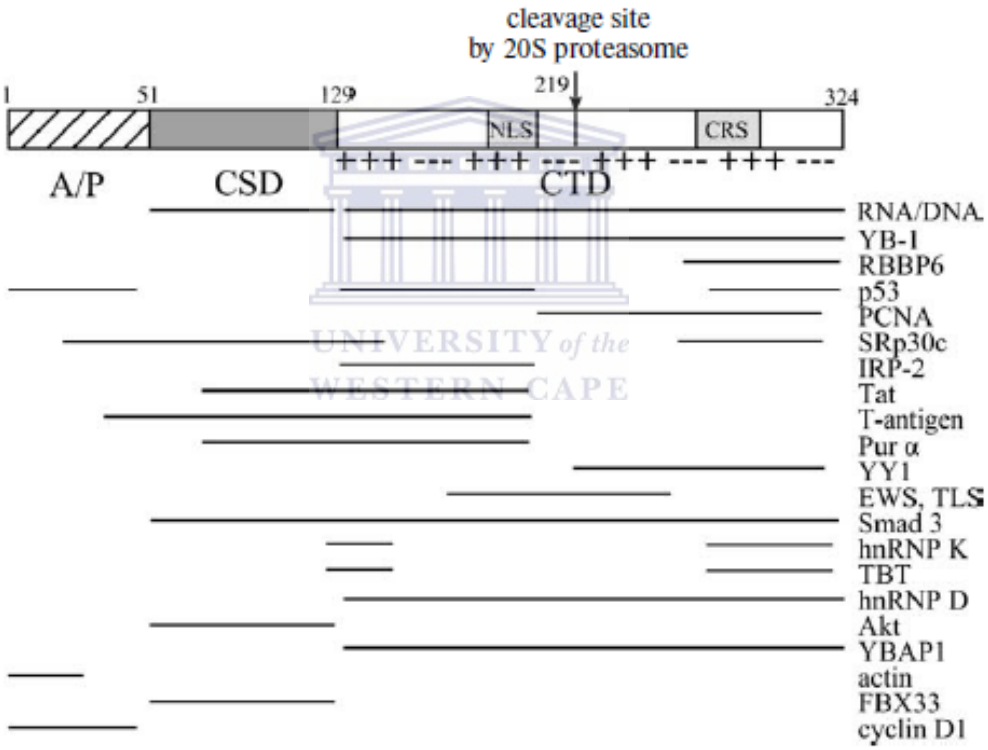

Figure 4: Schematic of the protein binding sites on YB-1. Most of the interactions involve the CTD due to the irregular and unstructured properties of this domain. Figure taken from Eliseeva *et al.*(2011).

1.3.2. Functions and regulation of YB-1

When YB-1 is localized to the nucleus its functions involve transcription, DNA repair and pre-mRNA splicing. YB-1 is a DNA binding protein that was initially identified bound to the promoters of the major histocompatibility complex II gene HLA-DRα, as well as the gene encoding the EGF receptor enhancer (Didier *et al*., 1988; Sakura *et al.,* 1988). Binding of YB-1 to these promoter regions was

thought to be dependent on the so-called Y-box sequence (5'-CTGATTGGC/TC/TAA-3'). However YB-1 has since been found to regulate genes without the Y-box sequence in their promoters. YB-1 has been described as a nucleic acid chaperone which can melt double-stranded helices in the promoter region and bind specifically to pyrimidine-rich strands (Dmitry *et al*., 2013). This may explain why YB-1 prefers to bind single-stranded DNA sequences (Izumi *et al*., 2001).

Genes that are transcriptionally regulated by YB-1 include genes involved in cell division, apoptosis, immune response, multi-drug resistance and tumour growth. In the case of the MDR1 gene which encodes the multi-drug resistance protein P-glycoprotein it was originally concluded that transduction required binding of YB-1 to the Y-box sequence in the MDR1 promoter (Bargou *et al*., 1997). However it was later found that YB-1 binding to the promoter region of MDR1 is dependent on it complexing with APE1 protein and histone acetyltransferase p300 as it had a higher affinity for MDR1 when in complex with APE1 and p300. (Dmitry *et al*., 2013). In 2007 Kaszubiak and co-workers reported that YB-1 has no effect in MDR1 regulation as the knock down of YB-1 had no effect on P-glycoprotein or MDR1 mRNA levels or drug sensitivity (Kaszubiak *et at*., 2007). The involvement of YB-1 in MDR1 regulation is therefore still a contentious topic. On the other hand YB-1 knock-out cell lines were sensitive to hypoxia, cisplatin treatment and temperature (Uchiumi *et al*., 2006). These contradictory finding may be cell type-dependent. Taken together these findings establish YB-1 as an important regulator of genes involved in cell differentiation, proliferation and stress response.

UNIVERSITY of the
WESTERN CAPE

YB-1 has a dual function in cell proliferation; at lower concentrations it promotes proliferation whereas at higher concentrations it suppresses proliferation. This dual nature was identified when YB-1 expression was inhibited by siRNAs which resulted in an increase in cell doubling time and an enlarged proportion of cells in the G1-phase (Bergmann *et al*., 2005). On the other side the suppression of YB-1 resulted in a decrease in the amount of cyclin D1 and an increase in concentration of cell cycle inhibitors p21 and p16 (Evdokimova *et al*., 2009). The reason for these dual functions is still poorly understood but may also be cell type dependent.

Combined with its potent function as an activator of proliferation, YB-1 also protects cancer cells against apoptosis. It achieves this by binding to the tumour suppressor p53 and hampering p53-dependent transcription of pro-apoptotic genes APAF1, NOXA and BAX (Lee *et al*., 2008). Another manner in which YB-1 inhibits apoptosis is by suppressing the transcription of the Fas-receptor (Homer *et al*., 2005).

The role of YB-1 in stress response is generally dependant on its localisation, either in the nucleus or in the cytoplasm. It is generally found in the cytoplasm but translocates to the nucleus upon treatment with DNA damaging agents such as xenobiotics or UV irradiation (Dmitry *et al.,* 2013). Once localised to the nucleus YB-1 transduces expression of genes that reduce the negative effect of these stresses, including MDR1. The exact mechanism of YB-1 translocation has been a highly contentious issue. Initially YB-1 was believed to shuttle to the nuclease by complexing with p53 during genotoxic stress (Lasham *et al.,* 2003). This mechanism was further complicated by the findings of Homer and co-workers that functional p53 in required for YB-1 nuclear translocation and not simply shuttling (Homer *et al.,* 2005). Furthermore Homer *et al* (2005) reported that YB-1 selectively inhibits the ability of p53 to cause cell death, by preventing transactivation of pro-apoptotic genes. This YB-1 may be a potential negative regulator of the p53 tumor suppressor.

Another highly contested mechanism of YB-1 nuclear translocation involves cleavage of YB-1 at residue 220 by the 20S proteasome (Sorokin *et al*., 2005). In 2005 Sorokin and co-workers reported that the N-terminal fragment contains a nuclear localisation signal (residues 186-205) and the C-terminal fragment contains a cytoplasmic retention signal (residues 267-293). Cleavage at residue 220 releases the N-terminal fragment to translocate to the nuclease, leaving the C-terminal fragment in the cytoplasm. Taking all of these proposed mechanisms into account Braithwaite and co-workers proposed the scenario for YB-1 translocation shown in Fig 5: upon genotoxic stress YB-1 is cleaved by the proteasome at residue 220, possibly as a result of phosphorylation at Ser 102. Meanwhile p53 is also activated to induce expression of an unknown Protein X which binds to the N-terminal fragment of YB-1, facilitating translocation of YB-1 to the nucleus and promoting growth while inhibiting p53-mediated apoptosis (Braithwaite *et al.,*2006).

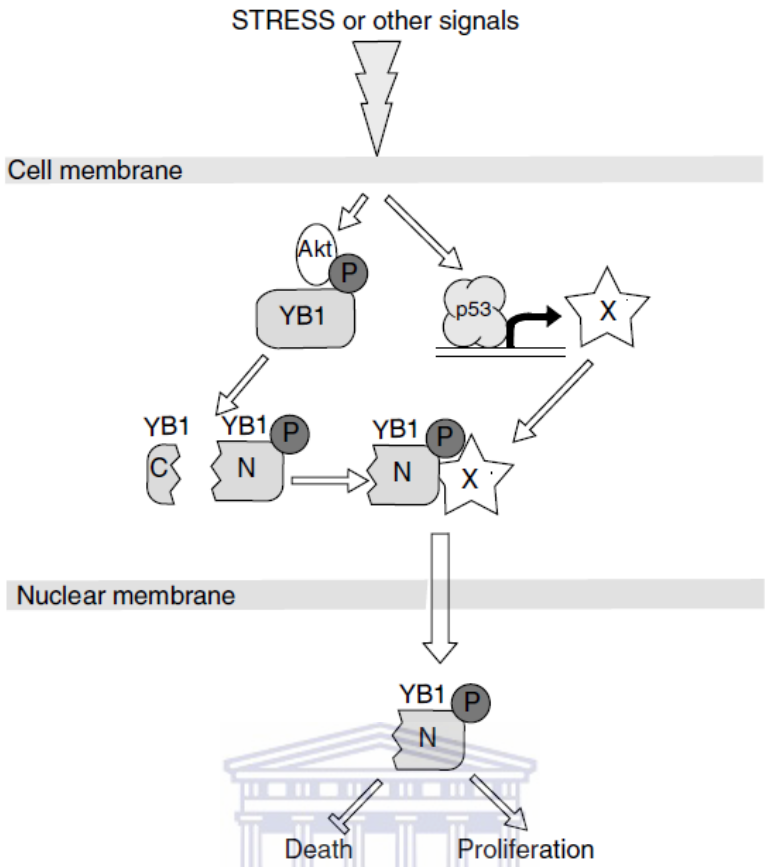

Figure 5: The proposed mechanism for YB-1 nuclear translocation. Following genotoxic stress YB-1 undergoes proteolysis following phosphorylation at serine 102. The same stress activates p53 to induce gene X expression which complexes with the N-terminal fragment of YB-1, shuttling it to the nucleus. Taken from Braithwaite *et al. (*2006)

UNIVERSITY of the
WESTERN CAPE

In subsequent years the mechanism for YB-1 has been further called into question by the findings of Cohen and co-workers, who maintain that cleavage of YB-1 does not take place at all and that the whole of YB-1 translocates to the nucleus following cells stress (Cohen *et al*., 2009). This proposal is supported by the findings of Woolley and co-workers that the findings of Sorokin and co-workers where influenced by antibody cross-reactivity (Woolley *et al*., 2011). However more recently van Rooyen and colleagues have reiterated that YB-1 undergoes proteolysis at residue 220, but that it is the C-terminus, rather than the N-terminus, that translocates to the nucleus (van Rooyen *et al.,* 2013). The true mechanism of YB-1 translocation and cleavage is therefore still a highly contentious issue that requires more investigation.

Transcription of YB-1 is triggered by the binding of transcription factors GATA1 and GATA2 to the GATA-motif, which is a specific sequence within the YB-1 promoter (Yamasaki *et al*., 2009). Transcription factors that bind to the Enhancer-box sequence within the YB-1 promoter include Twist or c-Myc and Max (Chen and Behringer. 1995; Uramoto *et al.,* 2002). YB-1 can also be ubiquitinated by RBBP6 and FBX33A, resulting in its complete degradation in the 26S proteasome

(Lutz *et al*., 2006; Chibi *et al.,* 2008). On the translational level YB-1 inhibits its own translation by binding to its own mRNA within both the 5' and 3' UTRs of YB-1 mRNA (Skabkina *et al.,* 2003). This self-inhibition of YB-1 translation is overcome by the binding of PABP within the YB-1 mRNA transcript, thereby displacing YB-1 (Skalweit *et al.,* 2003).

1.4. Murine Double Minute 2 (MDM2)

MDM2 is a RING finger-containing E3 ligase which is best known as the primary negative regulator of the p53 tumour suppressor protein. It was originally discovered as being amplified on double-minute chromosomes in transformed mouse fibroblasts (Fakharzadeh *et al*., 1991). MDM2 binds to p53 and ubiquitinates it, resulting in its degradation in the 26S proteasome. In turn, p53 induces the transcription of MDM2, leading to a negative feedback loop in which the two proteins suppress each other in the absence of genotoxic stress (Weinberg. 2006) (Fig 6).

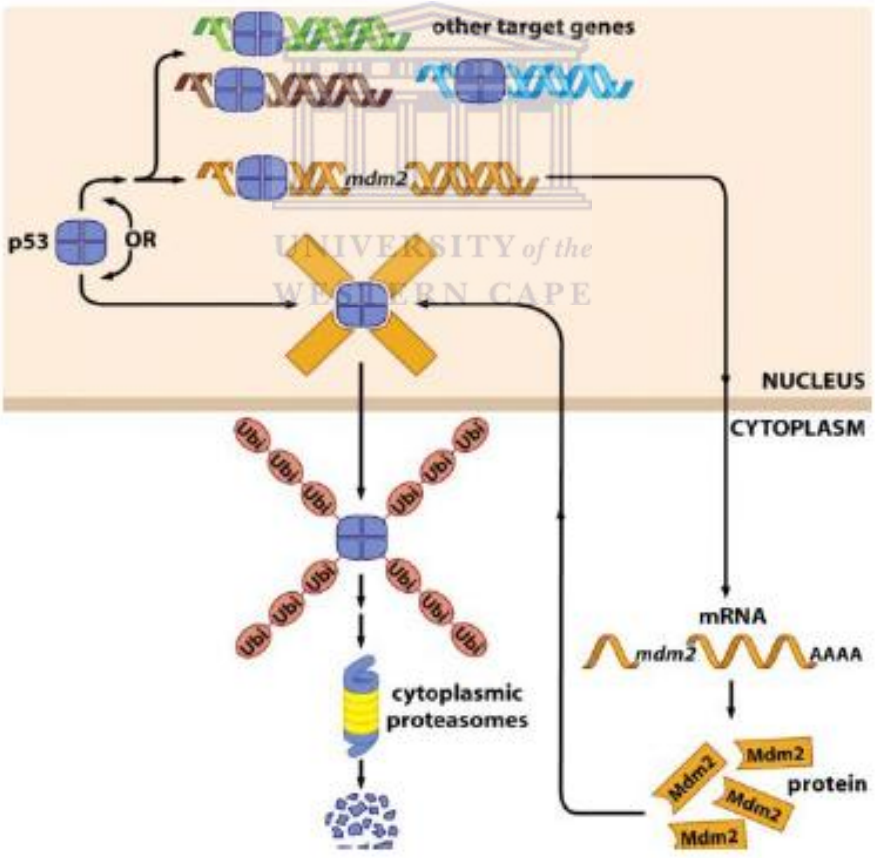

Figure 6: The p53/Mdm2 negative feedback loop. Under unstressed conditions p53 levels are generally kept low by binding Mdm2, which results in the ubiquitination and degradation of p53. But when the cell is under genotoxic stress, p53 gets post translationally modified (phosphorylation and acetylation), thus not allowing Mdm2 to bind and thus stabilizing p53 allowing its levels to rise, to stop the cell cycle or to trigger apoptosis (Appella *et al.,* 2002). Taken from Weinberg (2006).

Post-translation modifications of both proteins in response to a number of cellular stresses results in disruption of the interaction between MDM2 and p53, leading to up-regulation of both (Kruse and Gu. 2009). These modifications include phosphorylation and acetylation of p53 (Moll and Petrenko. 2003). Phosphorylation of MDM2 additionally has the effect of suppressing the E3 ligase activity of MDM2 in addition to disrupting its interaction with p53 (Cheng *et al*., 2011). Abolition of the interaction between MDM2 and p53 is considered to be a promising strategy for stabilising and activating p53 in tumour cells, and considerable effort has been devoted to understanding the structure of the interaction site and designing small molecules for the purpose of disrupting the interaction. Early successes were achieved with Nutlins, a family of molecules which bind to a hydrophobic pocket on the N-terminus of MDM2, thereby abolishing the binding of p53 (Bargonetti *et al.,* 2008) and the first examples of p53-stabilising drugs designed along these lines have recently entered clinical trials. More recently stapled peptides sMTide02 and sMTide2A, which bind to both MDM2 and MDMX (see below), were found to be more specific than Nutlins, showed less toxicity to p53-negative cells and induced a higher level of p53 reporter gene response than Nutlin in several cell-based reporter assays (Hoe *et al*. 2014).

Another binding partner of both MDM2 and p53 is MDMX, which is a close homologue of MDM2 (Linke *et al*., 2008). MDMX is a RING finger-containing protein but up to now it has not been shown to have any E3 ligase activity of its own. Both MDMX and MDM2 form homodimers through their respective RING finger domains, but form stronger heterodimers, again through their respective RING finger domains. Acting on its own *in vitro* MDM2 has been shown to be able to catalyse mono-ubiquitination of p53, but not poly-ubiquitination (Wang *et al.,* 2011). However it has recently been reported that the MDMX/MDM2 heterodimer is able to catalyse the poly-ubiquitination of p53, resulting in the proteasomal degradation of p53 (Wang *et al.,* 2011). Strategies aimed at producing therapeutics that disrupt the MDM2/MDMX heterodimer are also currently being pursued (Laurie *et al.,* 2007).

1.5. The ubiqutin-conjugating enzyme UbcH1

1.5.1. Ubiquitin Proteasome System (UPS)

Ubiquitination is the covalent attachment of ubiquitin to a substrate protein through a number of complex, specific and highly-regulated processes (Wolf *et al*., 2004). It typically requires the sequential action of three enzymes: the E1, or ubiquitin-activating enzyme, the E2, or ubiquitin-conjugating enzyme, and the E3, or ubiquitin-ligase enzyme (Fig 7). The E1 activates the C-terminal end of ubiquitin by hydrolysing ATP and using the energy to catalyse the formation of a high-energy

thiol-ester bond between its active cysteine and the C-terminal glycine of ubiquitin. The activated ubiquitin is then transferred from the E1 to the active site cysteine of the E2 by trans-esterification, forming a second thiol-ester linkage with a catalytic cysteine of the E2. Finally the E3 catalyses the transfer of the ubiquitin from the E2 to the substrate, forming an iso-peptide linkage between the C-terminal glycine of ubiquitin and the Ɛ-amino group of a lysine residue on the substrate (Wolf *et al.,* 2004).

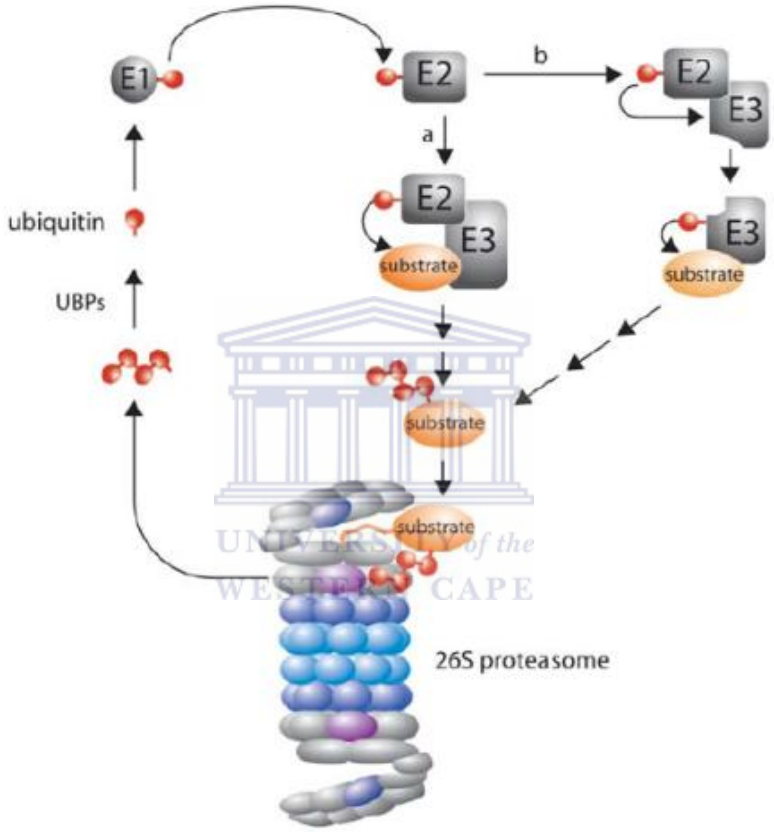

Figure 7: The Ubiquitin Proteasome System. The ubiquitination pathway and proteolysis of a poly-ubiquitinated substrate by the 26S proteasome. Taken from Wolf *et al,.* (2004).

Ubiquitin itself contains seven lysine residues, at positions 6, 11, 27, 29, 33, 48, and 63. After attachment of one ubiquitin monomer to a substrate, additional ubiquitin monomers may attach to one of the internal lysines forming a poly-ubiquitin chain (Pickart *et al,*. 2001). Ubiquitination can drastically alter the fate or function of a protein and plays a role in most, if not all, cellular processes. The best understood role of poly-ubiquitination is the tagging of substrates for degradation by the 26S proteasome, which is primarily associated with lysine48-linked chains. These are specifically recognised by the 19S cap of the 26S proteasome, leading to recruitment to the proteasome and subsequent degradation (Dantuma and Lindsten. 2009). Other linkages, such as those involving only

lysine 3, lysine 11 or lysine 63, are associated with DNA repair, endocytosis and the activation of protein kinases, but the precise fate of these tags is not yet fully understood (Dantuma and Lindsten. 2009).

1.5.2. Structure and function of UbcH1

UbcH1, which is also known as E2-25K or Huntington interacting protein 2 (Hip2) or by its official name UBE2K, is a 22.4 kDa ubiquitin-conjugating (E2) enzyme. It is unusual in its ability to catalyse poly-ubiquitination in the absence of an E3 ligase (Haldeman *et al,*. 1997) and to catalyse the formation of free (non-substrate-linked) poly-ubiquitin chains (Helderman *et al*., 1997). It is also unusual in being comprised of a C-terminal ubiquitin associating domain (UBA) in addition to the conserved E2 domain (Fig 8). The UBA domain appears to function primarily as a binding partner for ubiquitin as in the case of Cb1 E3 ligases (Zhou *et* al., 2008).

The 3D structure of UbcH1 has been solved by both crystallography and NMR, as shown in Figure 9 (Ko *et al.,* 2010). The E2 domain, comprising residues 1-153, consists of a four-stranded β-sheet (β1-β4), flanked by six alpha helices (α1-α6). The UBA domain, comprising residues 160-200, takes the form of a three-helix bundle (α7-α9) and is linked to the E2 by a short tether, residues 154-159.

UNIVERSITY of the
WESTERN CAPE

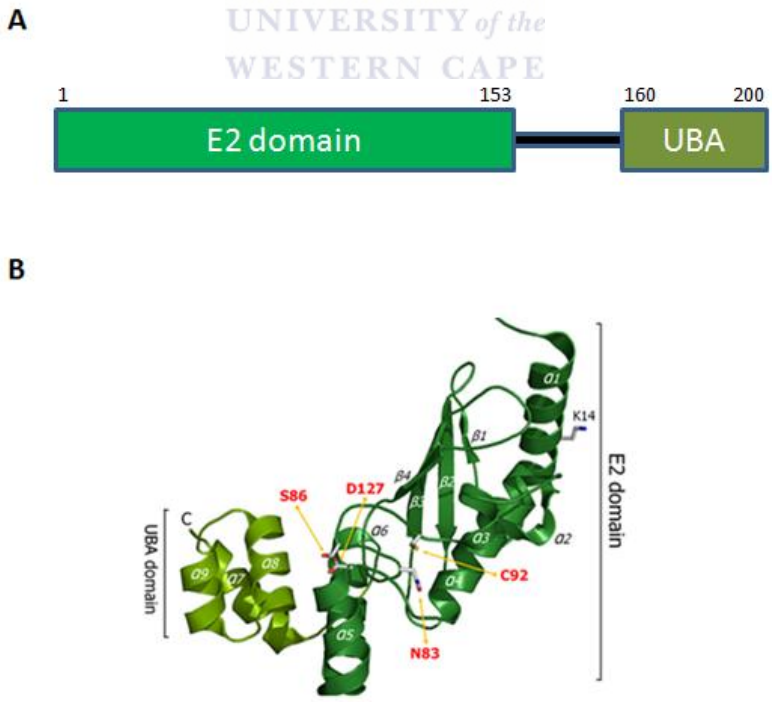

Figure 8: The domain organisation of UbcH1. A) UbcH1 is a 200 residue protein containing 2 domains: the E2 catalytic domain, residues 1-153, and the ubiquitin associated domain, residues 160-200. Adapted from Ko *et al.* (2010). B) Crystal structure of UbcH1 in which the E2 and UBA domains are coloured forest and pale green respectively. Cys-92, Asn-83, and Lys-14 (sumoylation site) Ser-86 and Asp-127, which form a hydrogen bond that modulates the active site, are also represented. Modified from Ko *et al.* (2010).

UbcH1 has also been reported to bind to the N-terminus of the Huntington protein, implicating it in the regulation of Huntington's disease through the ubiquitin proteasome pathway (Lee *et al,*. 2001). The standard model for the development of neurodegerative diseases like Alzheimer's and Huntington's involves accumulation of aggressive prion proteins in the brain. In 2003 Song and co-workers demonstrated, that through its UBA domain, UbcH1 binds a mutant form of ubiquitin known as ubiquitin-B (UBB), resulting from a frame-shift mutation. UBB can't be degraded in the 26S proteasome, resulting in the accumulation of UBB-conjugated substrates such as Huntington. Ko and colleagues later provided structural support for this mechanism (Ko *et al,*. 2010).

In addition to its function as an E2, UbcH1 also plays a role in repair of UV-damaged DNA (Koken *et al*., 1991). Schneider and colleagues later identified UbcH1 as being involved in the repair of alkylated and cross-linked DNA (Schneider *et al*., 1994). In 2013 Bae and colleagues identified UbcH1 as a direct binding partner for p53. They discovered that after genotoxic stress levels of p53 were lower when combined with over-expression of UbcH1 than when UbcH1 was absent. They went on to repeat the experiment but blocked the proteasome using MG132 and discovered p53 levels to be regulated in a proteasome dependant manner. An *in vivo* system was used in order to determine whether UbcH1 was responsible for the ubiquitination and degradation of p53. An UbcH1 mutant (S86Y) was used which is selectively inactivates poly-ubiquitin chain synthesis catalysed by UbcH1 as a negative control. In the presence of wild-type UbcH1 p53 was poly-ubiquitinated in the presence of MG132 but completely degraded in the absence of MG132. But when wild type UbcH1 was replaced by S86Y mutant UbcH1 p53 levels remained stable. This UbcH1 is a potential negative regulator of p53 (Bea *et al*., 2013).

1.6. Aims and Objectives

The primary aim of the work described in this thesis was to look for evidence *in vitro* of direct interactions between proteins expected to interact on the basis of their ubiquitination activity; in particular for interactions between RBBP6 and YB-1, since we have shown that the R3 fragment of RBBP6 is able to ubiquitinate YB-1 *in vitro*, and between RBBP6 and MDM2, since we have shown that R3 is able to ubiquitinate p53 with the assistance of MDM2. Also between RBBP6 and UbcH1, since we have found ubiquitination of YB-1 is optimal with UbcH1 as the ubiquitin-conjugating enzyme.

The interaction between the RING finger domain of RBBP6 and YB-1 had already been localised to the final 62 amino acids of YB-1 by Chibi and co-workers, both in yeast 2-hybrid studies and using *in vitro* transcribed/translated proteins (Chibi *et al.,* 2008). The aim here was to try to over-express a

larger fragment from the C-terminus of YB-1 containing the 62-residue region, to serve as a model system on which to perform a full structural characterisation of the interaction between YB-1 and RBBP6 and to study the ubiquitination of YB-1 by RBBP6. Hence the aim was to express a fragment of the C-terminus of YB-1 in bacteria, and show that it interacted with the RING finger of RBBP6 *in vitro*. We also aimed to show that the fragment was ubiquitinated by the R3 fragment of RBBP6; since the fragment would have a smaller number of lysine residues than full length YB-1, it should be possible to replace all but one of the lysines with arginines and in that way determine which lysine was the site for attachment of poly-ubiquitin chains.

In the case of the interaction between RBBP6 and MDM2 a direct interaction was reported by Li and co-workers in 2007. The aim of this study was to express the isolated domains of MDM2 and RBBP6 in bacteria and to conduct pull-down assays which would lay the foundation for future binding studies to identify the residues involved in the interaction.

In the case of RBBP6 and UbcH1 a direct interaction was expected because UbcH1 is able to act as an E2 in our ubiquitination assays of YB-1 by RBBP6. The aim of this study was to over-express both proteins in bacteria and conduct pulldown assays, followed by NMR-based interaction.

Questions to be addressed in this thesis include i) Do RBBP6 and YB-1 interact *in vitro?* Can we express a fragment of YB-1 in bacteria suitable for NMR-based structural studies? Can we identify amino acid residues involved in the interaction? ii) Can we identify a lysine residue or residues on YB-1 to which poly-ubiquitin chains become attached and, if so, can we abolish ubiquitination by mutating them to arginines? iii) Do RBBP6 and MDM2 interact *in vitro* and can we identify amino acid residues directly involved in their interaction? iv) Do RBBP6 and UbcH1 interact *in vitro* and can we identify amino acid residues directly involved in their interaction?

UNIVERSITY of the
WESTERN CAPE

Chapter 2

Methods and Materials

2.1. Antibodies used

Anti-RBBP6-RING:

Rabbit polyclonal custom-raised against residues 249-335 of human RBBP6 in the laboratory of Prof Dirk Bellstedt, Department of Biochemistry, University of Stellenbosch.

Anti-YB-1:

Rabbit poly-clonal custom-raised against residues 129-324 of YB-1 in the laboratory of Prof Antony Braithwaite, University of Sydney, Australia.

UNIVERSITY of the
WESTERN CAPE

Anti-MDM2:

Commercial rabbit poly-clonal raised against residues 393-424 of human MDM2, Cat. AB38618 (Abcam Plc, Cambridge, MA, USA).

2.2. Bacterial cultures

2.2.1. Bacterial strains used

Escherichia coli strain BL21 (DE3)pLysS: F- ompT gal dcm lon hsdSB(rB- mB-) λ(DE3) pLysS (Cm^R). chloramphenicol resistant

This strain was used to express recombinant proteins. Since it contains the lambda DE3 sequence integrated into its chromosome (containing the gene for RNA polymerase from phage T7) this strain is suitable for expression using the pET family of vectors.

Escherichia coli strain XL Gold: endA1 glnV44 recA1 thi-1 gyrA96 relA1 lac Hte Δ(mrcA)183 Δ(mcrCB-hsdSMR-mrr)173 tet^R F'[proAB $lacl^q$ZΔM15 Tn10(Tet^R Amy Cm^R].

Allows high-efficiency transformation with large plasmid inserts and was used for cloning. Antibiotic resistance against chloramphenicol and tetracycline.

2.2.2. Antibiotic selection

Ampicillin, kanamycin or chloramphenicol selection was achieved using concentrations of 100 µg/ml, 50 µg/ml, 35 µg/ml respectively both in solid and liquid media.

2.2.3. Bacterial transformation

Chemically competent cells were thawed on ice and 50 µl were added to 100-500 ng of the plasmid DNA solution, gently mixed and incubated for 30 min on ice. The cells were heat shocked by transfer to a 42 °C heat block for 90 seconds and incubated again on ice for 2 min, after which 500 µl of pre-warmed LB broth was added and the mixture incubated at 37 °C shaking for an hour to allow for the expression of the antibiotic resistance marker. The transformed cells (100 µl) were then plated onto pre-warmed nutrient agar plates containing the appropriate antibiotic and the plates incubated overnight at 37 °C.

UNIVERSITY of the

2.3. DNA cloning

2.3.1. Isolation of plasmid DNA

A single colony of transformed *E. coli* XL GOLD was inoculated into 5-10 ml of LB containing the appropriate antibiotic. The inoculated broth was incubated at 37 °C with vigorous shaking for 16 hours after which the cells were pelleted by centrifugation at 10000 rpm for 5 minutes in a microcentrifuge. Plasmid DNA was isolated using the GeneJET Miniprep kit (Thermo Fisher Scientific, Carlsbad, California, United States), according to the manufacturer's instructions.

2.3.2. PCR amplification of gene fragments

Generally, reactions consisted of 50-100 ng template DNA, 1x PCR buffer, 0.25 mM of each dNTP, 1U *Taq* DNA polymerase and 10 pmol of forward and reverse gene specific oligonucleotides, in a final volume of 50 µl. Oligonucleotide melting temperatures (Tm) were calculated using the online tool Oligo Calc found at www.basic.northwestern.edu/biotools/oligocalc.html and thermal cycling was carried out using the following procedure:

95 °C for 2 minutes (Initial denaturation)

90 °C for 1 min (Denaturation)

(Tm -5 °C) for 1 min (Annealing) — 30

72 °C for 1 min/kb (Extension)

72 °C for 5 min (Final extension)

2.3.3. Restriction enzyme digestion of DNA

Restriction enzymes were used according to the manufacturer's instructions. Generally, 1 µg of plasmid DNA or PCR products were digested with 1 unit of the desired restriction enzymes in a 50 µl reaction volume containing 1 x buffer. Reactions were incubated at the appropriate temperature for 1 hour. Digested DNA was analysed by electrophoresis in 1x TBE on 0.8 - 1 % agarose gels.

2.3.4. Ligation of DNA

Vectors used for cloning were prepared as described in Section 2.3.1. Plasmid DNA was digested with the appropriate restriction enzymes as described in Section 2.3.3. In general, vectors were digested with different enzymes, leaving non-compatible ends. These vectors were used in ligation reactions following purification using GeneJET Gel Extraction kit (Thermo Fisher Scientific) to remove the restriction enzymes. Generally, 50-100 ng of cloning vectors were used for ligations. Inserts were prepared as described in Section 2.3.2. and digested with the same enzymes as in Section 2.3.3. Both the cloning vectors and inserts were purified using a GeneJET Gel Extraction kit (Thermo Fisher Scientific). Ligations were set up in 20 µl at a vector: insert ratios of 1:3 and 1:5. Each reaction volumes contain 1x buffer and 1.0 Weiss unit of T4 ligase. Ligation reactions were allowed to proceed at room temperature for 2 hours. This is followed by bacterial transformation as described in Section 2.2.3.

UNIVERSITY of the
WESTERN CAPE

2.3.5. Agarose gel electrophoresis of DNA

DNA was analysed by electrophoresis on 0.8 or 1% agarose gels. Gels were prepared by adding the required volume of 1x TBE to the appropriate mass of electrophoresis grade agarose. The agarose was boiled and cooled to 55 °C followed by the addition of GRGreen Nucleic Acid stain 10000x (Labgene Scientific, Châtel-St-Denis, Switzerland) to a final concentration of 1x and poured onto a gel casting tray. DNA loading buffer was added the DNA to a final concentration of 1x and loaded onto the gel. The DNA marker was loaded in the first lane to show the sizes of the bands. The DNA was visualized by subjecting the gel to UV light at 365 nm.

2.4. Recombinant protein expression

2.4.1. Protein expression in rich media

E. coli BL21 (DE) pLysS cells transformed with expression constructs were grown overnight at 37 °C on nutrient agar plates containing the appropriate antibiotic. Single colonies were picked and used to inoculate 100 ml of LB containing the appropriate antibiotics. This culture was grown overnight at 37 °C on a rotary shaker. The culture was scaled up to 1 litre by the addition of 900 ml of LB medium containing the appropriate antibiotic and grown at 37 °C until the culture reached an optical density at 550 nm of 0.5. Recombinant protein expression was induced by the addition of IPTG to a final concentration of 0.5 mM. Induction was carried out overnight at 30 °C. Overnight cultures were transferred to 250 ml polypropylene tubes and the cells harvested by centrifugation at 6000 rpm for 30 minutes at 4 °C.

2.4.2. Protein expression in labelled media

For ^{15}N labelling of recombinant protein, proteins were expressed in minimal medium (see Table 2.1) supplemented with 18.7 mM ^{15}N-NH_4Cl (Cambridge Isotope Laboratories, Inc., Tewksbury, MA, USA) as the sole nitrogen source. Expression was carried out as described in Section 2.4.1.

2.5. Protein purification

UNIVERSITY of the
WESTERN CAPE

2.5.1. Protein extraction

Cell pellets were thawed on ice and resuspended in extraction buffer for the purification of 6xHis fusion proteins, the extraction buffer was supplemented with 40 mM imidazole (Table 2.1). After which they were lysed on ice by sonication, which was carried out in 30 second bursts, followed by 30 seconds rest on ice, repeated for 5 minutes. The lysate was cleared by centrifugation at 14000 rpm for 30 minutes at 4 °C.

2.5.2. Affinity purification

A disposable plastic column containing 5 ml of the appropriate media (glutathione agarose or nickel sepharose) was washed with 3 column volumes (CV) of 8 M urea, 5 CV of water, 3 CV of 100 mM acetate buffer pH 4.5, 3 CV 100 mM borate buffer pH 8.5 and then equilibrated with 5 CV of wash buffer (see Table 2.1). The crude lysate was added to the column and the flow through collected after which the column was washed with 3 CV of wash buffer and each CV collected. The bound proteins were then eluted with the appropriate buffer: in the case of GST fusion proteins, the elution buffer contained 20 mM reduced glutathione, while 500 mM imidazole was used to elute 6xHis

tagged proteins. Finally, the column was washed and stored in 1 M NaCl containing 0.2 % NaN_3. Purified fractions were analysed by SDS-PAGE.

2.5.3. Cleavage of recombinant protein

3C protease from human rhinovirus was expressed in the laboratory as a GST-fusion protein and purified as described in Sections 2.4 and 2.5. GST-fusion proteins were cleaved with 3C protease in a Snakeskin™ dialysis bag (Thermo Fisher Scientific) with a 3.5 kDa MWCO. The tubing was then placed in 2 L of cleavage buffer in a 5 L beaker at 4 °C overnight with stirring. Following cleavage the GST tag and the GST-3C was separated from the target protein by returning the cleaved sample to a glutathione agarose column as described in Section 2.5.2. The target protein was collected in the flow-through with the cleaved GST, the uncleaved GST-fusion and GST-3C remaining immobilised on the column.

2.5.4. Size exclusion chromatography

Protein samples were concentrated into 0.5 - 1 ml and then loaded onto a calibrated Superdex 75 16/600 column (Amersham Biosciences, Pittsburgh, USA), operated on an ÄKTA FPLC chromatography platform (GE Healthcare, Little Chalfont, UK). 2 ml elution fractions were collected for a total elution volume of 1 CV.

UNIVERSITY of the
WESTERN CAPE

2.5.5. HisTRAP affinity chromatography

6xHis tagged proteins were loaded onto a 5 ml HisTRAP column (GE Healthcare, Little Chalfont, UK) operated on an ÄKTA FPLC chromatography system equilibrated with 3 CV of wash buffer. The column was washed with 4 CV of wash buffer and the bound protein was eluted using a 0 - 500 mM concentration gradient of imidazole and collected in 2 ml fractions.

2.6. SDS-PAGE gel electrophoresis

Proteins were fractionated on 16 % denaturing polyacrylamide gels (SDS-PAGE) prepared using Laemmli's method (Laemmli, 1970). Gel was prepared as follows:

Resolving gel 16 %	**Stacking gel 4 %**
1.6 ml dH_2O	1.5 ml dH_2O
1.3 ml Separating buffer	0.625 ml Stacking buffer
2 ml acrylamide (40% acrylamide:bis-acrylamide)	0.375 ml acrylamide (40 % acrylamide:bis-acrylamide)

52.4 µl 10 % SDS	25 µl 10 % SDS
30 µl 10 % APS	12.5 µl APS
3.75 µl TEMED	2.5 µl TEMED

Samples were prepared by adding equal volumes of sample and 2x SDS sample buffer and boiling at 95 °C for 10 minutes. Samples were then loaded onto the gel and separated using a Mini-PROTEAN Tetra Cell (BioRAD, Hercules, CA, USA). Upon completion the gel was stained with Coomasie staining solution for 15 minutes and destained with destaining solution until the background was clear.

2.7. Immuno-detection of proteins

Following separation on SDS-PAGE as described in Section 2.6, proteins were transferred onto PVDF membrane (0.2 µm Immun-Blot, BioRAD, BioRad, Hercules, CA, USA) using the Trans-Blot® Turbo™ Transfer System (BioRad) in transfer buffer (see Table 2.1). Following transfer non-specific binding was blocked by incubating the membrane in 1 % casein in PBS-T for 1 hour at room temperature with shaking. This was followed by incubation with primary antibodies for 1 hour at room temperature with shaking. The membrane was then washed for 3 x 10 minutes with PBS-T following which it was incubated with secondary antibodies for 1 hour at room temperature with shaking. The membrane was then washed for 3 x 10 minutes with PBS-T. The blot was then developed in Clarity™ ECL Western Blotting Substrate (BioRad) and visualized on the ChemiDoc system from UVP (Nuffield road, Cambridge UK).

UNIVERSITY of the
WESTERN CAPE

2.8. Affinity pull-down assays

GST pull-down assays were performed using GST-tagged “bait” and un-tagged “prey” proteins. Equal molar quantities of GST-tagged bait proteins or GST (to serve as negative control) were added to 20 µl of 50 % glutathione agarose slurry. Equal amounts of prey were added to both baits and incubated overnight at 4 °C with rolling. An additional negative control was included from which the bait protein was omitted altogether. The beads were pelleted by centrifugation and washed 3 times with 1 ml wash buffer. Finally the beads were re-suspended in 40 µl of SDS sample buffer, boiled for 5 minutes at 95 °C and 10 µl loaded onto an SDS-PAGE gel. Prey proteins were immuno-detected with the appropriate antibodies as described above.

2.9. Co-immunoprecipitation

Co-immunoprecipitation assays were conducted in a similar manner as GST pull-down assays, with the exception that bait proteins were precipitated using antibodies conjugated to agarose, which were themselves precipitated with Protein A/G-conjugated agarose. Protein A/G is a protein with high affinity for immunoglobulin molecules such as the primary antibodies targeting the bait protein. In this case both the bait and prey proteins were present in mammalian cell lysates. 100 µg of each lysate was mixed with 20 µl Protein A/G-conjugated antibodies against one of the proteins of interest which were then incubated overnight at 4 °C with rolling. The beads were pelleted by centrifugation and washed 3 times with 1 ml wash buffer. Finally the beads were resuspended in 30 µl sample buffer, boiled for 5 minutes at 95 °C and 10 µl separated on 16% SDS-PAGE gels. Precipitated proteins were immunodetected with the appropriate antibodies as described before.

UNIVERSITY of the
WESTERN CAPE

Chapter 3

Investigation of interactions involved in the regulation of YB-1 by RBBP6

3.1. Introduction

The RING finger domain of Retinoblastoma Binding Protein 6 has previously been shown in a yeast 2-hybrid assay to interact directly with the C-terminal 62-amino acids of Y-Box Binding Protein-1 (Chibi *et al.,* 2008). Chibi and co-workers went on to confirm the interaction by expressing the two regions in an *in vitro* transcription/translation system and conducting immunoprecipitation assays. Subsequent attempts to express the relevant fragment of YB-1, residues 262-324, at larger scale in bacteria proved unsuccessful due to poor solubility (Victor Muleya, MSc thesis, UWC, 2011). In this work we set out to identify a larger fragment of the C-terminus of YB-1 that would be suitable for large-scale expression in bacteria and subsequent NMR-based interaction studies, with the aim of identifying residues directly involved in the interaction.

UNIVERSITY of the
WESTERN CAPE

The region of YB-1 spanning residues 220-324, denoted YB-$1_{220\text{-}324}$, was selected since this fragment corresponds to the C-terminal fragment reportedly released from YB-1 by proteasomal cleavage (Sorokin *et al*., 2005; van Rooyen *et al.,* 2013), suggesting that it may be independently folding and resistant to proteolysis. With a molecular mass of 12.5 kDa, YB-$1_{220\text{-}324}$ would be the ideal size for NMR-based interaction studies and for structure determination. Since YB-1 is known to form oligomers (Evdokimova *et al.,* 1995), which give rise to high backgrounds in *in vitro* ubiquitination assays, it was hoped that the fragment would serve as a "cleaner" substitute for YB-1 in these assays. The selected fragment corresponds to approximately half of the C-terminus, making it possible that the reduced numbers of the charges may render it less likely to oligomerise. Investigating ubiquitination using a smaller fragment may also aid in identifying the target lysine, since with only four lysines in YB-$1_{220\text{-}324}$ as opposed to the sixteen in full length YB-1, systematic mutation of individual lysines to arginine becomes feasible.

This chapter describes bacterial expression and purification of YB-$1_{220\text{-}324}$ with an N-terminal GST and a C-terminal 6xHis tag, followed by affinity pulldown assays aimed a co-precipitating the isolated

RING finger domain of RBBP6 (RBBP6-RING). The latter was used since it was the domain originally shown to interact with YB-1 in yeast 2-hybrid assays (Chibi *et al.,* 2008). Furthermore RBBP6-RING is known to be suitable for large-scale expression in bacteria and its ^{15}N-HSQC NMR spectrum has been previously assigned and published (Kappo *et al.,* 2012), which would allow for immediate identification of resonances perturbed during binding. A hemagglutinin tag (HA) was included between the GST tag and YB-$1_{220\text{-}324}$ for future immunodetection using anti-HA antibodies. However the HA tag was not used in this study as antibodies recognising YB-$1_{220\text{-}324}$ and RBBP6-RING were used instead.

The chapter continues by describing *in vitro* investigations of two interactions which are suggested by unpublished results generated by other members of our laboratory. These are the putative interaction of RBBP6-RING with the ubiquitin-conjugating enzyme UbcH1, which is suggested by Dr Andrew Faro's finding that RBBP6 catalyses poly-ubiquitination of YB-1 using UbcH1 as E2 (A. Faro and D.J.R. Pugh, manuscript in preparation). The second putative interaction involves RBBP6-RING and the oncogenic protein Murine Double Minute 2 (MDM2), which is suggested by Ms Lauren Jooste's finding that RBBP6 cooperates with MDM2 in ubiquitinating p53 *in vitro* (L. Jooste, A. Faro and D.J.R. Pugh, manuscript in preparation). If verified this result would confirm and extend the report of Li and co-workers that RBBP6 cooperates with MDM2 *in vivo* to suppress levels of p53 during development (Li *et al*., 2007). The above two studies are preliminary studies aimed at establishing optimal conditions for future, more focussed, investigations using Nuclear Magnetic Resonance spectroscopy (NMR).

The chapter begins with description of a side-project whose aim was to generate a bacterial expression construct coding for the DWNN domain from RBBP6, terminating immediately following the di-glycine (-GG) motif which represents a key feature of vertebrate DWNN domains. This motif is found at exactly the same structural position as the di-glycine motif in ubiquitin, raising the possibility that the DWNN domain becomes covalently attached to substrate proteins in a process which has been dubbed "DWNNylation". Before it can be attached to substrate proteins *in vivo* ubiquitin is enzymatically processed to expose the –GG motif and recombinant ubiquitin used in *in vitro* ubiquitination assays is designed to terminate immediately following the –GG. The aim was therefore to produce an expression construct encoding DWNN-GG for use by co-workers conducting DWNNylation assays. An HA tag was included immediately upstream of DWNN-GG for immunodetection using anti-HA antibodies; the construct was designed in such as way that it could be re-used to generate HA-tagged versions of existing constructs cloned into pGEX-6P-2.

3.2. *Generation of a GST-HA-DWNN-GG expression construct*

3.2.1. *Cloning of HA-DWNN-GG into pGEX-6P-2*

The first task was to modify the pGEX-6P-2 expression vector to insert a hemagglutinin (HA) immunotag between the 3C protease site and the multiple cloning cassette (MCC), at the same time as inserting the cDNA coding for DWNN-GG between the BamHI and XhoI sites of the MCC. This was done by amplifying HA-BamHI-DWNN-GG flanked by 5'-BglII and 3'-XhoI sites and cloning it into the BamHI/XhoI sites of pGEX-6P-2, as described in Section 2.3. Since BglII and BamHI produce compatible overhangs, the BglII/BamHI site would be destroyed whereas the internal BamHI site would be preserved, regenerating the MCC downstream of the BglII site. This was done so that the DWNN domain could later be excised and replaced with any other cDNA previously cloned into the BamHI/XhoI sites of pGEX-6P-2. This latter feature was exploited below for generation of the GST-HA-YB-$1_{220-334}$-6xHis construct.

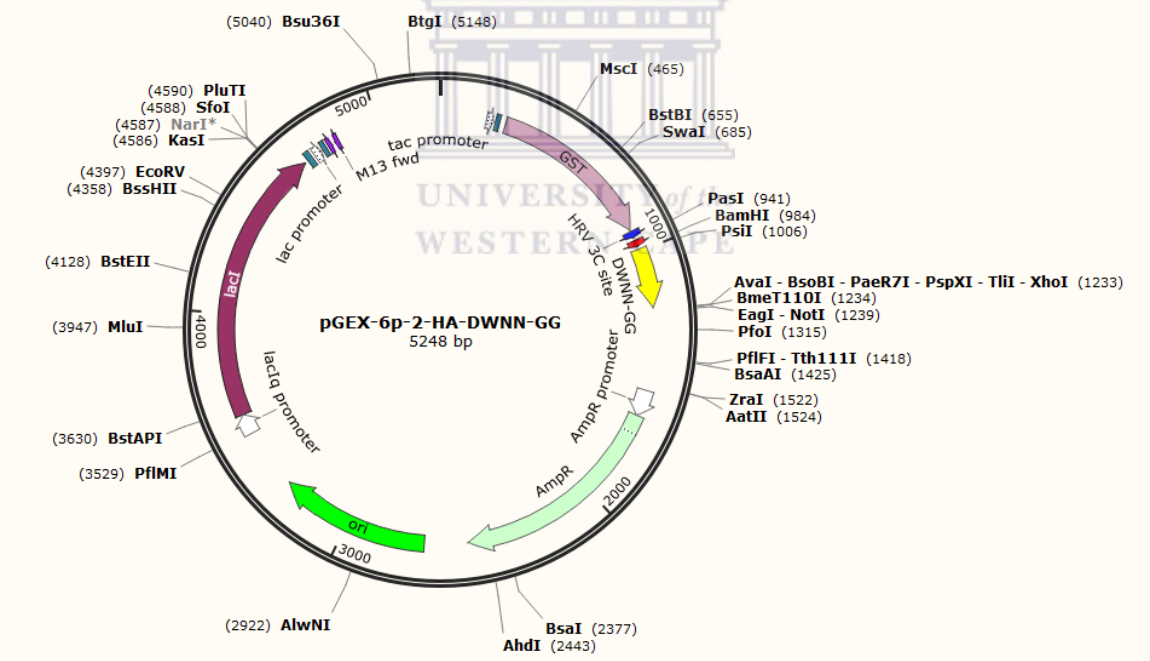

Figure 3.1: Construct map of pGEX-HA-DWNN-GG. pGEX-6P-2 vector with the GST (Purple) fused HA-DWNN-GG (HA-tag red and DWNN-GG in yellow) gene separated by a HRV 3C cleavage site (Red).

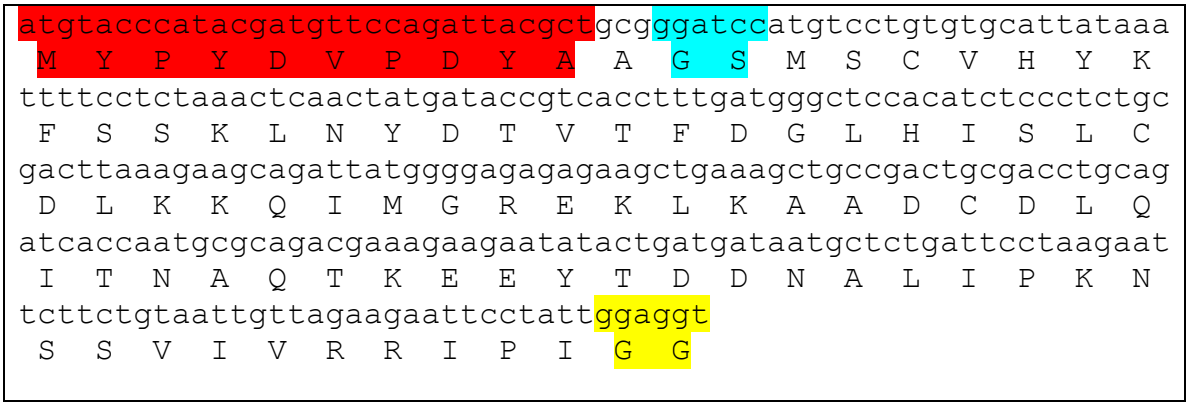

Figure 3.2: DNA sequence and amino acid translation of HA-DWNN-GG. DWNN comprises residues 1-79 of RBBP6, terminating after the –GG motif highlighted in yellow, BamHI indicated in turquoise and HA tag in red.

The primers are shown in Table 3.1. The reverse primer contains two stop codons (5'-TGA|TGA) immediately preceding the XhoI site (green); the underlined bases are complimentary to the template. The forward primer contains the sequence coding for the HA tag, highlighted in purple, flanked by BglII (yellow) and BamHI (turquoise) sites at the 5'- and 3'-ends respectively. Following amplification and cloning into the BamHI and XhoI sites of the pGEX-6P-2 expression vector, the BamHI/BglII sites were both destroyed, leaving the internal BamHI site on the 3'-end of the HA tag. This allowed the DWNN-GG domain to be subsequently excised with BamHI and XhoI and replaced with any other BamHI/XhoI fragment. An existing pGEX-6P-2 construct encoding residues 1-118 of RBBP6 was used as the template.

UNIVERSITY of the
WESTERN CAPE

Table 3.1: **Oligonucleotides used to amplify the HA-DWNN-GG fragment**. The HA tag is shown in purple and the restriction enzymes sites in yellow (Bgl II), blue (BamHI) purple and green (XhoI). Two stop codons are shown in red. Underlines bases are complimentary to the template.

Primer name	Primer sequence	Primer melting temperature
Forward primer	5'- GAG GCGAGA TCTATG TAC CCA TAC GAT GTT CCA GAT TAC GCT GCG GGA TCC ATG TCC TGT GTG CA -3'	62 °C
Reverse primer	5'-GAG GCGCTC GAGTCA TCA ACC TCC AAT AGG AAT TCT TCTAA -3'	62 °C

As can be seen in Figure 3.3(A), the HA-DWNN-GG fragment was successfully amplified as a 294 bp amplicon (lane 2) The amplicon was digested with BglII and XhoI restriction enzymes (Thermo Fisher Scientific) and cloned into the BamHI and XhoI sites of the pGEX-6p-2 vector. Putative positive clones were screened by colony-PCR using the HA-DWNN-GG-specific primers shown in Table 3.1 (see Fig 3.3 B), and by extraction of plasmid DNA followed by restriction digest with BamHI and XhoI to

release an insert of approximately 294 bp (Fig 3.3 C). The DNA sequences of positive clones were confirmed by DNA sequencing at Inqaba Biotechnical Industries (Pty) Ltd (Hatfield, South Africa) and found to be 100 % in agreement with the expected sequence (Appendix).

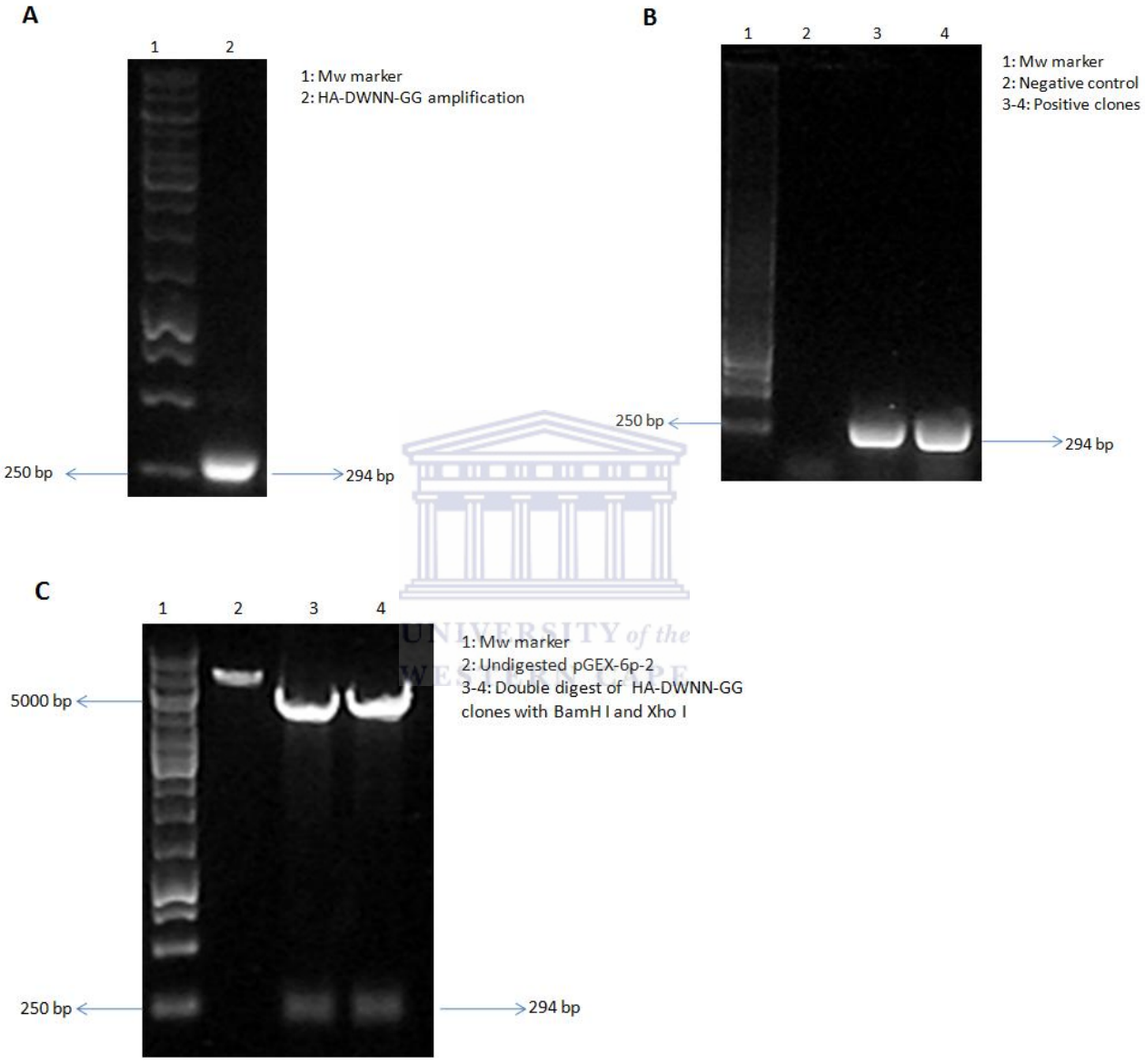

Figure 3.3: Successful cloning of HA-DWNN-GG into pGEX-p6-2. (A) The HA-DWNN-GG fragment was amplified from the pGEX-6P-2-RBBP6-DWNN construct. Lane 2 contains a ~294 bp band which corresponds to the HA-DWNN-GG amplicon size. (B) Putative positive colonies were screened using colony-PCR and amplified a band of the expected size of ~294 bp (lanes 3 and 4) Lane 2 contains negative control to which no template DNA was added. (C) Screening of colonies testing positive using colony-PCR was digested with BamH I and Xho I. The release of a fragment of 294 bp (lanes 3 and 4) confirm that the cloning was successfully carried out.

3.2.2. Expression and purification of HA-DWNN-GG

HA-DWNN-GG was expressed solubly as a GST-fusion protein in *E. coli* BL21 cells and purified away from cellular proteins using glutathione-affinity chromatography, as described in Section 2.5. GST-HA-DWNN-GG migrated on 16 % SDS-PAGE at the expected size of 40 kDa, as can be seen as seen in lanes 6-9 of Fig 3.4(A).

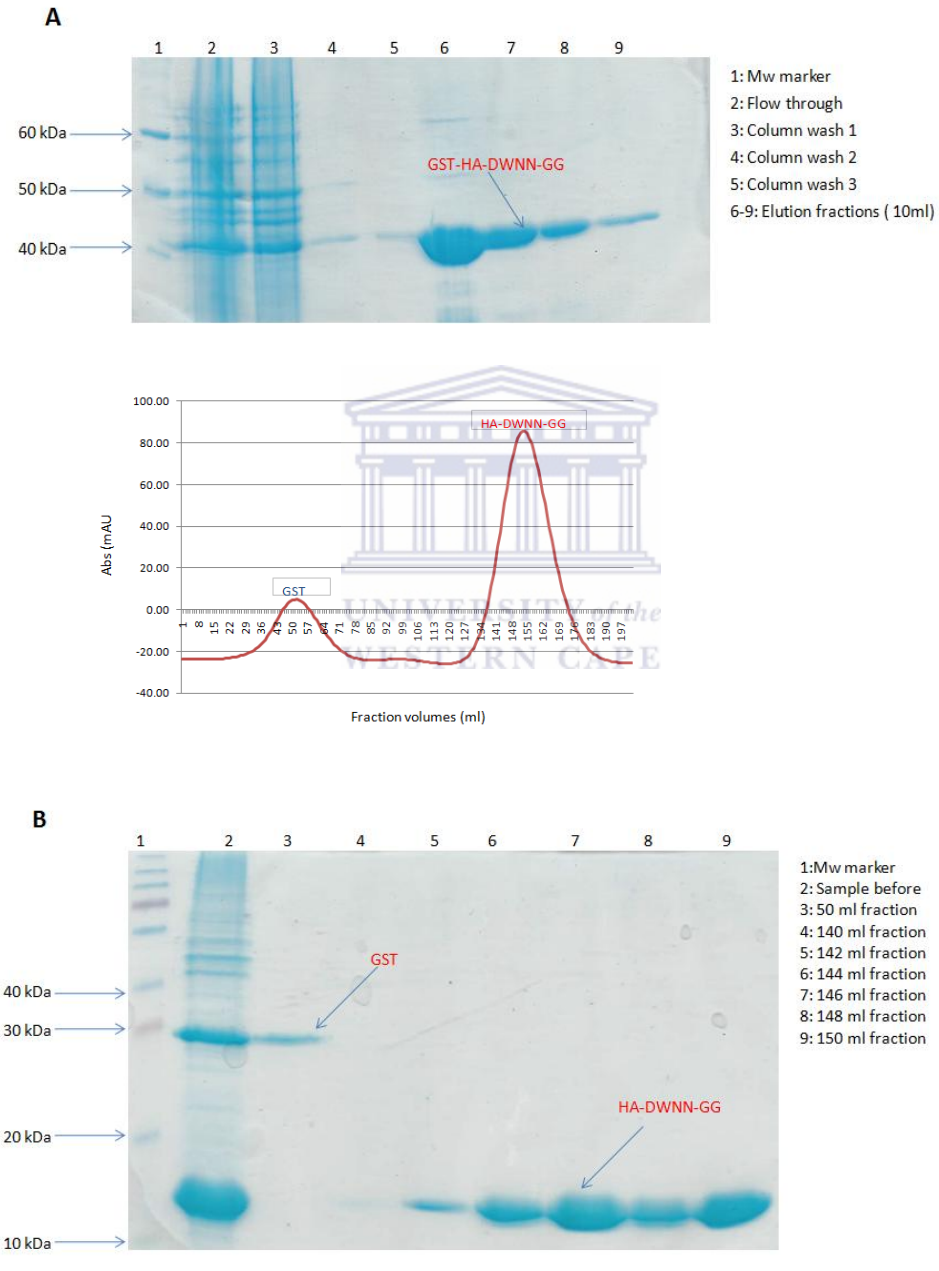

Figure 3.4.: Purification of HA-DWNN-GG. (A) GST-HA-DWNN-GG was purified using a glutathione agarose column. Lanes 5-9 contain 40 kDa bands which correspond to the expected size of GST-HA-DWNN-GG. (B) Following cleavage with 3C protease, HA-DWNN-GG was purified away from GAT using a second round of glutathione affinity chromatography (data not shown) and finally using size exclusion chromatography on a calibrated Hiload Superdex 75 16/600 SEC column. (C) SEC yielded two well-separated peaks which turned out to be HA-DWNN-GG (lanes 6-9) and GST (lane 2).

Eluted fractions were pooled and incubated overnight at 4 ^{o}C with 3C protease to cleave the GST tag using the protease recognition site incorporated into the vector between GST and the HA tag. The sample was simultaneously dialysed to remove free glutathione. The cleaved sample was subjected to a second round of glutathione affinity chromatography to remove cleaved GST, uncleaved fusion and GST-3C protease, and the target protein was collected in the flow through. Residual GST was removed using size exclusion chromatography on the ÄKTA FPLC chromatography system using a calibrated Hiload Superdex 75 16/600 SEC column (GE Healthcare, Little Chalfont. UK). Fractions corresponding to the peaks in the resulting chromatogram were analysed on SDS PAGE, as shown in Fig 3.4(B). HA-DWNN-GG, with a molecular weight of 14 kDa (lanes 4-9), was well separated from GST (26 kDa) (lane 2), yielding a highly purified sample of HA-DWNN-GG.

3.3. RBBP6 interacts with YB-1 in mammalian cell lysates

3.3.1. Co-immunoprecipitation of YB-1 by RBBP6

Prior to attempting to localise the interaction between RBBP6 and YB-1 *in vitro*, we first attempted to reproduce the reported interaction between endogenous RBBP6 and YB-1 in mammalian cell lysates. We began by investigating whether endogenous RBBP6 was able to precipitate full length YB-1 from HeLa cell lysate. Immunoprecipitation was carried out using 100 µg lysate and a rabbit poly-clonal antibody raised against bacterially-expressed RBBP6-RING. As a negative control the anti-RBBP6-RING antibody was replaced with an anti-HA antibody. Following immunoprecipitation and extensive washing the samples were resuspended in 30 µl sample buffer and 15 µl separated on SDS-PAGE and detected using a poly-clonal antibody raised against residues 129-324 of YB-1. Details of the antibodies used are provided in 2.1. The positive control (lane 2), which was not subjected to immunoprecipitation, contains a fifth of the lysate used in the immunoprecipitation.

Lane 4 of Figure 3.5 shows that the anti-RBBP6 antibody was able to co-precipitate a protein at approximately 50 kDa, which is consistent with full-length endogenous YB-1, whereas the anti-HA antibody in lane 3 was not. The anti-RBBP6 antibody also co-precipitated a fragment of between 20 and 30 kDa which, since the antibody targets an antigen on the C-terminus of YB-1, is most likely to correspond to a C-terminal isoform or degradation fragment of YB-1. This is consistent with previous reports that RBBP6 interacts with the C-terminus of YB-1 (Chibi *et al.,* 2008). Both co-precipitated bands are visible in the non-precipitated lysate following longer exposure (lane 2, panel (B), which corresponds to the dotted area in panel A), which is as expected.

The amount of lysate added to the immunoprecipitation in lane 4 was five times that loaded in lane 2, but only 15 µl out of the of the final resuspended volume of 30 µl was loaded; hence if all of the YB-1 added to the immunoprecipitation in lane 4 were co-immunoprecipitated, we should expect a relative intensity of lane 4 relative to lane 2 of 2.5. The band in lane 4 is already weak, but no band is visible in lane 2, so the intensity looks somewhat more than 2.5-fold less. On the other hand a band is visible in panel B, which was subjected to 50 s of exposure, compared to 5 s for panel (A), which represents a 10-fold sensitivity enhancement. Hence if all of the YB-1 added to the immunoprecipitation in lane 4 were co-immunoprecipitated, we should expect an intensity of the bands in panel B to be 10/2.5 = 4 times more intense than those in lane 4 of panel A. While quantifying the relative intensity is difficult, it does appear to be consistent with 4, in which case we may suspect that the interaction between endogenous RBBP6 and YB-1 is fairly strong.

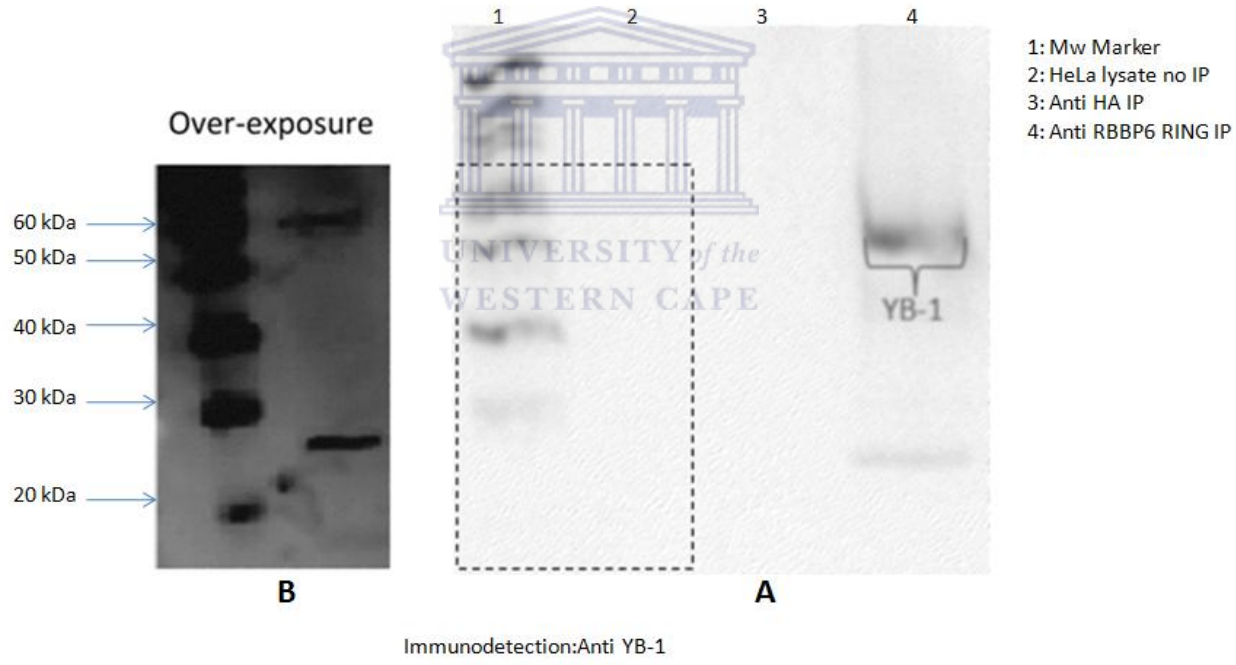

Figure 3.5: Endogenous RBBP6 is able to co-precipitate endogenous YB-1. (A) Western blot detected using an antibody raised against the C-terminus of YB-1. Equal amount of HeLa lysate was added to lanes 3 and 4. An antibody raised against RBBP6-RING is able to precipitate endogenous YB-1 (lane 4), whereas a non-specific antibody (anti-HA) is not (lane 3). The band at 50 kDa is consistent with full length YB-1. The band between 20 and 30 kDa is likely to be either a C-terminal isoform of YB-1 or else a C-terminal degradation product, since the antibody recognises the C-terminus of YB-1. Lane 2 contains lysate only and was not subjected to immunoprecipitation. Although endogenous YB-1 is not visible in lane 2, it is visible when the western blot is exposed for ten times longer, as shown in panel (B).

UNIVERSITY of the WESTERN CAPE

3.4. The RING finger of RBBP6 interacts with the CTD of YB-1 in vitro

3.4.1. Expression and purification of the RING finger domain from RBBP6

Having verified the interaction between endogenous full length YB-1 and RBBP6, we next investigated the interaction between smaller fragments *in vitro*: the RING finger domain of RBBP6 and the C-terminal fragment of YB-1, YB-$1_{220-324}$. The RING finger domain, $RBBP6_{249-335}$, was selected because it was the fragment used in the yeast 2-hybrid assay which originally identified YB-1 as an interaction partner of RBBP6 (Chibi *et al*., 2008*)*. The RING finger has subsequently been shown to express solubly in high quantities and to be suitable for NMR interaction studies (Kappo *et al.,* 2012). Furthermore the ^{15}N-HSQC NMR spectrum of RBBP6-RING has been fully assigned, which means that NMR resonances found to be perturbed during binding can be immediately assigned to residues in the domain, allowing mapping of the interaction surface.

A pGEX-6P-2 expression construct for $RBBP6_{249-335}$ was already available in the laboratory. The domain was expressed as a fusion with GST and purified using glutathione affinity chromatography. GST-RBBP6-RING was found to migrate at the expected size of 37 kDa, as seen in the eluted fractions (Fig. 3.6(A), lanes 6-9). The GST tag was removed using 3C protease and separated from RBBP6-RING using size exclusion chromatography, as shown in panels (B) and (C). SDS-PAGE analysis showed that RBBP6-RING, which has a molecular weight of 10.2 kDa (lanes 4-8), was very efficiently separated from GST (26 kDa, lane 2) and from a number of higher molecular weight contaminants apparent in lane 10. The apparent molecular weight of RBBP6-RING (around 15 kDa) is somewhat higher than expected for a 10 kDa protein, but this is consistent with earlier reports (Kappo et al, 2012).

For NMR studies the RBBP6 RING finger domain was successfully expressed as a ^{15}N-labelled protein by expressing it in M9 minimal media supplemented with ^{15}N ammonium chloride as the sole nitrogen source (Cambridge Isotope Laboratories, Inc., Cambridge, Mass, USA), as described in Section 2.4.2. ^{15}N-labelled GST-RBBP6-RING was solubility expressed (Fig 3.7 A) and purified using glutathione affinity chromatography, as shown in Fig. 3.7(A), lanes 6-9. Following cleavage with 3C protease ^{15}N-RBBP6-RING was successfully separated from GST using size exclusion chromatography, as shown in panel (B), lanes 4-10. As with unlabelled RBBP6-RING, the protein migrates as a smear around 15 kDa. Fractions containing ^{15}N-RBBP6-RING fractions were pooled and concentrated to 150 µM, which is considered adequate for NMR chemical shift perturbation studies.

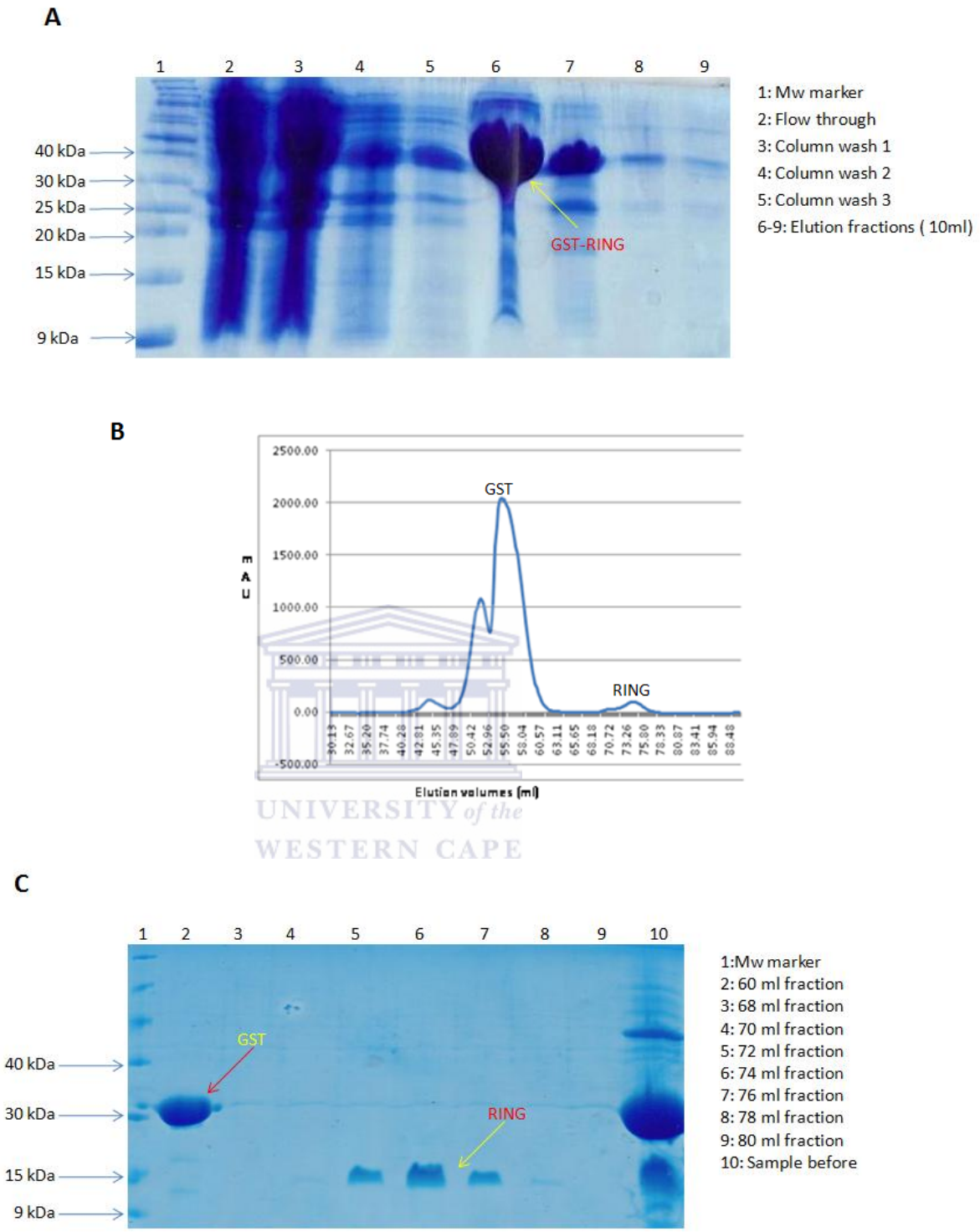

UNIVERSITY of the
WESTERN CAPE

Figure 3.2.: Purification of the RBBP6 RING finger domain. (A) RBBP6 RING finger domain was purified using a glutathione agarose column. Lanes 6-9 contain 37 kDa bands which correspond to the expected size of GST-RBBP6 RING. The purified protein was then cleaved with recombinant 3C protease. (B) Following cleavage concentrated RBBP6 RING was further purified using Size Exclusion Chromatography on a calibrated Hiload Superdex 75 16/600 SEC column. (C)Lane 10 contains a concentrated sample which was loaded on the column and contained three major bands 37 kDa, 26 kDa and 15 kDa corresponding to GST-RING, GST and the RBBP6 RING finger respectively. Lane 2 correspond to the fraction were GST eluted and Lanes 4-8 contain the fractions where the RBBP6 RING eluted.

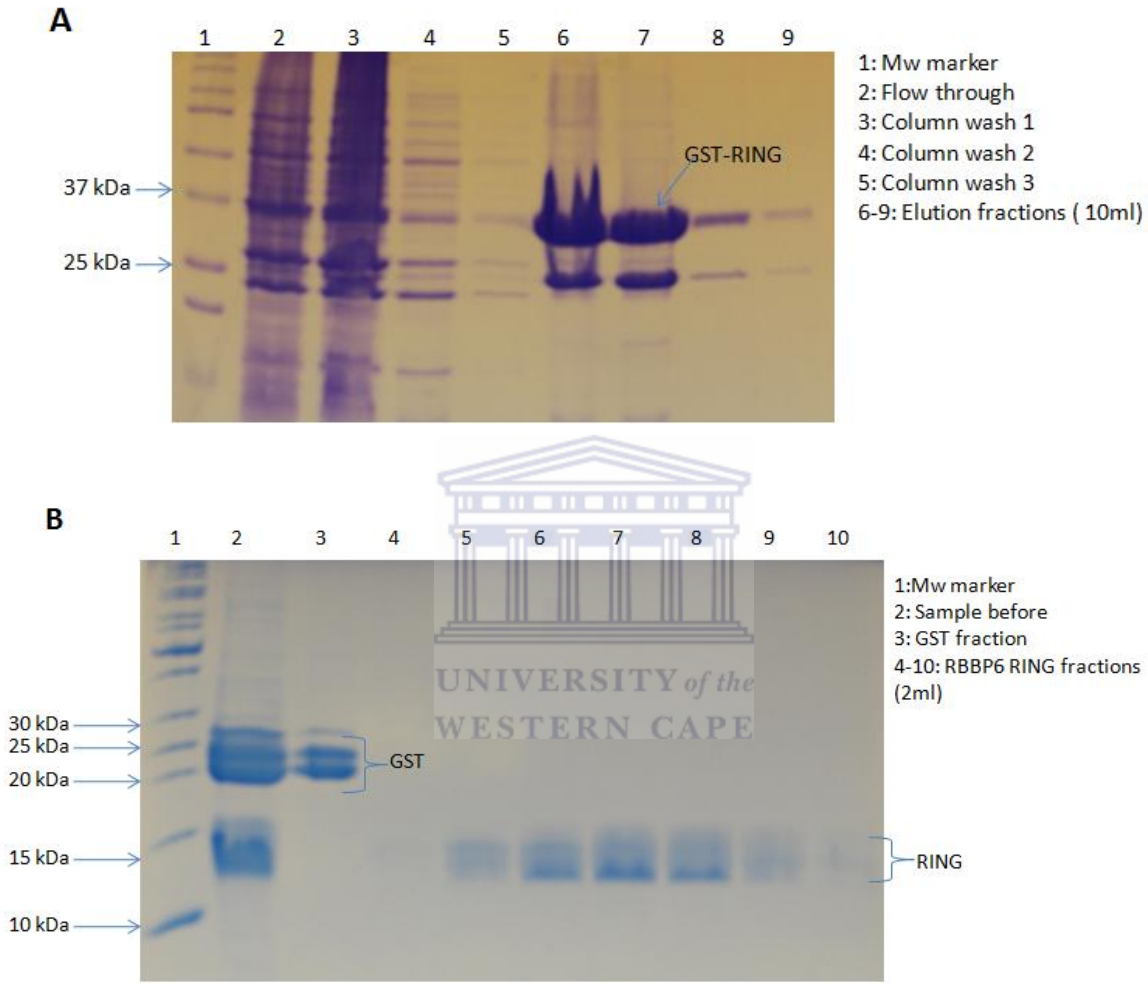

Figure 3.7: Purification of ^{15}N-labelled RBBP6-RING finger domain. (A) RBBP6 RING finger domain was purified using a glutathione agarose column. Lanes 6-9 contain 37 kDa bands which correspond to the expected size of GST-RBBP6 RING. (B) Following cleavage concentrated RBBP6 RING was further purified using Size Exclusion Chromatography. Lane 1 contained a concentrated sample containing GST and the RBBP6 RING finger. Lane 3 contain the fraction were GST was eluted and Lanes 4-9 contain the fractions were the RBBP6 RING finger domain eluted.

UNIVERSITY of the WESTERN CAPE

3.4.2. Cloning of wild type YB-1$_{220-324}$ for expression in bacteria

The region of YB-1 selected for *in vitro* studies was residues 220 – 324, dubbed YB-1$_{220-324}$ (Fig 3.8). As described earlier this includes the 62-residue region identified in a yeast 2-hybrid screen as interacting with the RING finger of RBBP6 (Chibi *et al.,* 2008). It also coincides with the C-terminal fragment reported to be separated from full length YB-1 by cleavage in the proteasome (Sorokin et al, 2005; van Rooyen *et al.,* 2013), and hence characterising its expression would lay the groundwork for future structural and functional studies on the fragment.

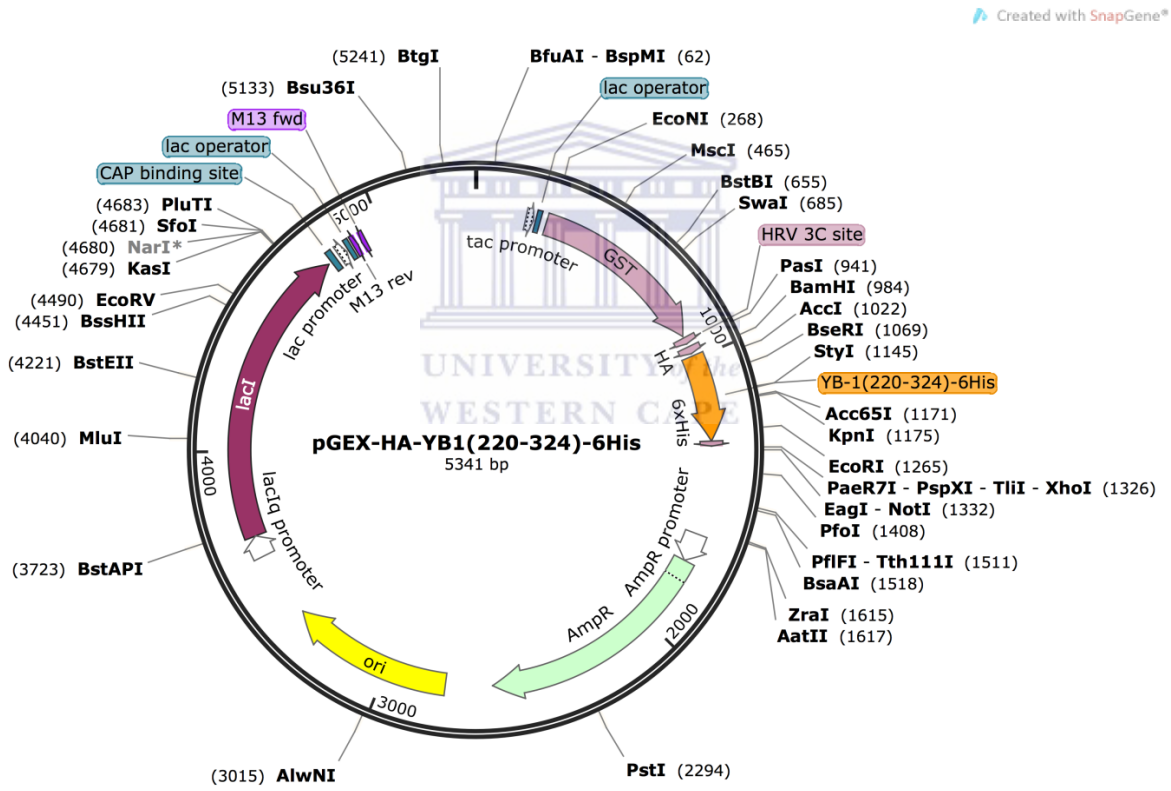

Figure 3.8: Construct map of pGEX-HA-YB-1$_{220-324}$ -6xHis. pGEX-6P-2 vector with the GST (Purple)-fused HA-YB-1$_{220-324}$-6xHis (HA-tag light purple, YB-1$_{220-324}$ in oranje and 6xHis-tag in brown light purple) gene separated by a HRV 3C cleavage site (purple).

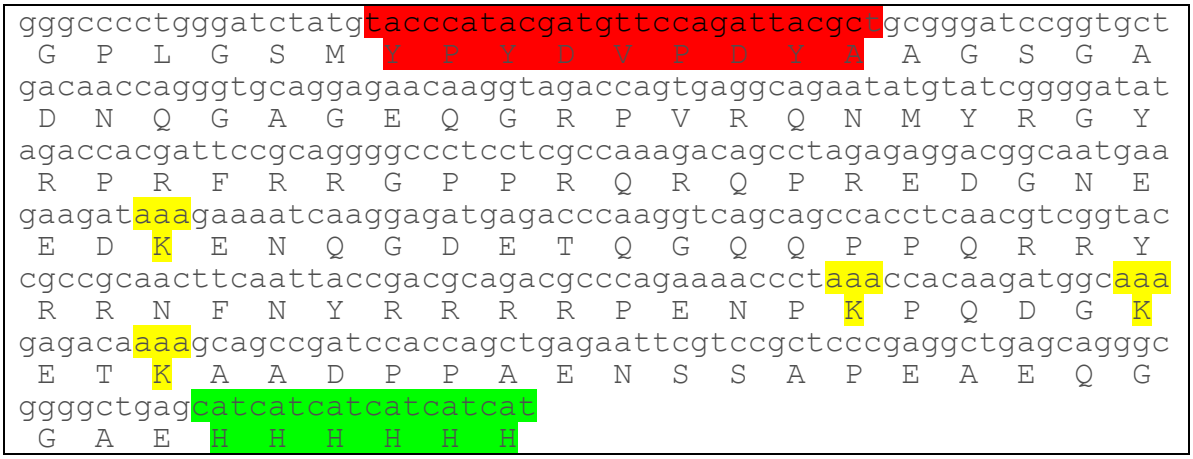

Figure 3.9: DNA sequence and mRNA translation of HA-YB-1$_{220-324}$. YB-1$_{220-324}$ comprises residues 220-324 of YB-1 followed by a 6xHis tag. HA tag indicated in red and 6xHis tag indicated in green. The four lysines are indicated in yellow. BamHI and XhoI sites (turquoise and red respectively) were added to the ends to facilitate cloning into the same sites in the vector. The significance of the KpnI site (GGTACC – indicated in blue) is explained below.

The fragment was amplified from full length YB-1 using the primers shown in Table 3.2 and cloned into the pGEX-HA-DWNN-GG construct described above, following excision of the DWNN-GG with BamHI and XhoI. Because YB-1 had previously been seen to be susceptible to degradation from the C-terminus a 6His tag was incorporated into the reverse primer (shown in green), to facilitate purification of full length YB-1$_{220-324}$ and not degradation products. The amino acid sequence of the protein following removal of GST is shown in Figure 3.9.

UNIVERSITY of the
WESTERN CAPE

Table 3.2: **Oligonucleotides used to amplify the YB-1$_{220-324}$ fragment**. The restriction enzymes sites are coloured (BamHI turquoise and XhoI red) and 6xHis in green. What do the underlined bps signifiy? Where is the underlining in the forward primer?

Primer name	Primer sequence	Primer melting temperature
Forward primer	5′- GAG GCGGGA TCCGGT GCT GAC AAC CAG GGT G -3′	62 °C
Reverse primer	5′-GAG GCGCTC GAG TTA ATG ATG ATG ATG ATG ATG CTC AGC CCC GCC CTG CTC-3′	64 °C

A 348 bp amplicon corresponding to YB-1$_{220-324}$ was successfully amplified using full length YB-1 as template, as shown in lane 3 of Figure 3.10(A). The amplicon was digested with BamHI and XhoI and cloned into the pGEX-HA-DWNN-GG vector following excision of the DWNN-GG fragment with the same restriction enzymes. Putative positive clones were screened by colony-PCR using the primers in Table 3.2 and confirmed by digestion of plasmid DNA to release the insert, as shown in Figure 3.10, panels (B) and (C). Positive clones were confirmed by DNA sequencing (Inqaba Biotechnical Industries (Pty) Ltd) and found to be 100 % in agreement with the expected sequence (Appendix).

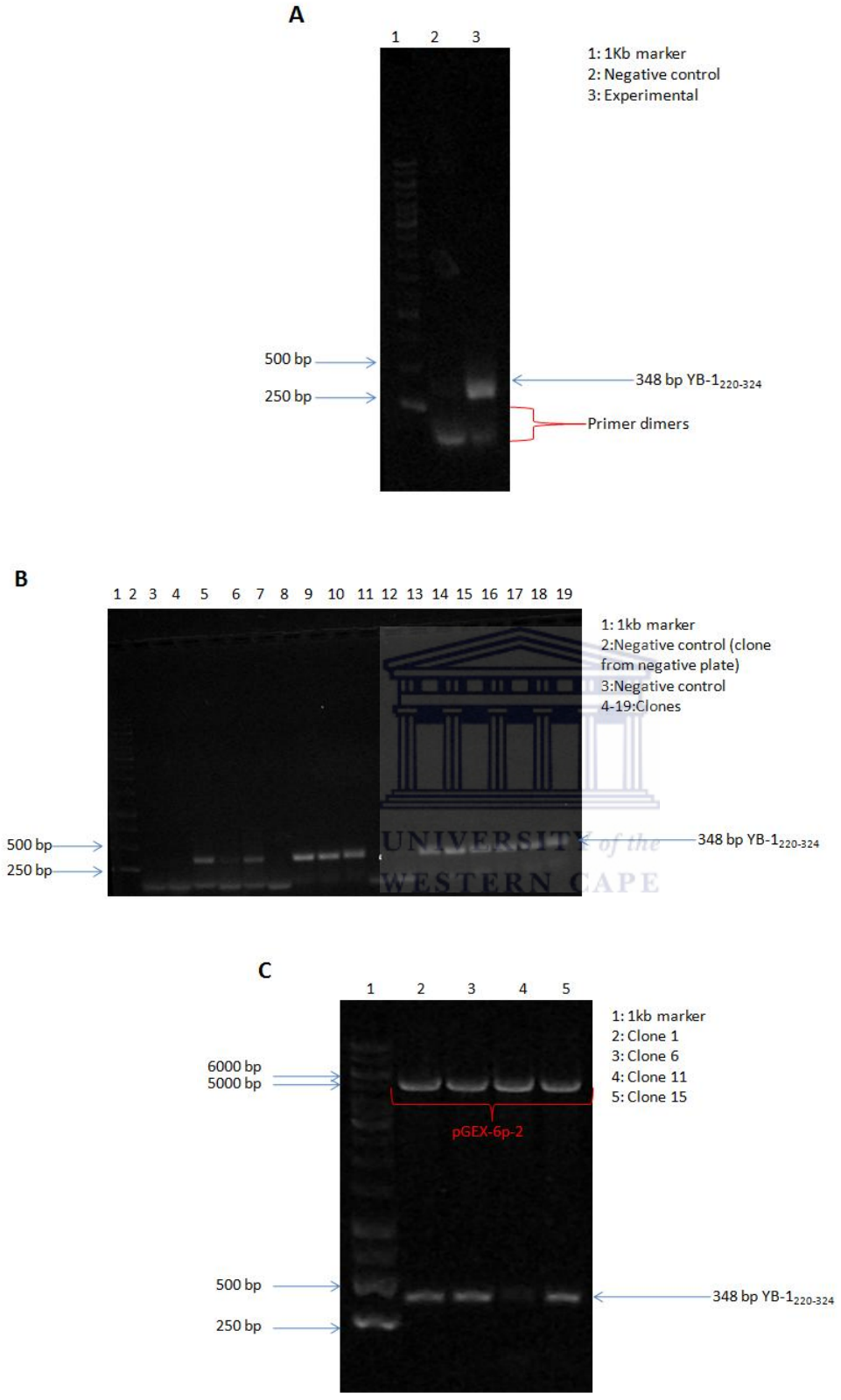

Figure 3.10: Cloning of wild type YB-$1_{220-324}$ into pGEX-HA-DWNN-GG. (A) The YB-$1_{220-324}$ fragment was amplified from the pGEX-YB-1_{FL} construct. Lane 3 contains a 348 bp band which corresponds to the YB-$1_{220-324}$ amplicon size. Lane 2 contains a no template DNA control which is negative containing only primer dimers. (B) Putative positive colonies were screened using colony-PCR. Lanes 2 and 3 contained negative controls in which no template DNA and a no-insert colony were used respectively. Lanes 4-19 contain amplicons of putative positive colonies. (C) Screening of positive colonies by digesting with BamHI and XhoI to release the YB-$1_{220-324}$ insert. Lanes 2-5 all contain a 348 bp insert corresponding to YB-$1_{220-324}$.

3.4.3. Cloning of YB-1$_{220-324}$-RRRR and -RKKK mutants

Another motivation for cloning of the YB-1$_{220-324}$ fragment was the hope that it would serve as a well-behaved substrate for *in vitro* ubiquitination studies of YB-1 by RBBP6. Full length YB-1 has been shown by Dr Andrew Faro, a co-worker in the laboratory, to be poly-ubiquitinated by RBBP6 *in vitro*. Since RBBP6 is known to interact with the C-terminus of YB-1, we expected that YB-1$_{220-324}$ would also be ubiquitinated by RBBP6. YB-1$_{220-324}$ contains only four lysines (see Fig 3.9) rather than the sixteen in full length YB-1, making it feasible to replace them individually with arginines in order to determine if ubiquitination was taking place exclusively on any one of them.

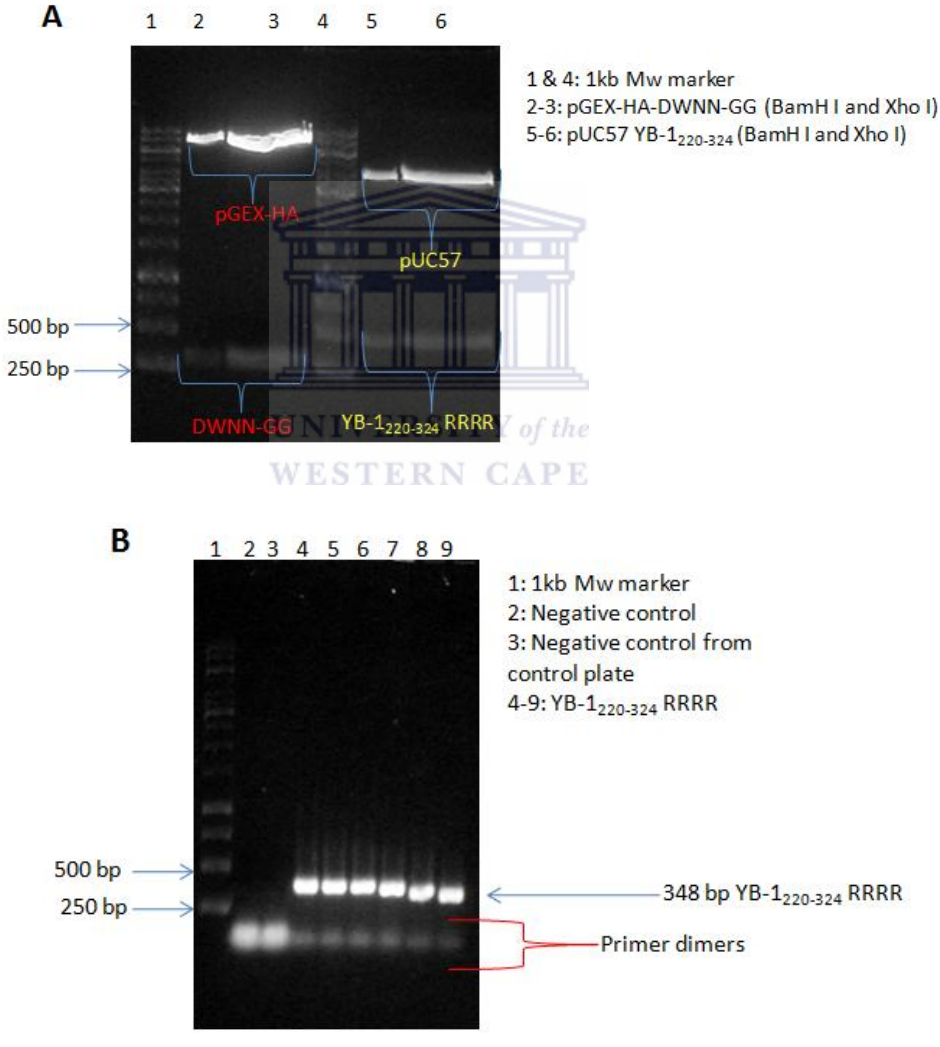

Figure 3.11: Sub-cloning of YB-1$_{220-324}$-RRRR mutant into pGEX-HA-DWNN-GG. (A) YB-1$_{220-324}$-RRRR mutant was sub-cloned from a pUC57 vector into a pGEX-6p-2-HA vector (pGEX-HA-ΔDWNN-GG). Lanes 2 and 3 contain the pGEX-HA-DWNN-GG vector digested with BamHI and XhoI releasing the DWNN-GG insert 232 bp and the pGEX-HA vector 5.7 kb. Lanes 5 and 6 contain the pUC57 YB-1$_{220-324}$-RRRR mutant construct digested with BamHI and XhoI releasing the YB-1$_{220-324}$-RRRR mutant 348 bp. (B) Screening of putative positive colonies using colony pcr. Lane 2 and 3 contains no template DNA and background negative colony controls. Lanes 3-9 contain amplicons of the expected size of YB-1$_{220-324}$-RRRR 348 bp.

UNIVERSITY of the
WESTERN CAPE

We began by replacing all four lysines with arginines, since this would serve as a useful negative control for ubiquitination of wild type YB-$1_{220\text{-}324}$. The construct was dubbed YB-$1_{220\text{-}324}$-RRRR, to distinguish it from YB-$1_{220\text{-}324}$-KKKK, which is better known as wild type YB-$1_{220\text{-}324}$. To save time YB-$1_{220\text{-}324}$-RRRR, flanked by BamHI and XhoI sites and incorporating the C-terminal 6xHis tag also present in wild type YB-$1_{220\text{-}324}$, was synthesised by Genscript Inc. (Piscataway, NJ, USA) and delivered in a pUC57 plasmid. The insert was released using BamHI and XhoI (Fig 3.11(A), lanes 5-6) and sub-cloned into the pGEX-HA-DWNN-GG plasmid following excision of DWNN-GG (Fig 3.11(A), lanes 2-3). Putative positive clones were screened by colony-PCR using the primers in Table 3.2, as shown in Figure 3.11(B). The sequences were verified by direct sequencing and found to be 100 % in agreement with the expected sequence, including replacement of codon AAA, corresponding to lysine, with CGC, corresponding to arginine, in four places (Appendix).

The next step involved mutation of the first lysine, lysine-247, to arginine. We realised that rather than use PCR-based mutagenesis, which carries a significant risk of introducing unwanted mutations, the same effect could be achieved using sub-cloning alone for which the risk of mutations is less. As can be seen from Figure 3.9, YB-$1_{220\text{-}324}$ contains a KpnI site (GGTACC, indicated in blue) between the first and the second lysines. Hence sub-cloning the KpnI/XhoI fragment from YB-$1_{220\text{-}324}$-RRRR into the KpnI/XhoI sites of wild type YB-$1_{220\text{-}324}$ would replace lysines 2, 3 and 4 with arginines, producing a construct dubbed “KRRR”. This was successfully achieved, as shown in Figure 3.12. The sequences were verified by direct sequencing and were found to be 100 % in agreement with the expected sequence, including replacement of codon AAA, corresponding to lysine, with CGC, corresponding to arginine, in positions 2, 3 and 4 (Appendix).

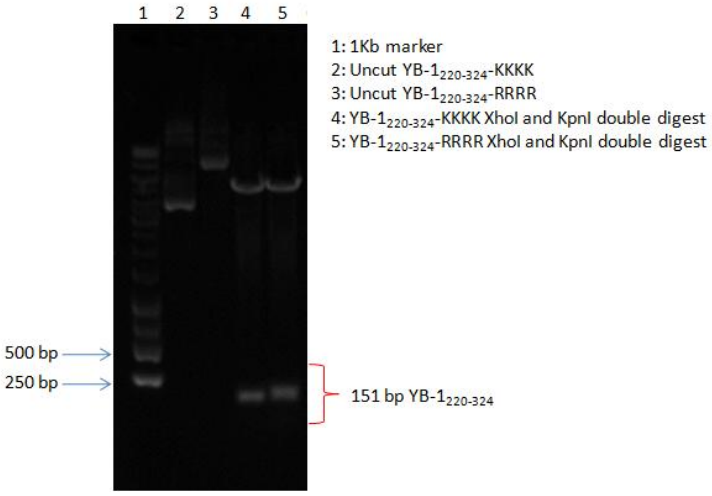

Figure 3.12: Sub-cloning of YB-$1_{220\text{-}324}$-KRRR mutant into pGEX-HA-DWNN-GG. YB-$1_{220\text{-}324}$-KRRR was constructed by sub-cloning the KpnI/XhoI fragment from YB-$1_{220\text{-}324}$–RRRR into wild type YB-$1_{220\text{-}324}$. Lanes 2 and 3 contain the uncut wild type YB-$1_{220\text{-}324}$ and YB-$1_{220\text{-}324}$ -RRRR constructs respectively. Lanes 4 and 5 contain the same constructs digested with XhoI and KpnI releasing a 151 bp insert in each case.

3.4.4. Expression and purification of wild type YB-1$_{220-324}$ and the RRRR and RKKK mutants

The pGEX-HA-YB-1$_{220-324}$-6xHis construct was transformed into the *E. coli* BL21 expression host and used to over-express wild type GST-HA-YB-1$_{220-324}$-6xHis. Taking advantage of the GST tag the fusion protein was purified using glutathione affinity chromatography, followed by nickel ion affinity, as shown in Figures 3.13(A). The fusion protein migrates at the expected molecular weight of approximately 40 kDa, corresponding to 27 kDa (GST) plus 12.5 kDa (YB-1$_{220-324}$-6xHis). Unfortunately a number of lower molecular weight bands were present despite the use of two purification methods. Nevertheless the GST-tag was cleaved using 3C protease and separated from YB-1$_{220-324}$ using a second round of glutathione affinity chromatography.

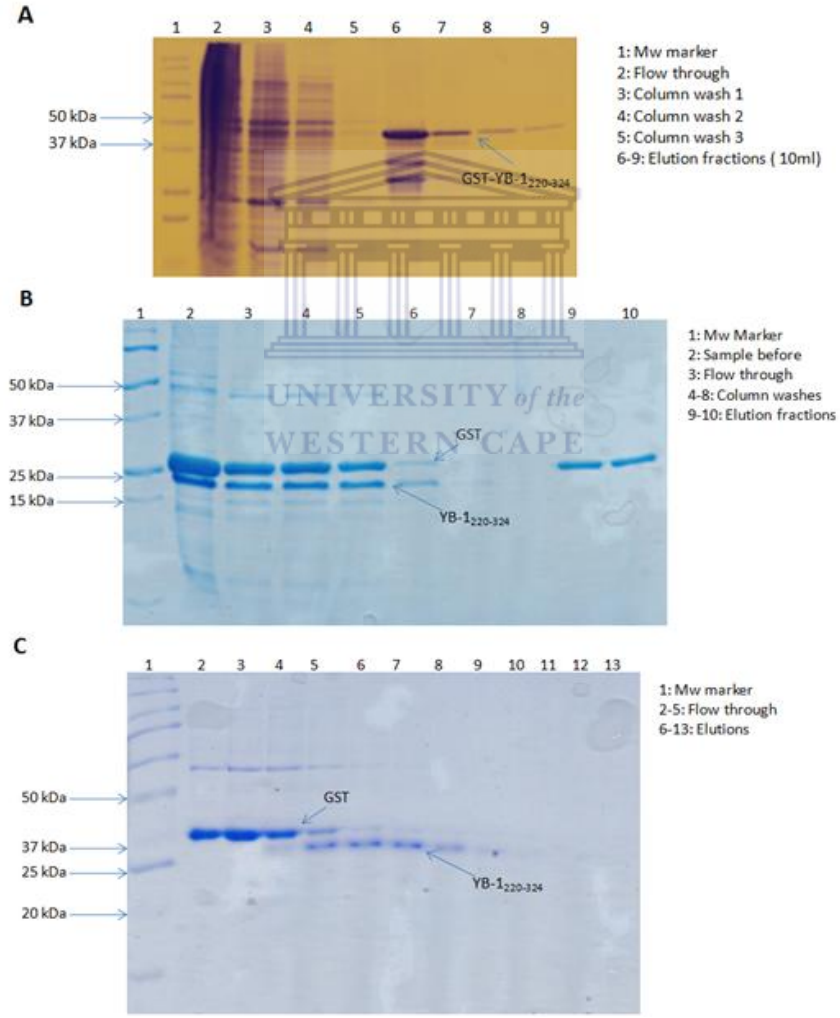

Figure 3.13: Purification of HA-YB-1$_{220-324}$-6xHis fusion protein (A) YB-1$_{220-324}$ was first purified using a glutathione agarose column, taking advantage of the N-terminal GST tag. Lanes 6-9 contain a 40 kDa band corresponding to the expected size of GST-HA-YB-1$_{220-324}$-6xHis. (B) Following cleavage with GST-HRV 3C GST and HA-YB-1$_{220-324}$ was separated on a glutathione agarose column. Lane 2 contains the cleaved sample before purification with 2 major bands 26 and 24 kDa in size corresponding to the size of GST and YB-1$_{220-324}$. Lanes 4-8 contain the column wash fractions which contain both GST and YB-1$_{220-324}$. Lanes 9 and 10 contain the elution fractions which contain GST. (C) YB-1$_{220-324}$ was further purified using a HisTrap affinity column. Lanes 2-4 contain the flow through fractions which contain GST and GST-HRV 3C. Lane 6-10 contains the elution fractions which contain YB-1$_{220-324}$ and residual GST.

Figure 3.13(B) confirms that the fusion protein was efficiently cleaved by the 3C protease, producing two distinct bands, and confirms that the top band is GST, since it is eluted from the column by free glutathione (lanes 9 and 10). Surprisingly HA-YB-$1_{220-324}$-6xHis,, which is the lower band, migrates at an effective molecular weight of approximately 24 kDa, which is almost twice the expected size of 12.5 kDa. Although some of the GST was retained by the column and eluted in lanes 9 and 10, the procedure did not result in effective separation of GST from HA-YB-$1_{220-324}$-6xHis in lanes 3-6.

Taking advantage of the C-terminal 6xHis-tag, nickel ion affinity chromatography was used to remove the remaining GST. Figure 3.13(C) shows that this method was more successful in separating the two proteins, with most of the GST remaining in the flow through and most of HA-YB-$1_{220-324}$-6xHis being eluted from the column following addition of 500 mM imidazole, with much reduced contamination by GST. Samples of YB-$1_{220-324}$-RRRR and YB-$1_{220-324}$-KRRR were expressed in the same way, with efficiencies similar to that of the wild type, as shown in Figures 3.14(A) and (B) respectively.

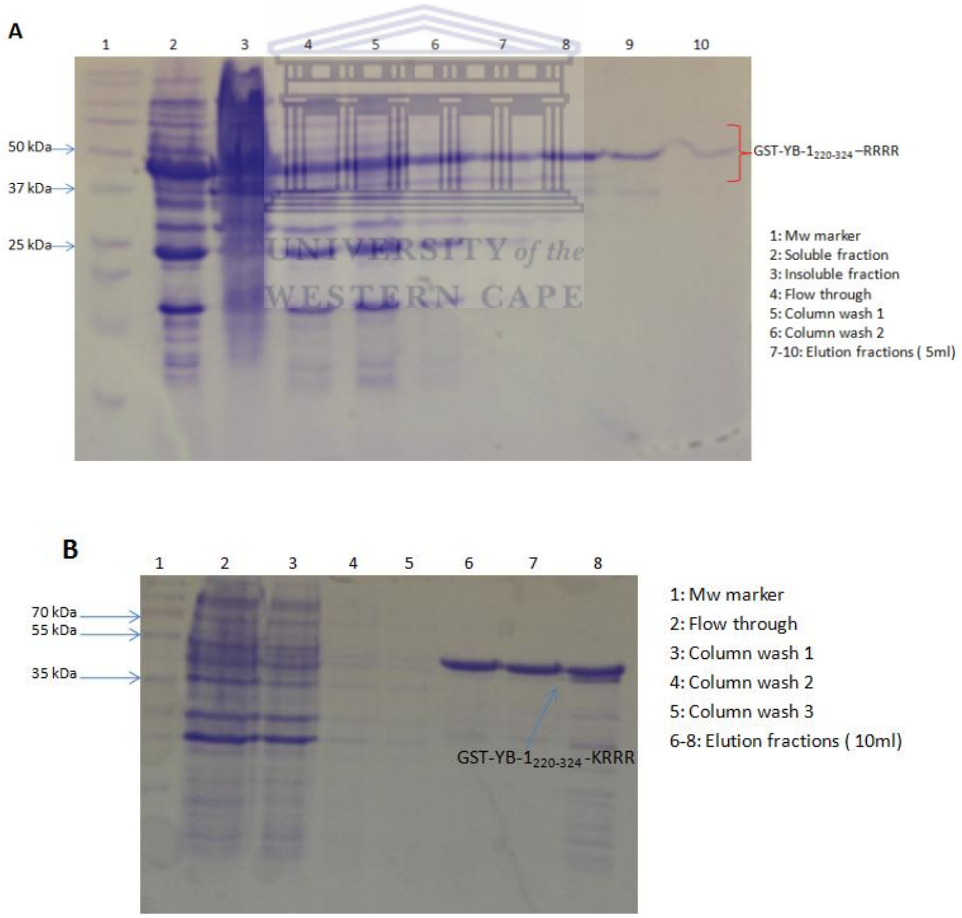

Figure 3.14: Expression and purification of GST-HA-YB-$1_{220-324}$ mutants -RRRR and -KRRR. (A) HA-YB-$1_{220-324}$-RRRR was purified using a glutathione agarose column. Lanes 7-10 contain a 40 kDa band that corresponds to the expected size of GST-HA- YB-$1_{220-324}$-6xHis-RRRR. (B) Glutathione agarose purification of GST-HA-YB-$1_{220-324}$-6xHis-KRRR. Lanes 7-10 contain a 40 kDa band that corresponds to the expected size of GST-HA-YB-$1_{220-324}$-6xHis-KRRR.

3.4.5. The RING finger of RBBP6 and the YB-1$_{220-324}$ fragment co-precipitate each other in GST pull-down assays

Interaction between full length YB-1 and RBBP6 in human cell lysate was shown in Section 3.5. In order to investigate whether the YB-1$_{220-324}$ fragment of YB-1 interacts directly with the RING finger of RBBP6 *in vitro*, GST affinity pulldown assays were performed using GST-RBBP6-RING-conjugated to glutathione agarose beads as "bait" and wild type HA-YB-1$_{220-324}$-6xHis as "prey". The expected molecular weight of HA-YB-1$_{220-324}$-6xHis is 12.5 kDa. Following incubation and extensive washing the proteins retained by the beads were analysed by western blotting using the polyclonal anti-YB-1 antibody described in Section 2.1. As shown in Figure 3.15, GST-RBBP6-RING was able to pull down HA-YB-1$_{220-324}$-6xHis (lane 5), whereas neither GST alone (lane 3) nor the glutathione-conjugated beads alone were able (lanes 4). Although small amounts of HA-YB-1$_{220-324}$-6xHis are evident in lanes 3 and 4, there is significantly less than in lane 5, and is most likely due to insufficient washing of the beads.

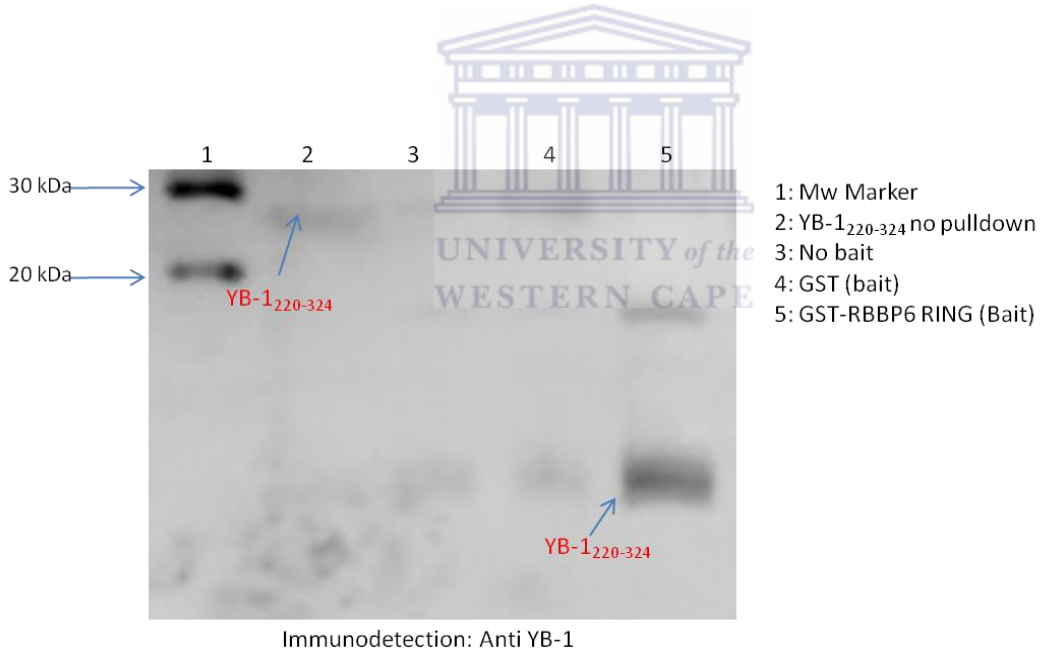

Figure 3.15: Immunodetection of wild type HA-YB-1 $_{220-324}$-6xHis (KKKK) precipitated by GST-RBBP6-RING. GST-RBBP6-RING is able to precipitate YB-1$_{220-324}$-6xHis (lane 5), whereas GST and the glutathione-conjugated beads alone cannot (lanes 4 and 3 respectively). Equal amounts of HA-YB-1$_{220-324}$-6xHis and equal amounts of glutathione agarose were added to lanes 3, 4 and 5. Ten times less YB-1$_{220-324}$ was added to lane 2, which was not subjected to pull-down, compared to lanes 3-5.

In lanes 3-5 HA-YB-1$_{220-324}$-6xHis predominantly migrates at its expected molecular weight of 12.5 kDa, whereas when loaded directly onto the gel it migrates at around 24 kDa (lane 2), which is consistent with its behaviour during purification (Fig 3.13, (C) and (D)). Smaller amounts can be seen at both molecular weights in all lanes. This anomalous behaviour of the C-terminus of YB-1 has been reported previously (Evdokimova *et al.,* 1995) and may be the result of the highly charged nature of

the CTD of YB-1. Nevertheless lanes 3-4 suggest that the change in its behaviour may be the result of the presence of the glutathione agarose.

Taking a more quantitative approach, lanes 3-5 contain 10 times the amount of prey as was loaded in lane 2 (which was loaded directly onto the gel without precipitation). After the final wash glutathione agarose pellets were re-suspended in 30 µl SDS sample buffer, of which 15 µl was loaded on a SDS PAGE gel for analysis. Hence if all of the prey in lane 5 were pulled down we would expect the signal in lane 5 to be 10/2 = 5 x more intense than that in lane 2. The differing banding patterns in lane 2 and lane 5 make comparisons difficult, but a rough estimate suggests that the signal in lane 5 is of the order of 5 times that in lane. Hence we conclude that HA-YB-$1_{220\text{-}324}$-6xHis does interact with the RING finger of RBBP6, and that the interaction is relatively strong.

To further confirm the interaction the roles of the bait and prey were swopped around: GST-HA-YB-$1_{220\text{-}324}$-6xHis was used as bait and RBBP6-RING as prey. The results were analysed by western blotting using a polyclonal antibody targeting RBBP6-RING (Section 2.1), which detected a single band below 20 kDa, as can be seen in lane 3 of Figure 3.16, which was loaded directly onto the gel without pull-down. Equal amounts of RBBP6-RING were loaded in lanes 6 and 8 (nothing was loaded in lane 7). GST-HA-YB-$1_{220\text{-}324}$-6xHis was able to pulldown RBBP6-RING (lane 8), whereas neither GST alone (lane 6) nor the glutathione-conjugated beads (lane 5) were able to, at least to the same extent.

UNIVERSITY of the
WESTERN CAPE

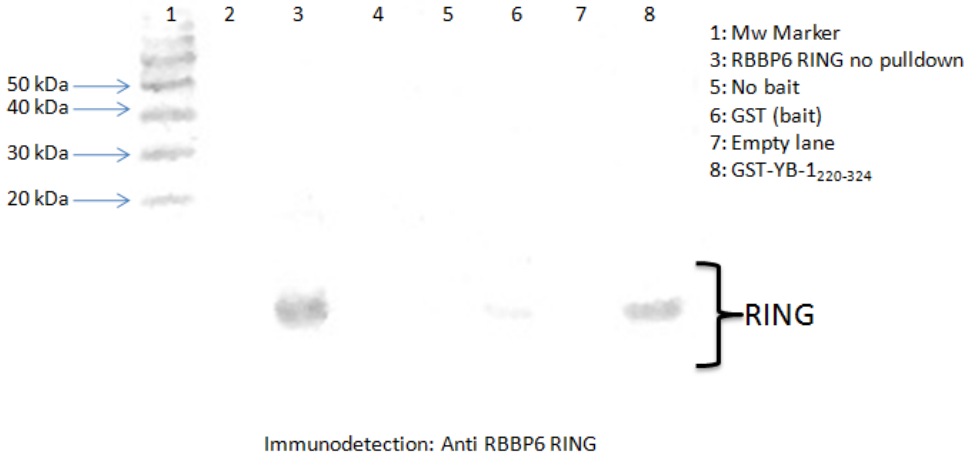

Figure 3.16: Immunodetection of RBBP6 RING precipitated by GST-HA-YB-$1_{220\text{-}324}$-6xHis. Equal amounts of RBBP6 RING and glutathione agarose was added to lanes 5,6 and 8. GST-YB-$1_{220\text{-}324}$ WT is able to precipitate RBBP6 RING 10 kDa Lane 8, whereas GST and the beads Lanes 6 and 5 respectively cannot. The faint band in lane 6 is much less intense compared to lane 8 and represents background. Lane 3 contains the RBBP6 RING as a control. Equal amounts of RBBP6-RING and glutathione agarose beads were added to lanes 5-8 and pull down assays conducted as described previously. Five times less RBBP6-RING was added to lane 3 then pulldown lanes and no pull down was carried out, to serve as a molecular weight marker for RBBP6-RING.

Again taking more quantitative approach lanes 5-8 contain 5 times as much RBBP6-RING as lane 3. After the final wash glutathione agarose pellets were resuspended in 30 µl SDS sample buffer of which 10 µl was loaded on a SDS PAGE gel for analysis. Hence if all of the prey in lane 8 were pulled down we would expect the signal in lane 8 to be 5/3 = 1.7 x more intense than that in lane 3. In actual fact the signal in lane 8 is of the order of half as much as that in lane 3, which suggests that significantly less than 100 % of RBBP6-RING was precipitated. While this result disagrees with that from the reciprocal assay, it nevertheless provides independent confirmation that a significant interaction exists between the RING finger of RBBP6 and the YB-$1_{220-324}$ fragment of YB-1.

As has been mentioned above, a co-worker has shown, using samples prepared as part of this work, that wild type HA-YB-$1_{220-324}$-6xHis is ubiquitinated by RBBP6 whereas the RRRR mutant is not, as expected, due to the absence of lysines. Since we have shown above that HA-YB-$1_{220-324}$-6xHis interacts directly with RBBP6-RING, an alternative explanation for the lack of ubiquitination of HA-YB-$1_{220-324}$-6xHis-RRRR that needs to be ruled out is that HA-YB-$1_{220-324}$-6xHis-RRRR does not interact directly with RBBP6-RING. In order to investigate this possibility a GST-pull down assay was used to investigate whether HA-YB-$1_{220-324}$-RRRR could co-precipitate RBBP6-RING. Consistent with the previous result, wild type HA-YB-$1_{220-324}$-6xHis (lane 5) precipitates RBBP6-RING significantly better than either GST alone (lane 4) or when no bait is present (lane 3). Surprisingly, lane 6 suggests that HA-YB-$1_{220-324}$-6xHis-RRRR co-precipitates RBBP6-RING significantly better than wild type HA-YB-$1_{220-324}$-6xHis (lane 5 Nominally equal amounts of wild type and mutant HA-YB-$1_{220-324}$-6xHis and equal amounts of RBBP6-RING were added to lanes 5 and 6, and although the amounts might not have been exactly equal, it is unlikely that any differences would account for the large differences between the bands in lanes 5 and 6. Ideally the western blot should have been stripped and re-probed with antibodies against YB-1 in order to show that the amounts of wild type and mutant HA-YB-$1_{220-324}$-6xHis were in fact equal. Nevertheless we can conclude that HA-YB-$1_{220-324}$-6His-RRRR interacts with RBBP6-RING at least as well as with wild type HA-YB-$1_{220-324}$-6His and therefore the lack of ubiquitination of YB-$1_{220-324}$-6His-RRRR by RBBP6 can only be due to the absence of lysine residues. It is therefore a suitable negative control for wild-type YB-$1_{220-324}$ in ubiquitination assays as it still binds to RBBP6 but can't be ubiquitinated.

UNIVERSITY of the WESTERN CAPE

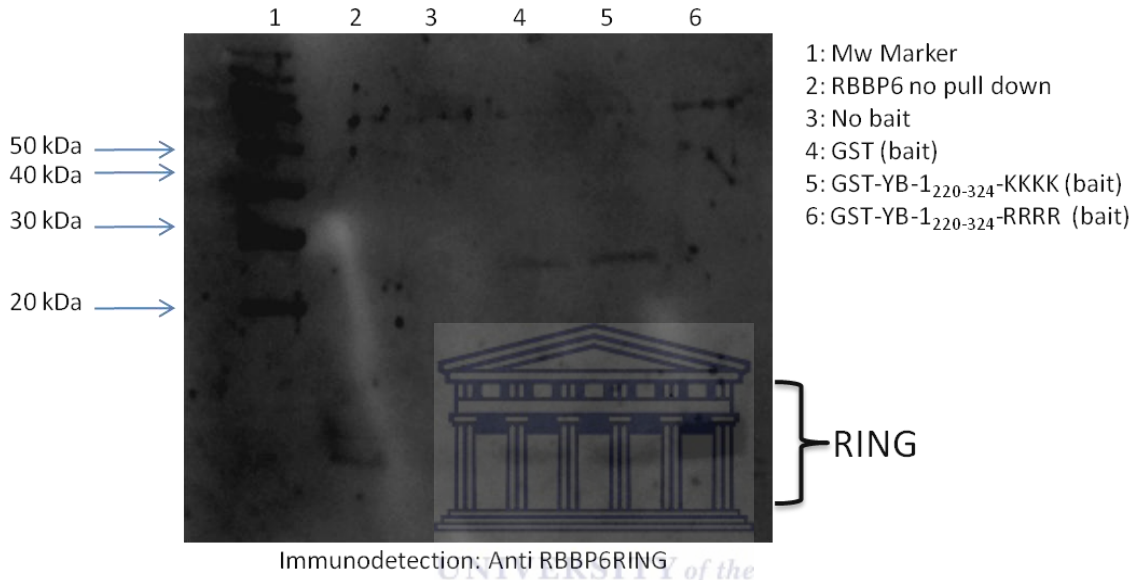

UNIVERSITY of the
WESTERN CAPE

Figure 3.17: Immunodetection of RBBP6-RING precipitated by GST-HA-YB-$1_{220-324}$-6xHis-KKKK and -RRRR. GST-YB-1_{220-32}-KKKK and -RRRR are able to precipitate RBBP6-RING 10 kDa (lanes 5 and 6 respectively), whereas GST and the beads (lanes 3 and 4 respectively) cannot. The feint band in lane 4 is much less intense compared to lanes 5 and 6 and represents background. Equal amounts of RBBP6-RING and glutathione agarose beads were added to lanes 3-6 and pull down assays conducted as described previously. RBBP6-RING was added to lane 2 but no pull down was carried out

3.5. UbcH1 interacts with the RING finger of RBBP6 in vitro

3.5.1. Expression and purification of UbcH1

A cDNA construct encoding UbcH1 was obtained from the Addgene repository (Plasmid No: 31436, deposited by Prof. Rachel Klevit, University of Washington, Seattle) and cloned into the pGEX-6P-2 bacterial expression vector by Ms Lauren Jooste, a co-worker in the Pugh laboratory at UWC. The final construct was fully validated by direct DNA sequencing. GST-UbcH1 was expressed in *E. coli* BL21 and purified away from the endogenous *E. coli* proteins using a gravity flow glutathione agarose column, as described earlier in this thesis. Significant quantities of the 48.4 kDa fusion protein (GST 26 kDa; UbcH1 22.4 kDa) can be seen migrating at approximately 50 kDa in lanes 6-9 of Figure 3.18(A).

Uncleaved GST-UbcH1 was used for the pull-down assay described below. For NMR analysis the GST tag was cleaved using 3C protease and separated from UbcH1 by a second round of glutathione affinity chromatography, with GST being retained by the column and UbcH1 collected in the flow through (see Figure 3.18(B)). This procedure was complicated by the similarity in size between GST (26 kDa, lane 7) and UbcH1 (22.4 kDa, lanes 2 and 3), requiring a number of rounds of purification to eliminate residual GST. During this process UbcH1 appears to have become partially proteolysed, yielding a fragment around 18 kDa in addition to the 22.4 kDa bands, as seen in Figure 3.18 (B). Final purification and exchange into NMR buffer was carried out using a Hiload Superdex 75 16/600 SEC column, as shown in Figure 3.18(C), by which time the lower, presumably proteolysed fragment, was predominant. Mass spectrometric analysis confirmed that the sample contained only fragments of between 19 and 20 kDa, as shown in Figure 3.18(D), compared with the expected mass of 22.4 kDa. Since the ubiquitin-associated domain (UBA) of UbcH1 comprises the last 40 residues of the protein (residues 160 – 200), with a molecular weight of around 4.5 kDa, and is attached to the E2 domain via a flexible linker, it is highly probable that the UbcH1 sample had been truncated near the beginning of the UBA.

UNIVERSITY of the
WESTERN CAPE

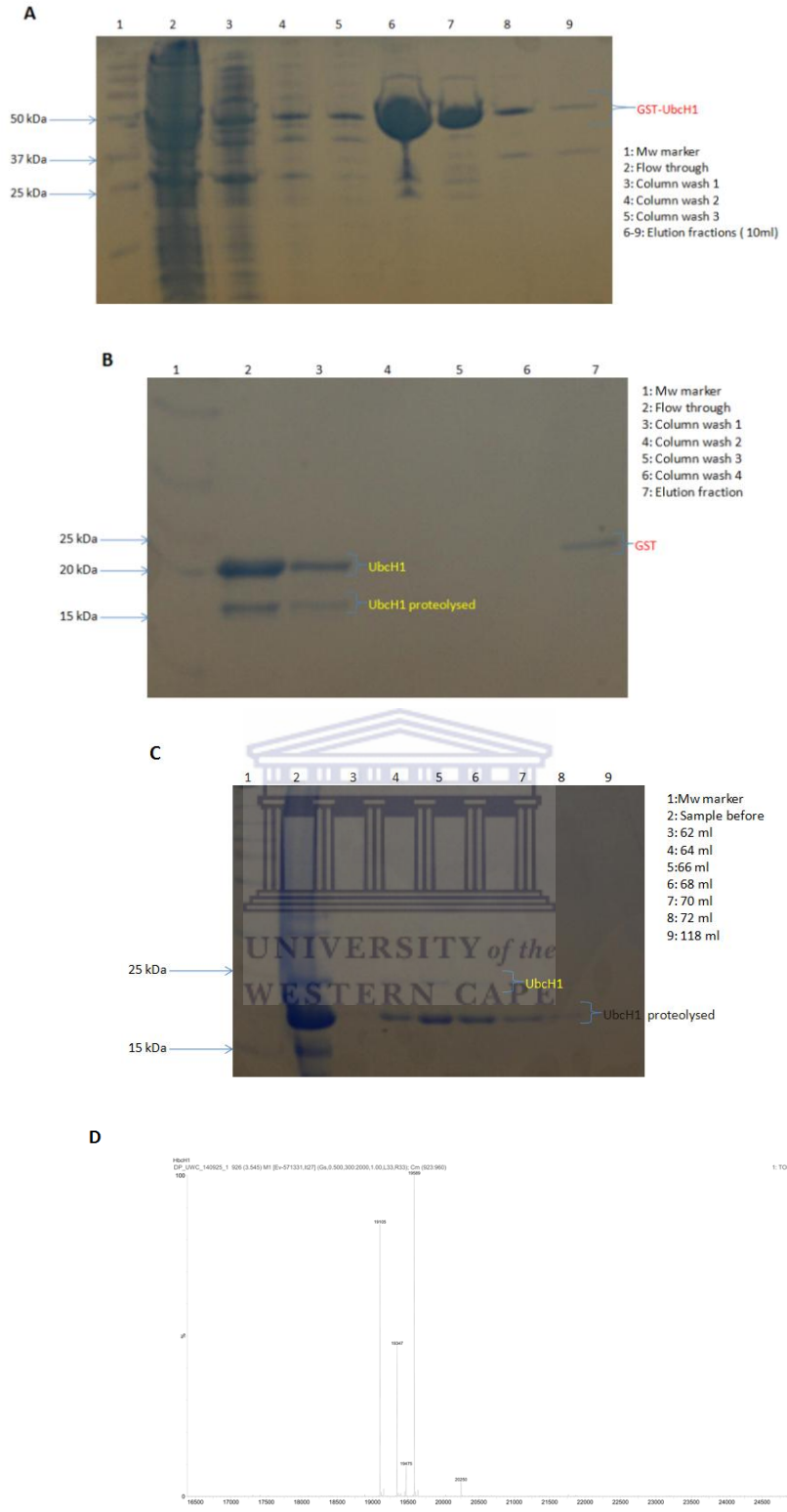

Figure 3.18: Expression and purification of UbcH1. (A) UbcH1 was purified using a glutathione agarose column. Lanes 6-9 contain ~50 kDa bands which correspond to the expected size of GST-UbcH1 (GST 26 kDa and UbcH1 22.4 kDa). The purified protein was then cleaved with recombinant 3C protease. (B) Following cleavage the protein was purified from GST using a glutathione agarose column. UbcH1 underwent partial proteolysis with two major bands ~22 kDa and ~18 kDa in lanes 2 and 3. (C) Concentrated UbcH1 was further purified using Size Exclusion Chromatography. Lane 1 contained a concentrated sample containing multiple bands with two major bands 22 kDa and 19 kDa corresponding to UbcH1 and UbcH1 degradation product respectively. (D) Mass spectrometry spectrum of pooled sample confirming the presence of fragments with masses around 19 and 20 kDa, compared to the expected mass of 22.5 kDa. This is likely to be the result of proteolytic removal of the UBA domain which makes up the last 40 residues of UbcH1.

3.5.2. UbcH1 binds to the RING finger domain of RBBP6 in vitro

A glutathione-affinity pull-down assay was carried out using GST-UbcH1 as bait and the RING finger of RBBP6 (RBBP6-RING) as prey, as shown in Figure 3.19. Equal quantities of glutathione-conjugated agarose and RBBP6-RING were added to each of lanes 4-6 and immunodetection of RBBP6-RING was carried out using a poly-clonal rabbit antibody raised against recombinant RING finger as described earlier in this thesis.

GST-UbcH1 was was able to precipitate RBBP6-RING very effectively (lane 6), whereas isolated GST was not (lane 5) and nor was the glutathione-conjugated agarose alone (lane 4). Comparison with lane 3, which contains only, RBBP6-RING, to which no pull down was applied, confirms that what is precipitated in lane 6 is indeed RBBP6-RING, but significantly more concentrated than that in lane 3.

The strength of the signal in lane 6 suggests that a large fraction of the prey has been precipitated. More quantitatively, 10 times the amount of RBBP6-RING was added to the precipitation assay (lane 6) than what was added to lane 3, which was not subject to pull down. A ¼ of the final precipitate was loaded in lane 6. Hence if all of the prey were precipitated we would expect the signal in lane 6 to be ¼ * 10 = 2.5 times as intense as that in lane 3. It looks significantly more intense than that, which throws some doubt on the result. Unfortunately neither an anti-UbcH1 nor an anti-GST antibody was available in the laboratory, so the interaction could not be repeated the other way around. Nevertheless we conclude that a definite interaction was observed between RBBP6-RING and UbcH1.

UNIVERSITY of the
WESTERN CAPE

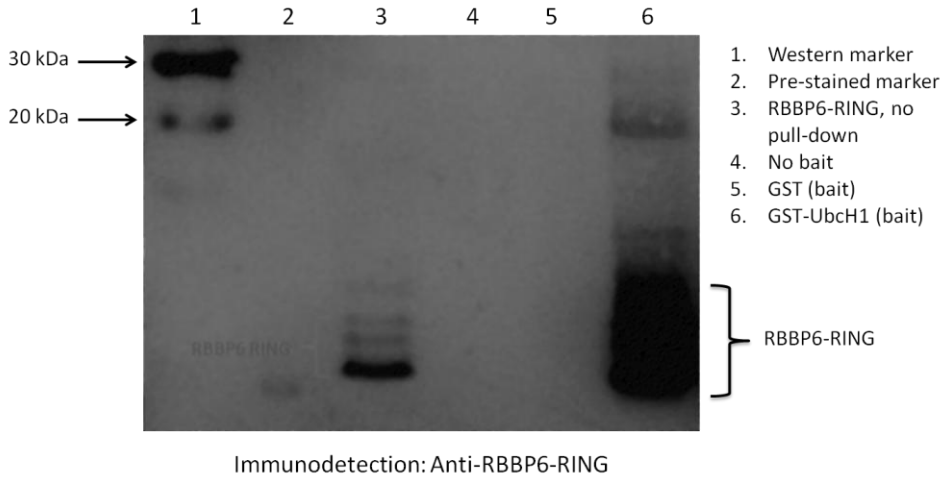

Figure 3.19: Immunodetection of recombinant RBBP6 RING precipitated by GST-UbcH1. Equal amounts of bacterially-expressed RBBP6-RING and glutathione-agarose beads were added to lanes 4-6. Bait proteins were added as indicated in the key. GST-UbcH1 was able to pull-down RBBP6-RING (lane 6), which is clearly the same protein as was added to lane 3, but which was not subjected to precipitation. When GST alone was used as bait (lane 5), or the bait was omitted altogether (lane 4), RBBP6-RING not was co-precipitated.

3.5.3. Chemical shift perturbation of ^{15}N-labelled RBBP6-RING finger by un-labelled UbcH1

The interaction between UbcH1 and the RING finger domain of RBBP6 was investigated further by NMR chemical shift perturbation assay. This assay investigates the chemical shift changes produced in the ^{15}N-HSQC spectrum of a ^{15}N-enriched protein when a second, un-labelled, protein is added. The un-labelled protein is not detected in the ^{15}N-HSQC spectrum; only its effects on the spectrum of the labelled protein are detected. The assay has been shown to be a very sensitive measure of protein-protein interactions (Ko *et al*. 2010); where the ^{15}N-HSQC of the labelled protein has been assigned, as it has in the case of RBBP6-RING, the assay allows for immediate identification of residues adjacent to the interaction interface.

A ^{15}N-labelled sample of RBBP6-RING was expressed and purified as described in the previous section. As is evident from Figure 3.18 UbcH1 expressed very well but was partially proteolysed during the purification steps. UbcH1 was concentrated into 400 µl without any major aggregation to a final concentration of 31.3 mg/ml, which for a 22.4 kDa protein corresponds to 1.4 mM. A 0.15 mM sample of 100 % ^{15}N-enriched RBBP6-RING was produced as described in Section 3.4 and used to record a ^{15}N-HSQC spectrum at 500 MHz for 8 hours. As seen in Figure 3.20(A) the spectrum shows good dispersion of resonances in both the ^{1}H and ^{15}N dimensions, which is indicative of a folded protein. The spectrum is also consistent with the assigned spectrum published by Kappo and co-workers (Kappo *et al.* 2012), although it is a much weaker sample. 20 µl, 60 µl, 100 µl and 140 µl of unlabelled UbcH1, corresponding to labelled:unlabelled molecular ratios of 1:0.3, 1:0.9, 1:1.5 and 1:2.2 respectively, were then added, and a ^{15}N-HSQC spectrum recorded following each addition, each taking 8 hours to record. An overlay of the spectra, each in a different colour, is shown in Figure 3.20(B).

A number of chemical shift changes are visible, such as those indicated by squares and shown in Figure 3.20(B). However the directions and magnitudes of these shifts are consistent with concentration-induced effects produced by the increases in volume brought about by addition of UbcH1. RBBP6-RING is known to be a mixture of monomer and homo-dimer at these concentrations, with the NMR spectrum being a population-weighted average of the two conformations (Kappo *et al.* 2012). Even small reductions in concentration will shift the equilibrium towards the monomeric conformation, with corresponding effects on the spectrum. Comparison of panels (C) of Figure 3.20 with Figure 5 of Kappo *et al* (2012) shows that the chemical shift perturbations in this study are consistent with the low-concentration end of the concentration range used by Kappo and co-workers. This is as expected because the concentrations used in this study are in the range 150 µM –

120 µM (150 µM * dilution factor 600 µl/740 µl), whereas those used by Kappo and co-workers range from 1000 µM – 25 µM.

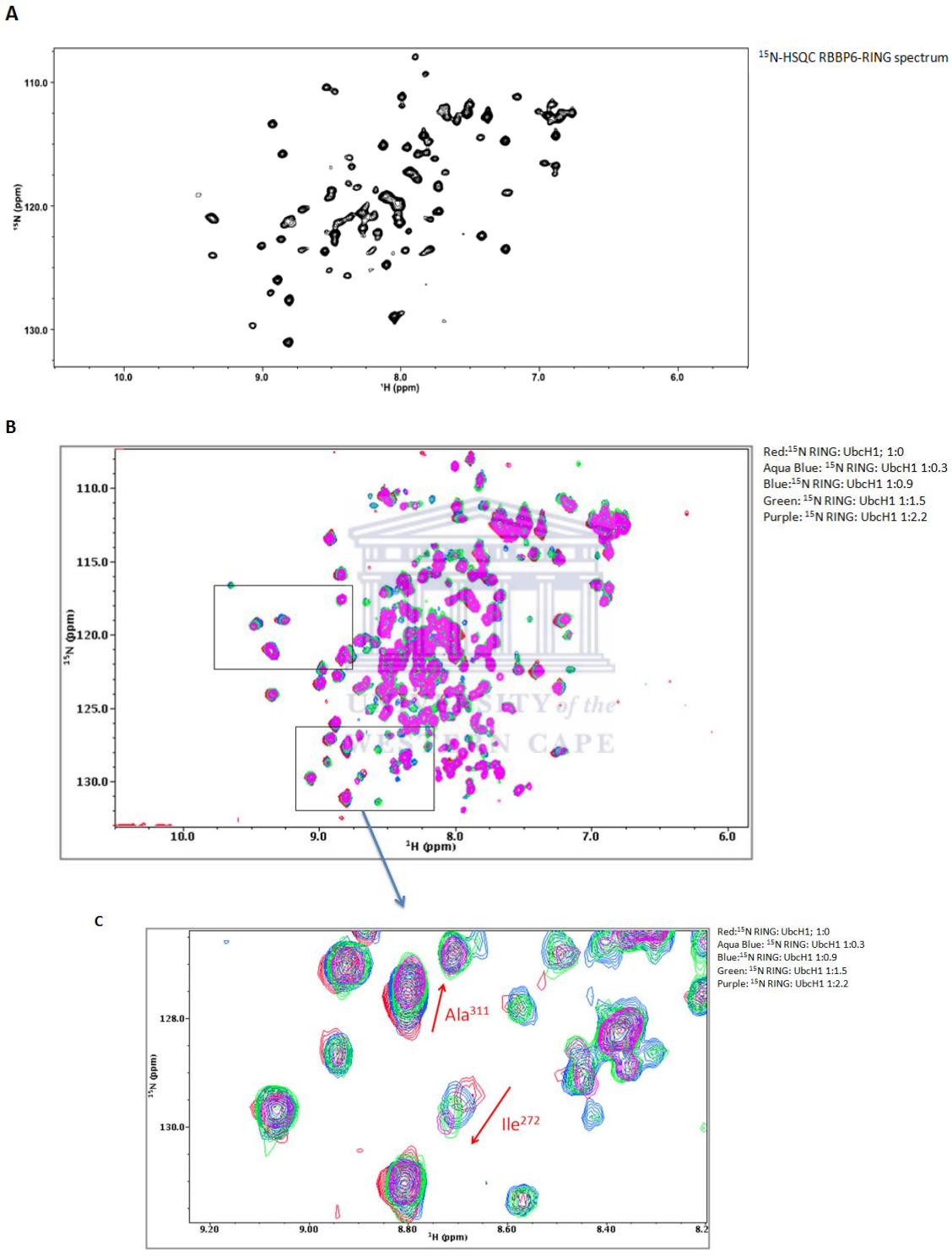

Figure 3.20: ^{15}N-HSQC spectra of the RBBP6 RING finger with and without unlabelled UbcH1. A) ^{15}N-HSQC spectrum of the RING finger domain was acquired at 25 °C on a 500 MHz spectrometer. The spectrum shows good dispersion of resonances, in both the ^{1}H and ^{15}N dimensions, indicative of a folded protein. B) The overlay of the ^{15}N-HSQC RING spectrum with no unlabelled UbcH1 (red) overlaid with the ^{15}N-HSQC RING spectrum with 20 µl (blue), 60 µl (blue), 100 µl (green) and 140 µl (purple) unlabelled UbcH1. C) Zoomed in chemical shifts observed upon addition of unlabeled UbcH1 which illustrates the shift from dimer to monomer.

The conclusion to be drawn from Figure 3.20 is that any chemical shift perturbations produced in the RBBP6-RING spectrum by UbcH1, following subtraction of the concentration effect, are likely to be small. Hence the data does not support anything more than a weak interaction between RBBP6-RING and UbcH1 which contradicts the conclusion drawn from the pull down assay shown in Figure 3.19. However, since the mass spectrum in Figure 3.18 suggests that the sample of UbcH1 used in the assay does not include the UBA domain one possible explanation for the lack of interaction is that the UBA is required for the interaction. The samples used in the pull-down shown in Figure 3.18 did not undergo the drawn-out series of purification steps used for production of the NMR sample and therefore are less likely to have suffered proteolytic removal of the UBA domain.

A second conclusion to be drawn from the above NMR study is that any chemical shift perturbation studies based on the ^{15}N-HSQC spectrum of RBBP6-RING are likely to be complicated by the intrinsic concentration-dependence of the spectrum. One way of overcoming this problem would be to base the assay on the ^{15}N-HSQC of UbcH1 rather than of RBBP6-RING. This will involve optimisation of expression of UbcH1 in minimal media for production of ^{15}N-labelled samples of the protein. However the high levels of expression and the lack of difficulty in concentrating the sample to mM concentrations suggests that this approach has a good chance of succeeding.

An alternative approach would be to base the investigation on the ^{15}N-HSQC of a monomeric form of RBBP6-RING. We have previously reported that the N312D and K313E mutants of RBBP6-RING are monomeric and that their ^{15}N-HSQC spectra are significantly less sensitive to changes in concentration than the spectrum of the wild type (Kappo et al 2012). The line-shapes of the spectra are also narrower than those of the wild type, as would be expected due to the smaller effective molecular weight of the protein, with the result that both resolution and sensitivity would be improved, boosting the chances of successfully carrying out the assay. Unpublished data from the Pugh laboratory shows that both the wild-type and mutants forms of the RBBP6-RING are able to auto-ubiquitinate themselves with UbcH1 playing the role of E2 which suggests that the monomeric form of UbcH1 still interacts with RBBP6-RING. Nevertheless it would be prudent to begin by showing that the mutant forms show significant interaction with UbcH1 using pull down assays, before going to the trouble of carrying out the NMR-based assay.

UNIVERSITY of the
WESTERN CAPE

3.6. MDM2 interacts directly with the RING finger domain of RBBP6 in vitro

Li and co-workers reported previously that RBBP6 interacts with MDM2 *in vivo* (Li *et al*., 2007). Our own results suggest that the R3 fragment of RBBP6, which consists of the first 335 amino acids of full length RBBP6 and contains the DWNN domain, the zinc knuckle and the RING finger domain, cooperates with MDM2 *in vitro* in ubiquitinating p53. Hence we would expect to observe a direct interaction between the R3 fragment of RBBP6 and MDM2 in *in vitro* immunoprecipitation studies. The R3 fragment had previously been shown in our laboratory to be suitable for expression in bacteria. Before trying to conduct a fully *in vitro* interaction with bacterially expressed MDM2, we decided to use endogenous MDM2 present in mammalian cells.

3.6.1. Co-precipitation of endogenous MDM2 by the R3 fragment of RBBP6

R3 was expressed in bacteria as a fusion with GST by a co-worker in the laboratory, Miss Portia Matodzi Maumela. HeLa cell lysate was supplied by Miss Andronica Ramaila, another co-worker in the laboratory. A glutathione-affinity pull down assay was carried out using GST-R3 as the bait and MDM2 as the prey, detecting MDM2 by western blot using antibody AB38618 (Abcam – Cambridge, MA, USA). This antibody recognises an epitope within residues 393-424 of MDM2 and has been shown to detect a band of 55 kDa, which corresponds to the expected size of MDM2, in mouse lens cells (Geatrell *et al.,* 2009). Note that this is at variance with other data showing that MDM2 migrates as a 98 kDa protein on SDS-PAGE (Jiang *et al.,* 2013). Although not published data, a number of reviews on the manufacturer's webpage for this antibody show detection of a 55 kDa band, which provide evidence that the protein detected by this antibody is in fact MDM2.

As can be seen from Figure 3.21 GST-R3 was able to precipitate a 55 kDa protein from HeLa cell lysate (lane 5). A similar-sized protein was detected in lysate which had not been subject to precipitation (lane 2), which is as expected. A similar-sized protein was also detected when the pull down was carried out without any bait (lane 3) or with GST as bait (lane 4), but the intensities are much less than when GST-R3 was used as bait. This is likely to be due to insufficiently stringent conditions during the wash steps. Nevertheless Figure 3.21 represents clear evidence of direct interaction between the R3 fragment of RBBP6 and endogenous MDM2.

UNIVERSITY of the
WESTERN CAPE

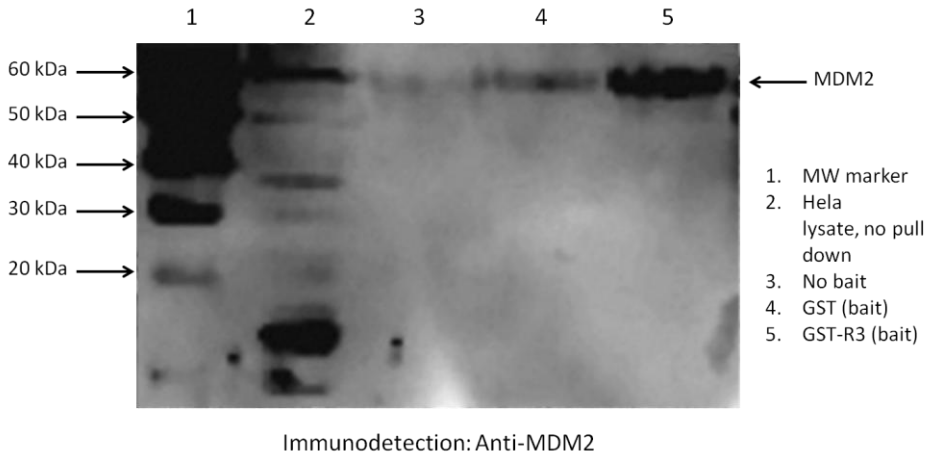

Figure 3.21: Immunodetection of endogenous MDM2 precipitated by GST-R3. Equal amounts of HeLa cell lysate and glutathione-agarose beads were added to lanes 3-5. Bait proteins were added as indicated in the key. GST-R3 was able to pull-down a protein of approximately 55 kDa (lane 5) which is also present in lysate not subjected to precipitation (lane 2). Smaller amounts of the same protein are present when no bait of GST is used as bait, but this is most likely to be due to insufficiently stringent washing of the beads.

3.6.2. Co-precipitation of recombinant RBBP6-RING by recombinant MDM2 in vitro

Encouraged by the interaction between recombinant R3 and endogenous MDM2 described above, we decided to investigate whether the interaction with MDM2 involves the RING finger of RBBP6. This time recombinatly-expressed, rather than endogenous, MDM2 was used as bait, fused to GST to facilitate pull down with glutathione agarose. Bacterially expressed RBBP6-RING was used as prey, detected using a rabbit polyclonal antibody raised against RBBP6-RING. Figure 3.22 shows that RBBP6-RING was precipitated when GST-MDM2 was used a bait (lane 5), but not when GST alone was used as bait (lane 4), nor when bait was left out altogether (lane 3).

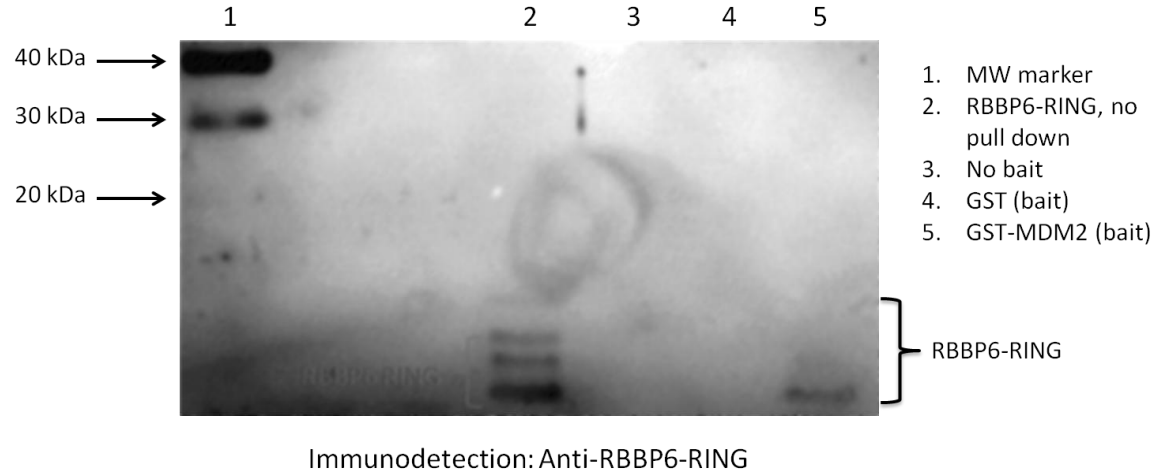

Figure 3.22: Co-precipitation of RBBP6-RING by GST-MDM2 *in vitro*. Equal amounts of bacterially-expressed RBBP6-RING and equal amounts of glutathione-agarose beads were added to lanes 3-5. Bait proteins were added as indicated in the key. GST-MDM2 was able to pull-down RBBP6-RING (lane 5) which is clearly the same protein as was added to lane 2, which was not subjected to precipitation. RBBP6-RING was not precipitated when GST alone was used a bait (lane 4) nor when bait was omitted altogether (lane 3).

The un-precipitated control in lane 2 contains 5 µl of the prey sample. 50 µl was RBBP6-RING was added to the precipitation (lane 5) 10x the amount added to lane 2 (which was not subjected to pull-down) and ¼ of the final precipitate was loaded in lane 5. Hence if all of the prey were precipitated we would expect the signal in lane 5 to be ¼ * 10 = 2.5 times as intense as that in lane 2. It looks significantly less intense than that, which may suggest that the interaction between GST-MDM2 and RBBP6-RING is relatively weak.

The above results, although preliminary, show a consistent interaction between RBBP6 and MDM2, using a variety of methods. Furthermore they suggest that the interaction can be localised to the RING finger domain of RBBP6.

UNIVERSITY of the
WESTERN CAPE

Chapter 4

Discussion and conclusions

The primary aim of this study was to gain further insight into the role RBBP6 plays in the regulation of the cancer-associated proteins YB-1 and p53. In particular we aimed to confirm, *in vitro*, the presence of interactions and to localise them where possible to fragments suitable for future NMR-based interaction assays. The study starts with a side project in which DWNN-GG, a fragment of the DWNN domain terminating immediately after the C-terminal di-glycine motif, was successfully cloned into pGEX-6P-2, including an HA tag inserted between the 3C protease site and the multiple cloning cassette, creating the construct pGEX-HA-DWNN-GG. The HA tag was inserted in such a manner that the DWNN-GG sequence could be excised and replaced with any other gene flanked by BamHI and XhoI sites, to yield a HA-tagged expression product. This property was used later in this thesis to generate the GST-HA-YB-$1_{220\text{-}324}$-6xHis expression construct. The pGEX-HA-DWNN-GG construct was designed to be used by co-workers investigating whether the DWNN domain becomes covalently attached to other proteins when added to mammalian cell lysate.

UNIVERSITY of the
WESTERN CAPE

The interaction between endogenous RBBP6 and YB-1 was confirmed in human lysate by precipitating RBBP6 and detecting YB-1. The interaction appeared to be a significantly strong based on a rough quantitative analysis. This is in good agreement with the findings of Chibi and co-workers (Chibi *et al.*, 2008) as well as our recent unpublished data that RBBP6 is able to poly-ubiquitinate YB-1 *in vitro*. In order to localise the interaction further on YB-1, the C-terminal fragment described by Sorokin and co-workers (Sorokin *et al.*, 2005), denoted YB-$1_{220\text{-}324}$, was successfully cloned and solubly over-expressed in bacteria. The RING finger from RBBP6 was similarly over-expressed and purified.

The expected interaction between YB-$1_{220\text{-}324}$ and RBBP6-RING was confirmed using GST pull-down assays, first with GST-RBBP6-RING as bait and YB-$1_{220\text{-}324}$ as prey, and then the other way around, significantly increasing the significance of the result. Attempts to over-express YB-$1_{220\text{-}324}$ on a scale suitable for NMR studies were unsuccessful due to protein stability issues. Performing the interaction assay the other way around – recording the ^{15}N-HSQC of ^{15}N-labelled YB-$1_{220\text{-}324}$ and adding unlabelled RBBP6-RING - may be a better strategy, since it would significantly reduce the

amount of YB-$1_{220-324}$ required, whereas RBBP6-RING expresses very efficiently and is amenable to being highly concentrated.

Since it contains 4 lysines compared to the 16 of YB-1, YB-$1_{220-324}$ should be an ideal substrate for identification of the lysine or lysines serving as attachment points for poly-ubiquitination. A mutant was first synthesised in which all four lysines were mutated to arginines, yielding a protein dubbed YB-$1_{220-324}$-RRRR. We then took advantage of a KpnI restriction enzyme site in YB-$1_{220-324}$ to sub-clone the last three arginines from YB-$1_{220-324}$-RRRR into wild type YB-$1_{220-324}$, yielding the YB-$1_{220-324}$-KRRR mutant. Due to time constraints the other 3 mutants could not be generated but will be the focus of future projects. Wild-type YB-$1_{220-324}$ and the RRRR mutant were successfully expressed in bacteria and donated to a co-worker for use in fully *in vitro* ubiquitination assays. The results indicate that the R3 fragment of RBBP6 is able to poly-ubiquitinate YB-$1_{220-324}$, which suggests that YB-$1_{220-324}$ may serve as a useful substrate for investigating ubiquitination of YB-1 by R3, and possibly for determination of the structure of the R3/YB-1 complex. As expected YB-$1_{220-324}$-RRRR could not be ubiquitinated by R3, although it still interacted with R3, and will therefore serve as a useful negative control in future ubiquitination studies. Time constraints did not permit investigation of the ubiquitination of the KRRR mutant.

UNIVERSITY of the
WESTERN CAPE

The demonstration of an interaction between YB-$1_{220-324}$ and its ubiquitination by RBBP6 provides *in vitro* confirmation of the report by Chibi and co-workers that RBBP6 suppresses YB-1 *in vivo* by promoting its ubiquitination and degradation in the 26S proteasome. Furthermore it provides a robust *in vitro* platform for future investigations of the regulation of this important oncogene. The aims of such investigations will include the design mutants of YB-1 which cannot be ubiquitinated by RBBP6, as well as the design of small molecules able to disrupt the interaction of YB-1 and RBBP6, both for use in functional studies. While it is true that the above strategies will increase the oncogenic potential of YB-1 rather than decrease it, they will nevertheless increase our understanding of the importance of the both RBBP6 and YB-1 in tumourigenesis. The regulation of tumourigenesis is the result of a balance of many pro- and anti-tumourigenic factors, and it is only by fully understanding both kinds of factors that we can hope to intervene effectively.

The *in vitro* interaction between RBBP6 and the ubiquitin-conjugating enzyme UbcH1 provides support to our data showing RBBP6 is able to poly-ubiquitinate YB-1 with the help of UbcH1 as ubiquitin-conjugating enzyme. The successful bacterial over-expression of NMR-quality samples of UbcH1 lays the foundation for future structural investigations of this interaction, including elucidation of the structure of the RBBP6-RING/ UbcH1 complex using NMR and identification of

amino acids whose mutation may modulate the activity of the pathway and would therefore be useful for future functional studies. The attempts reported here to validate and investigate the interaction using NMR were unsuccessful, most probably due to proteolytic cleavage of the UBA domain found at the C-terminus of UbcH1. From this it can be concluded that more care must be taken in purification of UbcH1. As in the case of YB-$1_{220\text{-}324}$ above, performing the interaction assay the other way around – recording the ^{15}N-HSQC of ^{15}N-labelled UbcH1 and adding unlabelled RBBP6-RING - may be a better strategy, since it would significantly reduce the amount of UbcH1 required.

The localisation of the previously-reported interaction between RBBP6 and MDM2 to the RING finger domain of RBBP6, both in lysate and in fully *in vitro* assays, lends support to our model in which RBBP6 and MDM2 interact though their respective RING finger domains. The successful use of bacterially-expressed MDM2 lays the groundwork for future *in vitro* assays aimed at further localising the interaction on MDM2.

UNIVERSITY of the
WESTERN CAPE

References

Appella, E. and Anderson, C. 2001. Post-translational modifications and activation of p53 by genotoxic stresses. *European journal of biochemistry.*268:567-589

Bae, Y., Jung, S., Kim, G., Rhim, H. and Kang, S. 2013. Hip2 ubiquitin-conjugating enzyme overcomes radiation-induced G2/M arrest. *Molecular Cell Research*. 1833: 2911–2921.

Basaki, Y., Taguchi, K., Izumi, H., Murakami, Y., Kubo, T., Hosoi, F., Watari, K., Nakano, K., Kawaguchi, H., Ohno, S., Kohno, K., Ono, M. and Kuwano, M. (2010.) Y-box binding protein-1 (YB-1) promotes cell cycle progression through CDC6-dependent pathway in human cancer cells. *European Journal of Cancer.* 46:954-965.

Bergmann, S., Royer-pokora, B., Fietze, E., Ju, K., Hildebrandt, B., Trost, D., Leenders, F., Claude, J., Theuring, F., Bargou, R., Dietel, M. and Royer, H. 2005. YB-1 provokes breast cancer through the induction of chromosomal instability that emerges from mitotic failure and centrosome amplification.*Cancer Research.*65: 4078–4087.

Braithwaite, W., Del Sal, G. and Lu, X. 2006. Some p53-binding proteins that can function as arbiters of life and death. *Cell death and differentiation*.13: 984–993.

UNIVERSITY of the
WESTERN CAPE

Brzovic, P., Keeffe, J., Nishikawa, H., Miyamoto, K., Fox, D., Fukuda, M., Ohta, T. and Klevit, R. 2002. Binding and recognition in the assembly of an active BRCA1/BARD1 ubiquitin-ligase complex. *Proceedings of the National Academy of Science United States of America.100: 5646-5651.*

Chattopadhyay, R., Das, S., Maiti, A., Boldogh, I., Xie, J., Hazra, T., Kohno, K., Mitra, S. and Bhakat, K. 2008. Regulatory role of human AP-Endonuclease (APE1/Ref-1) in YB-1 mediated activation of multidrug resistance gene MDR1. *Molecular and Cell Biology.* 28:7066-7080.

Chen, J., Tang, H., Wu, Z., Zhou, C., Jiang, T., Xue, Y., Huang, G., Yan, D. and Peng, Z. 2013. Overexpression of RBBP6 , alone or combined with mutant TP53 , is predictive of poor prognosis in colon cancer. 8:66524-66540

Cheng, Q., Cross, B., Li, B., Chen, L., Li, Z. and Chen, J. 2011. Regulation of MDM2 E3 ligase activity by phosphorylation after DNA damage. *Molecular and Cellular Biology*. 31: 4951–4963.

Chibi, M., Meyer, M., Skepu, A., Rees, D., Moolman-smook, J. and Pugh, D. 2008. RBBP6 interacts with multifunctional protein YB-1 through its RING finger domain , leading to ubiquitination and proteosomal degradation of YB-1. *Journal of Molecular Biology*.384: 908–916.

Cohen, S., Ma, W., Valova, V., Algie, M., Harfoot, R., Woolley, G., Robinson, P. and Braithwaite, W. 2009. Genotoxic stress-induced nuclear localization of oncoprotein YB-1 in the absence of proteolytic processing. *Oncogene*. 29: 403–410.

Dantuma, N. and Lindsten, K. 2010. Stressing the ubiquitin-proteasome system. *European Society of Cardiology.* 263: 2764-2772.

Didier, D., Schiffenbauer, J., Woulfe, S. and Zacheis, M. 1988. Characterization of the cDNA encoding a protein binding to the major histocompatibility complex class II Y box. *Proceedings of the National Academy of Science United States of America* 85: 7322–7326.

Eliseeva, I., Kim, E., Guryanov, S., Ovchinnikov, L. and Lyabin, D. 2011. Y Box Binding Protein 1 (YB 1) and its functions. *Biochemistry Moscow.* 76: 1402–1433.

Eliseeva, I., Lyabin, D. and Ovchinnikov, L. 2011. YB-1 protein : functions and regulation. *Wiley Interdisciplinary Reviews: RNA*. 5:95-110

UNIVERSITY of the
WESTERN CAPE

Evdokimova, V., Tognon, C., Ng, T., Ruzanov, P., Melnyk, N., Fink, D., Sorokin, A., Ovchinnikov, L., Davicioni, E., Triche, T. and Sorensen, P. 2009. Article translational activation of snail1 and other developmentally regulated transcription factors by YB-1 promotes an epithelial-mesenchymal transition. *Cancer Cell*. 15: 402–415.

Fakharzadeh, S., Trusko, S. and Georgel, D. 1991. Tumorigenic potential associated with enhanced expression of a gene that is amplified in a mouse tumor cell line. *European Molecular Biology Orginisation.* 1: 0–4.

Giammartino, D., Li, W., Ogami, K., Yashinskie, J., Hoque, M., Tian, B. and Manley, L. 2014. RBBP6 isoforms regulate the human polyadenylation machinery and modulate expression of mRNAs with AU-rich 3 9 UTRs.*Genes and Development.28*: 2248–2260.

Homer, C., Knight, D., Hananeia, L., Sheard, P., Risk, J., Lasham, A., Royds, J. and Braithwaite, A. 2005. Y-box factor YB1 controls p53 apoptotic function. *Oncogene*.15: 8314–8325.

Izumi, H., Imamura, T., Nagatani, G., Ise, T., Murakami, T., Uramoto, H., Torigoe, T., Ishiguchi, H., Yoshida, Y., Nomoto, M., Okamoto, T., Uchiumi, T., Kuwano, M., Funa, K. & Kohno, K. 2001. Y box-binding protein-1 binds preferentially to single-stranded nucleic acids and exhibits 3 ′ → 5 ′ exonuclease activity. *Nucleic Acid Research*. 29: 1200–1207.

Kappo, M., Ab, E., Hassem, F., Atkinson, R., Faro, A., Mulaudzi, T., Poole, J., Mckenzie, J., Chibi, M., Rees, D. and Pugh, D. 2012. Solution structure of RING finger-like domain of Retinoblastoma-binding Protein-6 (RBBP6) suggests it functions as a U-box.*Journal of Biochemistry*.287:7146-58

Kim, H., Kim, K., Lledias, F., Kisselev, A., Scaglione, K., Skowyra,Gygi, D. and Goldberg, A. 2007. Certain pairs of ubiquitin-conjugating Enzymes (E2s) and ubiquitin-protein ligases (E3s) synthesize non degradable forked ubiquitin chains containing all possible isopeptide linkages.*The journal of biological chemistry.* 282:17375–17386.

Kloks, C., Lasonder, E., Hoffmann, A., Vuister, G., Grzesiek, S. and Hilbers, C. 2002. The solution structure and DNA-binding properties of the cold-shock domain of the human Y-box Protein YB-1. *Journal of Molecular Biology*.316: 317-26

Ko, S., Kang, G., Song, S., Lee, J., Shin, D., Yun, J., Sheng, Y., Cheong, C., Jeon, Y., Jung, Y., Arrowsmith, C., Avvakumov, G., Dhe-Paganon, S., Yoo, Y., Eom, S. and Lee, W. 2010. Structural basis of E2-25K/UBB+1 interaction leading to proteasome inhibition and neurotoxicity. *Journal of Biological Chemistr.*, 285: 36070–36080.

Kosarev, P., Mayer, K. and Hardtke, C. 2002. Evaluation and classification of RING finger domains encoded by the *Arabidopsis* genome. *Genome biology.* 3:1-12.

Krishna, S. 2003. Structural classification of zinc fingers. *Nucleic Acids Research*, 31: 532–550.

Lee, C., Dhillon, J., Wang, M., Gao, Y., Hu, K., Park, E., Astanehe, A., Hung, M., Eirew, P., Eaves, C.J. and Dunn, S. 2008. Targeting YB-1 in HER-2 overexpressing breast cancer cells induces apoptosis via the mTOR / STAT3 pathway and suppresses tumor growth in mice suppresses tumor growth in mice. *Cancer Research.*10: 8661–8666.

Lee, S. and Moore, C. 2014. Efficient mRNA polyadenylation requires a ubiquitin-like domain, a zinc knuckle, and a RING finger domain, all contained in the Mpe1 protein. *Molecular and cellular biology*. 34: 3955–67.

UNIVERSITY of the WESTERN CAPE

Li, L., Deng, B., Xing, G., Teng, Y., Tian, C., Cheng, X., Yin, X. and Yang, J. 2007. PACT is a negative regulator of p53 and essential for cell growth and embryonic development. *Proceedings of the National Academy of Science United States of America.*8: 7951-6

Linke, K., Mace, P., Smith, C., Vaux, D., Silke, J. and Day, C. 2008. Structure of the MDM2 / MDMX RING domain heterodimer reveals dimerization is required for their ubiquitylation in trans. *Cell Death and Differentiation.* 15: 841–848.

Lutz, M., Wempe, F., Bahr, I., Zopf, D. and Melchner, H. 2006. Proteasomal degradation of the multifunctional regulator YB-1 is mediated by an F-Box protein induced during programmed cell death. *Federation of European Biochemical Societies*.580: 3921–3930.

Mather, A., Rakgotho, M. and Ntwasa, M. 2005. SNAMA, a novel protein with a DWNN domain and a RING finger-like motif: a possible role in apoptosis. *Biochimica et biophysica acta*. 1727: 169–76.

Mbita, Z., Meyer, M., Skepu, A., Hosie, M., Rees, J. and Dlamini, Z. 2012. De-regulation of the RBBP6 isoform 3 / DWNN in human cancers. *Molecular Cell Biochemistry* : 249–262.

Miotto, B., Chibi, M., Xie, P., Koundrioukoff, S., Moolman-smook, H., Pugh, D., Chibi, M., Xie, P., Debatisse, M., He, F., Zhang, L. and Defossez, P. 2014. The RBBP6/ZBTB38/MCM10 axis regulates DNA replication and common fragile site stability. *Cell Reports*. 7: 575–587.

UNIVERSITY of the
WESTERN CAPE

Moll, U. and Petrenko, O. 2003. The MDM2-p53 Interaction The MDM2-p53 Interaction. *Molecular Cancer Research*. 1: 1001–1008.

Morisaki, T., Yashiro, M., Kakehashi, A., Inagaki, A., Kinoshita, H., Fukuoka, T., Kasashima, H., Masuda, G., Sakurai, K., Kubo, N., Muguruma, K., Ohira, M., Wanibuchi, H. and Hirakawa, K. 2014. Comparative proteomics analysis of gastric cancer stem cells. *PLOS ONE*. 9:110736.

Motadi, L., Bhoola, K. and Dlamini, Z. 2010. Immunobiology Expression and function of retinoblastoma binding protein 6 (RBBP6) in human lung cancer. *Immunobiology*. 216: 1065–1073.

Pickart, M. 2001. Mechanisms underlying ubiquitination. *Annu Rev Biochem.* 70:503–533.

Plechanovova, A., Jaffray, E., MacMahon, S., Johnson, K., Navratilova, I., Naismith, J. and Hay, R. 2012. Mechanism of ubiquitylation by dimeric RING ligase RNF4. *Nature Structural Molecular Biology.*18: 1052-1059.

Pretorius, A., Adebodun, H., Bankole., Meyer, M., February, F. and Rees, D.2013. Silencing of Mouse RBBP6 Using Interference RNA Implicates It in Apoptosis and the Cell Cycle. *International Journal of Biosciences.* 2: 50-59

Pugh, D., Ab, E., Faro, A., Lutya, P., Hoffmann, E. and Rees, D. 2006. DWNN, a novel ubiquitin-like domain, implicates RBBP6 in mRNA processing and ubiquitin-like pathways. *BMC Structural Biology.* 12: 1–12.

Schneider, R. 1994. The human ubiquitin-conjugating enzyme UbcH1 is involved in the repair of UV-damaged, alkylated and cross-linked DNA. *Federation of European Biochemical Societies*. 350: 1–4.

Shi, Y., Di Giammartino, D., Taylor, D., Sarkeshik, A., Rice, W., Yates, J., Frank, J. and Manley, J. 2009. Molecular Architecture of the Human Pre-mRNA 3' Processing Complex. *Molecular Cell*, 33: 365–376.

Simons, A., Melamed-bessudo, C., Wolkowicz, R., Sperling, J., Sperling, R., Eisenbach, L. and Rotter, V. 1997. PACT : cloning and characterization of a cellular p53 binding protein that interacts with Rb.*Oncogene*.14:145-155

Skabkina, O., Skabkin, M., Popova, N., Lyabin, D., Penalva, O., Ovchinnikov, L. and Penalva, L. 2003. Post-translation modification and degradation: Poly (A) -binding protein positively affects YB-1 mRNA translation through specific interaction with YB-1 mRNA. *Molecular Biology*. 40: 670-685.

Sorokin, A., Selyutina, A., Skabkin, M., Guryanov, S., Nazimov, I., Richard, C., Th'ng, J., Yau, J., Sorensen, P., Ovchinnikov, L. and Evdokimova, V. 2005. Proteasome-mediated cleavage of the Y-box-binding protein 1 is linked to DNA-damage stress response. *European Molecular Biology Organization.* 24: 3602–3612.

Sutherland, B., Kucab, J., Wu, J., Lee, C., Cheang, M., Yorida, E., Turbin, D., Dedhar, S., Nelson, C., Pollak, M., Grimes, H., Miller, K., Badve, S., Huntsman, D., Chen, M., Pallen, C. and Dunn, S. 2005. Akt phosphorylates the Y-box binding protein 1 at Ser102 located in the cold shock domain and affects the anchorage-independent growth of breast cancer cells. *Oncogene*. 1: 4281–4292.

Uchiumi, T., Fotovati, A., Shibahara, K., Shimada, T., Fukuda, T., Nakamura, T., Tsuzuki, T. and Kuwano, M. 2006. YB-1 Is Important for an Early Stage Embryonic Development. *Journal of Biological chemistry.* 281:40440-40449.

UNIVERSITY of the WESTERN CAPE

Uramoto, H., Izumi, H., Ise, T., Tada, M., Uchiumi, T., Kohno, K. and Chem, J. 2002. p73 Interacts with c-Myc to Regulate p73 Interacts with c-Myc to Regulate Y-box-binding Protein-1 Expression. *Journal of Biological chemistry.*227:31694-31699

Uversky, V. and Dunker, A. 2010. Understanding protein non-folding. *Proteins and Proteomics*, 1804: 1231–1264.

Van Roeyen, C., Scurt, F., Brandt, S., Kuhl, V., Martinkus, S., Djudjaj, S., Raffetseder, U., Royer, H., Stefanidis, I., Dunn, S., Dooley, S., Weng, H., Fischer, T., Lindquist, J. and Mertens, P. 2013. Cold shock Y-box protein-1 proteolysis autoregulates its transcriptional activities. *Cell communication and signalingI.*11: 63-70.

Vo, L., Minet, M., Schmitter, J., Lacroute, F. and Wyers, F. 2001. Mpe1, a zinc knuckle protein, is an essential component of yeast cleavage and polyadenylation factor required for the cleavage and polyadenylation of mRNA. *Molecular and cellular biology*, 21: 8346–8356.

Wang, X., Wang, J. and Jiang, X. 2011. MdmX protein is essential for Mdm2 protein-mediated p53 polyubiquitination. *The journal of biological chemistry.* 286:23725-23734.

Weinberg, R.A. 2006.*The biology of cancer,* USA, Garland science, Taylor and Francis group, LLC, pp. 307-356

UNIVERSITY of the
WESTERN CAPE

Witte, M. and Scott, E. 1997.The proliferation potential proteinrelated (P2P-R) gene with domains encoding heterogeneousnuclear ribonucleoprotein association and Rb1 bindingshows repressed expression during terminal differentiation. *Proceedings of the National Academy of Sciences of the United States* .94:1212-1217.

Wolf, D. 2004. From lysosome to proteasome : the power of yeast in the dissection of proteinase function in cellular regulation and waste disposal. *Cellular and Molecular Life Sciences*. 61: 1601–1614.

Woolley, A., Algie, M., Samuel, W., Harfoot, R., Wiles, A., Hung, N., Tan, P., Hains, P., Valova, V., Huschtscha, L., Royds, J., Perez, D., Yoon, H., Cohen, S., Robinson, P., Bay, B., Lasham, A. and Braithwaite, A. 2011. Prognostic association of YB-1 expression in breast cancers: A matter of antibody. *PLOS ONE*. 6:20603-20609

Wu, H., Pomeroy, S., Ferreira, M., Teider, N., Mariani, J., Nakayama, K., Hatakeyama, S., Tron, V., Saltibus, L., Spyracopoulos, L. and Leng, R. 2011. UBE4B promotes Hdm2-mediated degradation of the tumor suppressor p53. *Nature medicine*. 17: 347–55.

Yamasaki, S., Ivanov, P., Hu, G. and Anderson, P. 2009. Angiogenin cleaves tRNA and promotes stress-induced translational repression. *Journal of Cell Biology*. 185: 35–42.

Yang, W. and Bloch, D. 2007. Probing the mRNA processing body using protein macroarrays and autoantigenomics. *RNA.* 13 : 704–712.

Yoshitake, Y., Nakatsura, T., Monji, M., Senju, S., Matsuyoshi, H., Tsukamoto, H., Hosaka, S., Komori, H., Fukuma, D., Ikuta, Y., Katagiri, T., Furukawa, Y., Ito, H., Shinohara, M., Nakamura, Y. & Nishimura, Y. 2004. Proliferation Potential-Related Protein , an Ideal Esophageal Cancer Antigen for Immunotherapy , Identified Using Complementary DNA Microarray Analysis. *Clinical Cancer* Research. 10: 6437–6448.

Zhang, Y., Homer, C., Edwards, S., Hananeia, L., Lasham, A., Royds, J., Sheard, P. and Braithwaite, A. 2003. Nuclear localization of Y-box factor YB1 requires wild-type p53. *Oncogene*. 22: 2782–2794.

Zhou, Z., Gao, H., Zhou, C., Chang, Y., Hong, J., Song, X., Lin, D. and Hu, H. 2008. Differential ubiquitin binding of the UBA domains from human c-Cbl and Cbl-b: NMR structural and biochemical insights. *Protein Science*. 17: 1805–1814.

UNIVERSITY of the
WESTERN CAPE

Appendix

```
Query  1    ATGTACCCATACGATGTTCCAGATTACGCTGCGGGATCCATGTCCTGTGTGCATTATAAA  60
            ||||||||||||||||||||||||||||||||||||||||||||||||||||||||||||
Sbjct  1    ATGTACCCATACGATGTTCCAGATTACGCTGCGGGATCCATGTCCTGTGTGCATTATAAA  60

Query  61   TTTTCCTCTAAACTCAACTATGATACCGTCACCTTTGATGGGCTCCACATCTCCCTCTGC  120
            ||||||||||||||||||||||||||||||||||||||||||||||||||||||||||||
Sbjct  61   TTTTCCTCTAAACTCAACTATGATACCGTCACCTTTGATGGGCTCCACATCTCCCTCTGC  120

Query  121  GACTTAAAGAAGCAGATTATGGGGAGAGAGAAGCTGAAAGCTGCCGACTGCGACCTGCAG  180
            ||||||||||||||||||||||||||||||||||||||||||||||||||||||||||||
Sbjct  121  GACTTAAAGAAGCAGATTATGGGGAGAGAGAAGCTGAAAGCTGCCGACTGCGACCTGCAG  180

Query  181  ATCACCAATGCGCAGACGAAAGAAGAATATACTGATGATAATGCTCTGATTCCTAAGAAT  240
            ||||||||||||||||||||||||||||||||||||||||||||||||||||||||||||
Sbjct  181  ATCACCAATGCGCAGACGAAAGAAGAATATACTGATGATAATGCTCTGATTCCTAAGAAT  240

Query  241  TCTTCTGTAATTGTTAGAAGAATTCCTATTGGAGGT  276
            ||||||||||||||||||||||||||||||||||||
Sbjct  241  TCTTCTGTAATTGTTAGAAGAATTCCTATTGGAGGT  276
```

Figure A1: Alignment of the experimental sequence read of HA-DWNN-GG (Sbjct) with the expected sequence (Query): HA-tag indicated in green, BamHI site in red and di-glycine in yellow. Showed that the sequence was 100 % correct. Sequencing was carried out Inqaba biotech.

```
Query  1    GGATCCGGTGCTGACAACCAGGGTGCAGGAGAACAAGGTAGACCAGTGAGGCAGAATATG  60
            ||||||||||||||||||||||||||||||||||||||||||||||||||||||||||||
Sbjct  1    GGATCCGGTGCTGACAACCAGGGTGCAGGAGAACAAGGTAGACCAGTGAGGCAGAATATG  60

Query  61   TATCGGGGATATAGACCACGATTCCGCAGGGGCCCTCCTCGCCAAAGACAGCCTAGAGAG  120
            ||||||||||||||||||||||||||||||||||||||||||||||||||||||||||||
Sbjct  61   TATCGGGGATATAGACCACGATTCCGCAGGGGCCCTCCTCGCCAAAGACAGCCTAGAGAG  120

Query  121  GACGGCAATGAAGAAGATAAAGAAAATCAAGGAGATGAGACCCAAGGTCAGCAGCCACCT  180
            ||||||||||||||||||||||||||||||||||||||||||||||||||||||||||||
Sbjct  121  GACGGCAATGAAGAAGATAAAGAAAATCAAGGAGATGAGACCCAAGGTCAGCAGCCACCT  180

Query  181  CAACGTCGGTACCGCCGCAACTTCAATTACCGACGCAGACGCCCAGAAAACCCTAAACCA  240
            ||||||||||||||||||||||||||||||||||||||||||||||||||||||||||||
Sbjct  181  CAACGTCGGTACCGCCGCAACTTCAATTACCGACGCAGACGCCCAGAAAACCCTAAACCA  240

Query  241  CAAGATGGCAAAGAGACAAAGCAGCCGATCCACCAGCTGAGAATTCGTCCGCTCCCGAG  300
            ||||||||||||||||||||||||||||||||||||||||||||||||||||||||||||
Sbjct  241  CAAGATGGCAAAGAGACAAAGCAGCCGATCCACCAGCTGAGAATTCGTCCGCTCCCGAG  300

Query  301  GCTGAGCAGGGCGGGGCTGAGCATCATCATCATCATTAACTCGAG  348
            ||||||||||||||||||||||||||||||||||||||||||||||
Sbjct  301  GCTGAGCAGGGCGGGGCTGAGCATCATCATCATCATTAACTCGAG  348
```

Figure A2: Alignment of experimental sequence of wild type YB-1$_{220\text{-}324}$ (Sbjct) against the expected sequence (Query): The sequence was 100 % identical to the expected sequence performed at Inqaba Biotech facility, with four lysines (codon AAA), indicated in yellow, the flanking BamHI and XhoI sites indicated in turquoise and red respectively.

UNIVERSITY of the WESTERN CAPE

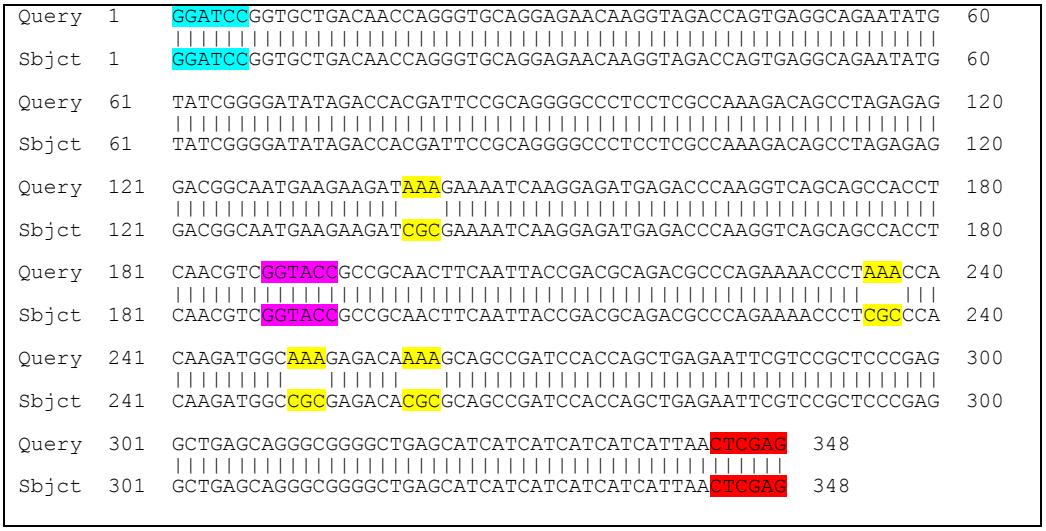

Figure A3: Alignment of the experimental sequence of the YB-$1_{220\text{-}324}$-RRRR mutant (Sbjct) against the expected sequence of the wild type (Query): The sequence was 100 % in agreement, with the exception of the four lysines (codon AAA), indicated in yellow, which have been replaced by arginines (codon CGC). The KpnI restriction site used for generation of the KRRR mutant is indicated in purple.

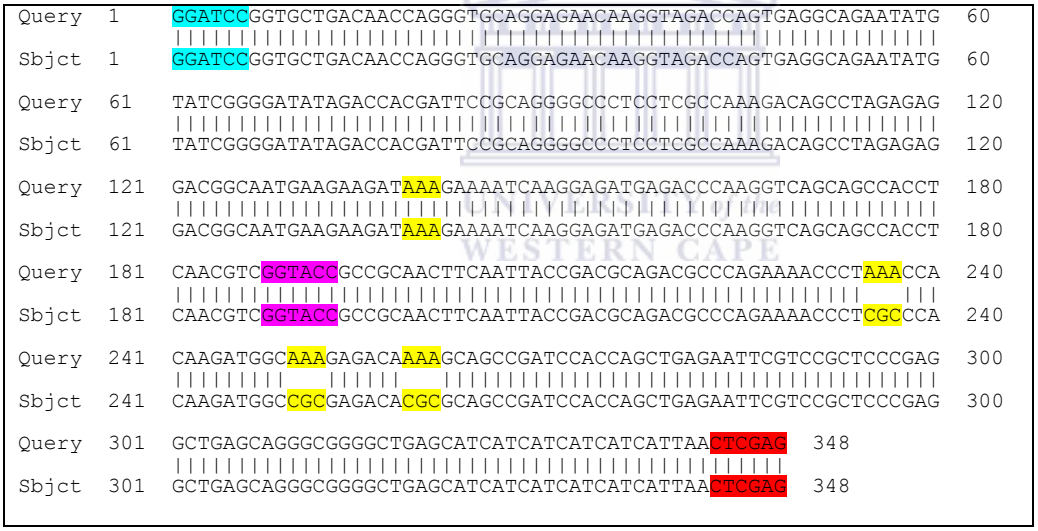

Figure A4: Alignment of the experimental sequence of the YB-$1_{220\text{-}324}$-KRRR mutant (Sbjct) against the expected sequence of the wild type (Query): The sequences are 100 % in agreement, with the exception of the last three lysines, indicated in yellow. The KpnI restriction site is indicated in purple.

B1. List of chemicals, kits and suppliers

Table B1: List of chemicals, kits and suppliers

Chemical	**Supplier**
40% 37.5:1 acrylamide: bis-acrylamide	Sigma
Agarose	Promega
Ammonium persulphate	Merck
Ampicillin	Roche
Boric acid	Merck
Bovine serum albumin	Roche
Calcium chloride	Merck
Clarity^{TM} ECL Western Blotting Substrate	Bio-rad
Coomassie Blue R-250	Sigma
Ethanol	Merck
Ethylene diamine tetra acetic acid (EDTA)	Merck
GeneJET Gel Extraction Kit	Thermo Fisher Scientific
GeneJET PCR Clean-up Kit	Thermo Fisher Scientific
GeneJET Plasmid Miniprep Kit	Thermo Fisher Scientific
Glacial acetic acid	Merck
Glutathione agarose	Sigma
Glycerol	Merck
Glycine	Merck
Hydrochloric acid	Merck
Imidazole	Sigma
Isopropanol	Merck
Luria Broth	Merck
N, N, N', N'-Tetra methylethylene-diamine (TEMED)	Sigma
Nickel sepharose	Amersham Biosciences
Nutrient agar	Merck
Potassium acetate	Merck
Potassium chloride	Merck
Protease inhibitor cocktail	Roche

UNIVERSITY of the
WESTERN CAPE

Restriction enzymes	Fermentas
Sodium chloride	Merck
Sodium dodecyl sulphate	Promega
Tris	Merck
Tryptone	Merck
Tween-20	Merck
Yeast extract	Merck

B2 List of general stock solutions and buffers

Table B2: List of general stock solutions and buffers

Buffer	**Composition/Preparation**
10 x PBS	1.37 M NaCl, 26.96 mM KCl, 88.75 mM $N_2HPO_4.2H_2O$, 15 mM KH_2PO_4 at pH 7.4
10x SDS electrophoresis buffer	50 mM Tris, 0.2% SDS and 500 mM glycine, pH 8.3
10x TBE	0.9 M Tris (pH 8.3), 0.89 M boric acid and 25 mM EDTA. This stock was stored at room temperature and diluted ten-fold for running agarose gels
2X SDS sample buffer	4 % SDS, 0.125 M Tris pH 6.8, 15 % glycerol and 1 mg/ml bromophenol blue. This buffer was stored at room temperature. 10 % β- mercaptoethanol was added to the buffer immediately prior use.
3C protease buffer	50 mM Tris, pH 8.0, 200 mM NaCl, 20 mM β-mercaptoethanol
Ammonium persulphate	A 10 % stock solution was prepared in deionised water. The solution was stored at 4 °C.
Ampicillin	A 100 mg/ml solution was made in deionised water, filter sterilised and stored at -20 °C.
Coomassie staining solution	40 % ethanol, 10 % acetic acid, 0.1 % Coomassie Blue R-250

UNIVERSITY of the WESTERN CAPE

Destaining solution	40 % ethanol, 10 % acetic acid.
IPTG	1 M stock solution was prepared in deionised water, filter sterilised and stored at -20 °C
Luria broth	1 % tryptone, 0.5 % yeast extract, 0.5 % NaCl and 0.2 % glucose
Minimal media	12.8 g/l Na2HPO4-7H2O, 3 g/l KH2PO4, 1 g/l NH4Cl and 0.5 g/l NaCl. The pH of this media was adjusted to 7.0 with NaOH and the solution was autoclaved. Immediately prior to use, the solution was supplemented with 2 ml of autoclaved 1 M MgSO4, 100 µl of autoclaved 1 M CaCl2 and 10 ml of filter-sterilized 20 % Glucose. The solution was stored at room temperature. For labeled minimal media 1g/liter ^{15}N- labeled NH4Cl was added to the media.
NMR buffer	100 mM Sodium phosphate buffer pH 6.0, 150 mM NaCl, 5 mM DTT and 0.02 % sodium azide.
PBS-T	1 X PBS and 0.1 % Tween
Protein elution buffer	20 mM Glutathione, 50 mM Tris-HCl pH 8.0 and 150 mM NaCl or 500 mM Imidazole, 50 mM Tris-HCl pH 8.0 and 150 mM NaCl
Protein extraction buffer	50 mM Tris, pH 8, 150 mM NaCl, 100 g/ml lysozyme, 10 mM-mercaptoethanol, 0.5 % Triton X-100, 20 µg/ml ZnSO4.
Protein wash buffer	50 mM Tris, pH 8.0, 150 mM NaCl and 10 mM β-mercaptoethanol.
Separating buffer	1.5 M Tris-HCl, adjusted to pH 8.8 with HCl. The buffer was stored at 4 °C.
Stacking buffer	0.5 M Tris-HCl, adjusted to pH 6.8 with HCl. The buffer was stored at 4 °C.

UNIVERSITY of the
WESTERN CAPE

UNIVERSITY of the
WESTERN CAPE